CHARACTERISATION OF VOLTAGE-GATED CALCIUM CHANNELS AND DETECTION OF THEIR AUTOANTIBODIES



by

KATHERINE S. LEYS

Neurosciences Group

Institute of Molecular Medicine

University of Oxford

A thesis submitted for the degree of

Doctor of Philosophy,

University of Oxford.

April 1991

ABSTRACT

K.S. Leys
Wolfson College, Oxford

D. Phil
Hilary Term, 1991

Characterisation of Voltage-Gated Calcium Channels and Detection of their Autoantibodies.

The Lambert-Eaton myasthenic syndrome (LEMS) is an autoimmune disorder of impaired neuromuscular transmission. It is associated with small cell lung carcinoma (SCLC) in 60% of patients. There is considerable evidence that the defect in LEMS is caused by autoantibodies to voltage-gated calcium channels (VGCCs) on the nerve terminal.

Two VGCC subtypes were demonstrated in cultured neuronal cell lines by the technique of K^+-induced $^{45}Ca^{2+}$ influx: one subtype was inhibited by dihydropyridines (DHPs), the other by ω-conotoxin (ωCgTx). These may correspond to L and N channels previously described for neuronal tissue. The presence of these VGCC subtypes was confirmed by radioligand binding studies using [^{3}H]-PN200-110 and ^{125}I-ωCgTx respectively.

Pooled LEMS IgG inhibited K^+-induced Ca^{2+} flux by 40% in SKNSH (human neuroblastoma) cells, while control IgG had no effect. The same LEMS pool reduced the density of ^{125}I-ωCgTx binding sites in SKNSH and MAR5 (human SCLC) cells by 57% and 43% respectively. These results provide further evidence that LEMS antibodies cause a loss of functional VGCCs.

78 LEMS and 88 control sera were tested for anti-VGCC antibodies by the precipitation of ^{125}I-ωCgTx-labelled VGCCs extracted from SKNSH cells. 42% of LEMS sera had significant levels of antibody (30-1466pM) compared to the healthy controls (<31pM). There was a high correlation between these results and those obtained using antigen extracted from MAR5 cells.

Raised antibody titres (30-82pM) were also found among SCLC patients (47%) and patients with rheumatoid arthritis or systemic lupus erythematosus (56%). The incidence of positive sera was not significant among patients with other neurological disorders, including myasthenia gravis.

Antibody titre did not correlate with disease severity across individuals. However, longitudinal studies in two LEMS patients showed an inverse relation between antibody titre and an electromyographic index of disease severity. Some of the antibodies detected may, therefore, be implicated in the neurological symptoms of LEMS. The assay may be a useful aid for the diagnosis of LEMS in some patients.

ACKNOWLEDGEMENTS

I am very grateful to Professor Newsom-Davis for his support throughout this study and to Dr. Angela Vincent for helpful advice, particularly concerning the radioimmunoassay.

I am indebted to my supervisor, Dr. Bethan Lang, for many hours of helpful discussions and for her constant encouragement and guidance.

I would like to thank my colleagues in the Neurosciences Group, Institute of Molecular Medicine and in particular to acknowledge the help of Irene Johnston.

Finally, I would like to thank my husband, David, for his support and patience.

TABLE OF CONTENTS

	Page
Abstract	1
Acknowledgements	2
Table of Contents	3
List of Figures	7
List of Tables	10
Abbreviations	11
Chapter 1: Introduction	
1.1. Autoimmune diseases	13
1.2. Lambert-Eaton myasthenic syndrome	14
1.2.1. Clinical and electrophysiological features of LEMS	15
1.2.2. Autoimmune aetiology of LEMS	16
1.2.3. Morphological changes in LEMS	19
1.2.4. Small cell lung carcinoma	21
1.2.5. Calcium flux studies	22
1.3. Voltage-gated calcium channels	23
1.3.1. Classification of VGCCs	23
1.3.2. Function of neuronal VGCCs	27
1.3.3. The dihydropyridine receptor	28
1.3.4. The ω-conotoxin receptor	36
1.4. Aims of project	41
1.4.1. Potassium-stimulated calcium flux in neuronal cell lines	41
1.4.2. Calcium antagonist binding to neuronal cell membranes	41
1.4.3. Immunoprecipitation of VGCCs by LEMS serum	42

Chapter 2: Materials and General Methods

2.1. Materials 43

2.2. Methods 44

2.2.1. Cell culture 44

2.2.2. Measurement of protein concentration 47

2.2.3. Preparation of IgG from plasma by the Rivanol method 48

2.2.4. Measurement of IgG concentration 49

2.2.5. Membrane preparation 49

2.2.6. Patients 50

2.2.7. Statistical methods 52

Chapter 3: Calcium flux studies

3.1. Introduction 53

3.2. Methods 55

3.3. Results 58

3.3.1. Voltage dependency of K^+-stimulated calcium flux 58

3.3.2. Time course of K^+-stimulated calcium flux 61

3.3.3. Net K^+-stimulated calcium flux in neuronal cell lines 61

3.3.4. The effect of antagonists on K^+-stimulated calcium flux 67

3.3.5. The effect of dibutyryl cAMP on K^+-stimulated calcium flux 78

3.3.6. The effect of LEMS IgG on K^+-stimulated calcium flux 81

3.4. Discussion 87

3.5. Summary 93

Chapter 4: Radioligand binding studies

4.1. Introduction 94

4.2. Methods 96

4.2.1. Binding of [^{3}H]-PN200-110 to cell membranes 96

4.2.2. Binding of ^{125}I-ω-conotoxin to cell membranes 97

4.3. Results 99

4.3.1. Time course of [^{3}H]-PN200-110 binding 99

4.3.2. [^{3}H]-PN200-110 binding to rat brain 99

4.3.3. [^{3}H]-PN200-110 binding to neuronal cells 105

4.3.4. Calcium dependency of [^{3}H]-PN200-110 binding 118

4.3.5. The effect of dibutyryl cAMP on [^{3}H]-PN200-110 binding 118

4.3.6. Time course of ^{125}I-ω-conotoxin binding 122

4.3.7. ^{125}I-ωCgTx binding to rat brain 122

4.3.8. ^{125}I-ωCgTx binding to neuronal cells 126

4.3.9. The effect of LEMS IgG on ^{125}I-ωCgTx binding 138

4.4. Discussion 142

4.5. Summary 150

Chapter 5: Immunoprecipitation studies

5.1. Introduction 151

5.2. Methods 153

5.3. Results 154

5.3.1. Assay conditions 154

5.3.2. Precipitation of ^{125}I-ωCgTx-VGCCs from SKNSH cells 157

5.3.3. Precipitation of ^{125}I-ωCgTx-VGCCs from MAR5 cells 169

5.3.4. Precipitation of ^{125}I-ωCgTx-VGCCs from rat brain 176

5.3.5. Correlation of anti-VGCC antibody titre with disease severity 178

5.3.6. Longitudinal studies of two LEMS patients 178

5.3.7. The co-existence of LEMS and MG in two patients 179

5.4. Discussion 186

5.5. Summary 193

Chapter 6: General discussion and future perspectives 194

Summary 201

References 203

LIST OF FIGURES

Page

1.1: Localisation of VGCCs at the neuromuscular junction 18

1.2: Modulation of VGCCs by LEMS IgG 20

1.3: Subunit structure of the skeletal muscle VGCC 30

1.4: Primary structure of the calcium channel α_1 subunit 32

3.1: Voltage dependency of calcium influx in SKNSH cells 59

3.2: Voltage dependency of calcium influx in Kelly cells 59

3.3: Time course of K^+-stimulated calcium flux in SKNSH cells 62

3.4: Time course of K^+-stimulated calcium flux in Kelly cells 62

3.5: Net K^+-stimulated calcium flux in 6 neuronal cell lines 64

3.6: Inhibition of K^+-stimulated calcium flux by nitrendipine 68

3.7: Inhibition of K^+-stimulated calcium flux by methoxyverapamil 70

3.8: Inhibition of K^+-stimulated calcium flux by ω-conotoxin 72

3.9: The additive effect of nitrendipine and ω-conotoxin on K^+-stimulated calcium flux 76

3.10: Inhibition of K^+-stimulated calcium flux by antagonists in dibutyryl cAMP-treated cells 79

3.11: The effect of pooled IgG on K^+-stimulated calcium flux 83

3.12: The effect of single IgG preparations on K^+-stimulated calcium flux 83

3.13: Inhibition of K^+-stimulated calcium flux by antagonists in IgG-treated cells 85

4.1: Time course of $[^3H]$-PN200-110 binding to PC12 membranes 100

4.2: $[^3H]$-PN200-110 binding to rat brain membranes 101

4.3: Inhibition of $[^3H]$-PN200-110 binding in rat brain membranes by antagonists 103

4.4: $[^3H]$-PN200-110 binding to PC12 membranes 107

4.5: Inhibition of $[^3H]$-PN200-110 binding in PC12 membranes by antagonists 109

4.6: $[^3H]$-PN200-110 binding to MAR5 membranes 111

4.7: $[^3H]$-PN200-110 binding to NG108 membranes 113

4.8: Inhibition of $[^3H]$-PN200-110 binding to NG108 membranes by antagonists 115

4.9: Calcium dependency of $[^3H]$-PN200-110 binding 119

4.10: The effect of dibutyryl cAMP on $[^3H]$-PN200-110 binding 121

4.11: Time course of ^{125}I-ωCgTx binding to SKNSH membranes 123

4.12: ^{125}I-ωCgTx binding to rat brain membranes 124

4.13: ^{125}I-ωCgTx binding to SKNSH membranes 127

4.14: Inhibition of ^{125}I-ωCgTx binding to SKNSH membranes by unlabelled ωCgTx 129

4.15: Inhibition of ^{125}I-ωCgTx binding to SKNSH membranes by divalent cations 130

4.16: ^{125}I-ωCgTx binding to MAR5 membranes 132

4.17: Inhibition of ^{125}I-ωCgTx binding to MAR5 membranes by unlabelled ωCgTx 134

4.18: ^{125}I-ωCgTx binding to NG108, PC12, IMR32 and Kelly membranes 135
4.19: The effect of IgG on ^{125}I-ωCgTx binding 140
5.1: The dependence of anti-VGCC antibody titre on antigen concentration 155
5.2: Precipitation of ^{125}I-ωCgTx-VGCCs from SKNSH cells by LEMS sera 162
5.3: Precipitation of ^{125}I-ωCgTx-VGCCs from SKNSH cells by control sera 164
5.4: Anti-VGCC antibody titres of 78 LEMS and 88 control sera using SKNSH antigen 166
5.5: Precipitation of ^{125}I-ωCgTx-VGCCs from MAR5 cells by LEMS and control sera 170
5.6: Anti-VGCC antibody titres of 28 LEMS and 40 control sera using MAR5 antigen 172
5.7: Correlation of anti-VGCC antibody titres using antigen extracted from SKNSH and MAR5 cells 174
5.8: Comparison of anti-VGCC antibody titre with indices of disease severity 180
5.9: Longitudinal studies of anti-VGCC antibody titre in two LEMS patients using SKNSH antigen 182
5.10: Longitudinal studies of anti-VGCC antibody titre in two LEMS patients using MAR5 antigen 184

LIST OF TABLES

	Page
1.1: Electrical and pharmacological properties of VGCC subtypes in chick DRG neurones	26
1.2: Comparison of DHP binding parameters in different tissues	35
1.3: The sensitivity of VGCCs to ωCgTx in different tissues	38
2.1: Origin and culture conditions of cell lines used	45
3.1: K^+-stimulated calcium flux in neuronal cell lines	66
3.2: Inhibition of K^+-stimulated calcium flux by antagonists	74
4.1: Properties of $[^3H]$-PN200-110 binding to neuronal membranes	117
4.2: Properties of ^{125}I-ωCgTx binding to neuronal membranes	137
5.1: Clinical details of the patients with Lambert-Eaton myasthenic syndrome	160
5.2: Anti-VGCC antibodies in LEMS and control sera using SKNSH neuroblastoma antigen	168
5.3: Comparison of anti-VGCC antibody titres using three sources of antigen	177

ABBREVIATIONS

ACh	Acetylcholine
AChR	Acetylcholine receptor
APUD	Amine precursor uptake and decarboxylation
AZP	Active zone particle
BSA	Bovine serum albumin
cAMP	Adenosine 3', 5' cyclic monophosphate
ωCgTx	omega-Conotoxin GVI A
CMAP	Compound muscle action potential
cpm	Counts per minute
D600	Methoxyverapamil
DHP	Dihydropyridine
DMSO	Dimethylsulphoxide
DRG	Dorsal root ganglion
EDTA	Ethylenediaminetetraacetic acid
ELISA	Enzyme-linked immunosorbent assay
epp	Endplate potential
FCS	Foetal calf serum
HAT	Hypoxanthine-aminopterin-thymidine
HC	Healthy controls
HLA	Human leukocyte antigen
HVA	High voltage-activated
Ig	Immunoglobulin
LEMS	Lambert-Eaton myasthenic syndrome
LVA	Low voltage-activated
mepp	Miniature endplate potential
MG	Myasthenia gravis
NCD	No cancer detected
NMJ	Neuromuscular junction

OND	Other neurological diseases
PBS	Phosphate buffered saline
PEI	Polyethyleneimine
PMSF	Phenylmethylsulphonylfluoride
PN200-110	A benzoxadiazol-substituted DHP (Weiland and Oswald 1985)
PTX	Phosphate/Triton X-100 buffer
RA	Rheumatoid arthritis
RIA	Radioimmunoassay
RS	Spearman's rank correlation coefficient
SCLC	Small cell lung carcinoma
SD	Standard deviation
SEM	Standard error of the mean
SLE	Systemic lupus erythematosus
SU	Status uncertain
Tris	Tris[hydroxymethyl]aminomethane
VGCC	Voltage-gated calcium channel

CHAPTER 1

INTRODUCTION

1.1. Autoimmune diseases

A wide range of diseases have been identified in which the body becomes sensitized to self components, either by the production of autoantibodies or autoreactive T cells. These can be divided into organ specific autoimmune diseases in which the self antigen is essentially localized to a given organ, for example thyrotoxicosis, and non-organ specific diseases in which the antigen is widespread throughout the body, resulting in the systemic deposition of autoimmune complexes. Examples of the latter include rheumatoid arthritis (RA) which is caused by self-reactivity to IgG, and systemic lupus erythematosus (SLE), which is associated with autoantibodies to DNA and nucleoproteins.

Evidence for the involvement of genetic factors in autoimmunity is provided by the familial incidence of autoimmune disorders and also the associations with particular HLA (human leukocyte antigen) specificities. There are frequent occurrences of more than one autoimmune disorder in the same individual.

Ideally, three criteria should be met for a disease to be defined as autoimmune: the presence of circulating antibodies or a cellular response to a specific antigen, transfer of the disease symptoms between species by injecting the active cells or antibodies (passive transfer), and induction of the disease by immunisation with the suspected antigen (active transfer) (Humphrey and White 1963).

An example of an organ specific autoimmune disease with a well characterised target antigen is myasthenia gravis (MG), a disorder of neuromuscular transmission (reviewed by Vincent 1990). The main clinical symptoms of MG are weakness and fatigue, with the muscles of the eye being particularly affected. Investigation of the compound muscle action potential (CMAP) in MG patients during a train of nerve stimuli shows an initial CMAP of normal amplitude that decreases to a plateau (decrement). The defect in MG is caused by antibodies which bind to the acetylcholine receptor (AChR) on the postsynaptic membrane of the neuromuscular junction. Physiological features of the disease are seen in mice after injection of MG immunoglobulin (Ig), and after immunisation with purified AChR, thus confirming an autoimmune basis for MG. The binding of antibody to its target results in a loss of functional AChRs principally by an increased rate of receptor degradation and complement-mediated lysis of the postsynaptic membrane. In addition, antibodies may directly inhibit acetylcholine (ACh) action by binding to the ACh binding site. Circulating anti-AChR antibodies are detected in about 90% of MG patients by the immunoprecipitation of ^{125}I-α-bungarotoxin-labelled human AChR. Research is currently in progress to define the precise antibody binding sites on the AChR.

1.2. Lambert-Eaton myasthenic syndrome

Myasthenic syndrome was first reported as a rare manifestation of lung cancer (Anderson et al 1953, Henson et al 1953), and was distinguished from myasthenia gravis after electrophysiological studies of patients by Lambert and his colleagues (Lambert et al

1956). Diseases which occur in association with neoplasia, but are not due to a direct effect of the tumour or its metastases are known as paraneoplastic disorders (Henson and Urich 1982). The Lambert-Eaton myasthenic syndrome is one of a group of neurological paraneoplastic disorders which includes subacute sensory neuropathy, cerebellar ataxia and opsoclonus (dancing eye syndrome). There is growing evidence that many of these disorders are caused by immunological cross-reactivity between the tumour and components of the target tissue. The most commonly associated tumour is small cell lung carcinoma (SCLC) which is thought to be neuroectodermal in origin (Pearse 1969). Neurological symptoms could, therefore, be produced by a cross-reactivity between tumour and neuronal antigens.

1.2.1. Clinical and electrophysiological features of LEMS

The clinical and electrophysiological features of 50 patients with LEMS have recently been reviewed (O'Neill et al 1988). The predominant clinical features of LEMS are proximal lower limb weakness, depressed tendon reflexes with post-tetanic potentiation and autonomic symptoms, in particular dryness of the mouth. LEMS is associated with SCLC in approximately 60% of cases. There are also occasional associations with tumours other than SCLC, but such occurrences may be fortuitous.

Electrophysiological tests of muscle from LEMS patients receiving a supramaximal nerve stimulus show a CMAP amplitude that is below the lower limit for normal controls. There is also an abnormal increase in this amplitude following maximal voluntary contraction of the muscle.

Studies of biopsied intercostal muscle have shown that the abnormality in LEMS is presynaptic, characterised by the reduced number of packets of acetylcholine (quanta) released from the nerve terminal after stimulation (Elmqvist and Lambert 1968). This reduction in endplate potential (epp) is not due to a defect in acetylcholine storage as levels of ACh in the nerve terminal do not differ from those of controls (Molenaar et al 1982). The quantal release of ACh is dependent on the entry of calcium into the nerve terminal. The resting non-quantal release of ACh, which is partly calcium-dependent, is also diminished in LEMS (Molenaar et al 1982). By contrast, the calcium-independent spontaneous release of transmitter (miniature endplate potential, mepp) is not significantly affected (Lambert and Elmqvist 1971). The abnormality in LEMS may, therefore, be explained by a presynaptic defect of calcium-dependent processes.

1.2.2. Autoimmune aetiology of LEMS

There is considerable evidence that LEMS is an autoimmune disorder (see review by Vincent et al 1989). Clinical evidence includes the association of LEMS with other diseases of autoimmune aetiology (Guttmann et al 1972, Lennon et al 1982, O'Neill et al 1988). O'Neill et al found that 34% of LEMS patients had a past or family history of an organ specific autoimmune disease. There are also associations with the major histocompatibility complex antigen HLA-B8 and with the IgG heavy chain marker Glm(2) suggesting an immunogenetic susceptibility to this disease (Willcox et al 1985). In addition, it has been shown that patients with LEMS respond to immunosuppressive drug therapy and to plasma

exchange, implying the involvement of a humoral factor (Newsom-Davis and Murray 1984).

The first experimental evidence for the presence of an autoantibody was provided by the results of passive transfer studies in mice (Lang et al 1981 and 1983). The IgG fraction of plasma from LEMS patients, injected into mice, reduced the CMAP amplitude and the quantal content of the endplate potential in the mouse diaphragm. The quantal content of the epp was studied over a range of calcium concentrations. At high concentrations the number of quanta released following nerve stimulation reached the same value as in control mice, suggesting that the number of available quanta was the same (Lang et al 1987). Further studies have shown that there is no effect of LEMS IgG on miniature endplate potentials and no evidence of postsynaptic deficit, nerve conduction failure or inability of the muscle to produce a response (Kim 1985, Kim 1986, Lang et al 1987). Thus the electrophysiological changes in mice are consistent with a reduction in the number of functional voltage-gated calcium channels (VGCCs) on the nerve terminal (Figure 1.1), resulting in a reduced level of calcium entry following nerve stimulation. The physiological effects of LEMS IgG in mice were maximal after a period of several days, coinciding with the rise of human IgG in mouse serum (Prior et al 1985, Lambert and Lennon 1988). By contrast, no immediate effect of IgG was observed on isolated mouse diaphragm for up to two hours (Prior et al 1985) or on <u>in vitro</u> preparations of rat and human neuromuscular junctions (Kim et al 1988). This implies a long-term effect of LEMS IgG on the nerve terminal.

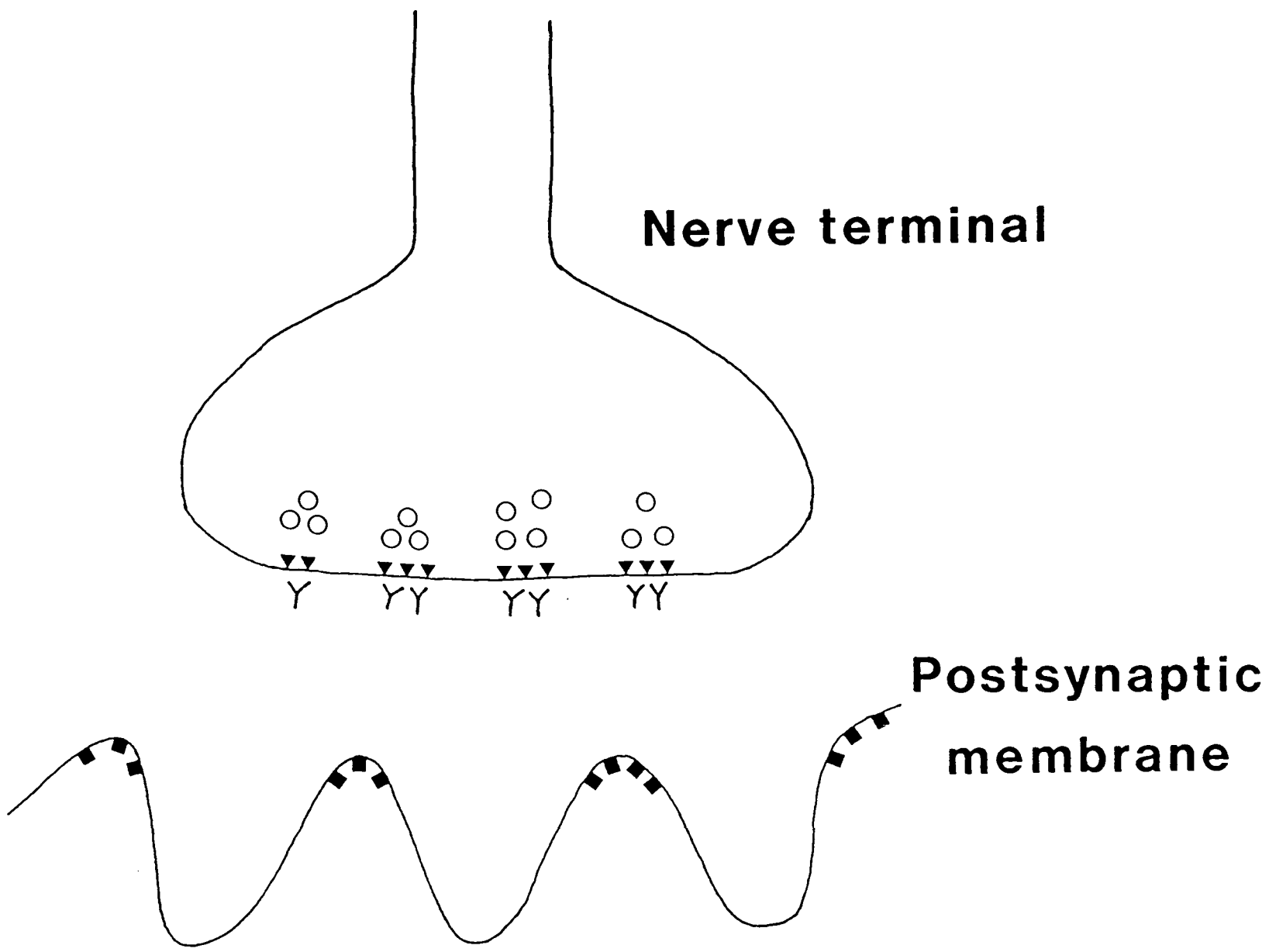


Figure 1.1: Localisation of VGCCs at the neuromuscular junction

Schematic representation of the neuromuscular junction showing the localisation of VGCCs on the presynaptic membrane of the nerve terminal. ▼ = VGCCs, O = synaptic vesicles, ■ = acetylcholine receptors, Y = LEMS IgG.

1.2.3. Morphological changes in LEMS

The freeze-fractured presynaptic membrane of the neuromuscular junction (NMJ) shows double parallel rows of particles at sites of synaptic vesicle release. These 'active zone particles' (AZPs) are thought to represent calcium channels (Pumplin et al 1981). Studies of biopsied intercostal muscle of LEMS patients showed a marked depletion of AZPs and a disruption of their normal array, while other presynaptic membrane particles were not affected (Fukunaga et al 1982) (Figure 1.2). Similar observations were made in freeze-fracture electromicrographs of muscle from mice treated with LEMS IgG (Fukunaga et al 1983), providing further evidence that the presynaptic calcium channel is the site of antibody attack in LEMS.

The mouse model has enabled the mechanism of action of LEMS IgG on AZPs to be investigated further. The initial alteration is a decrease in the distance between particles in a given row and between adjacent rows. The parallel orientation of the rows is then disturbed and the arrays become random clusters of particles (Fukuoka et al 1987) (Figure 1.2). These morphological changes are caused by divalent LEMS IgG and $F(ab')_2$, but not by monovalent Fab (Nagel et al 1988). The findings suggest that the two antigen-binding sites of the LEMS antibody cross-link adjacent AZPs which then aggregate into clusters. Particle density is then reduced by accelerated internalisation, ie., by the process of antigenic modulation. This mechanism agrees with the relative long-term effect of LEMS IgG mentioned above.

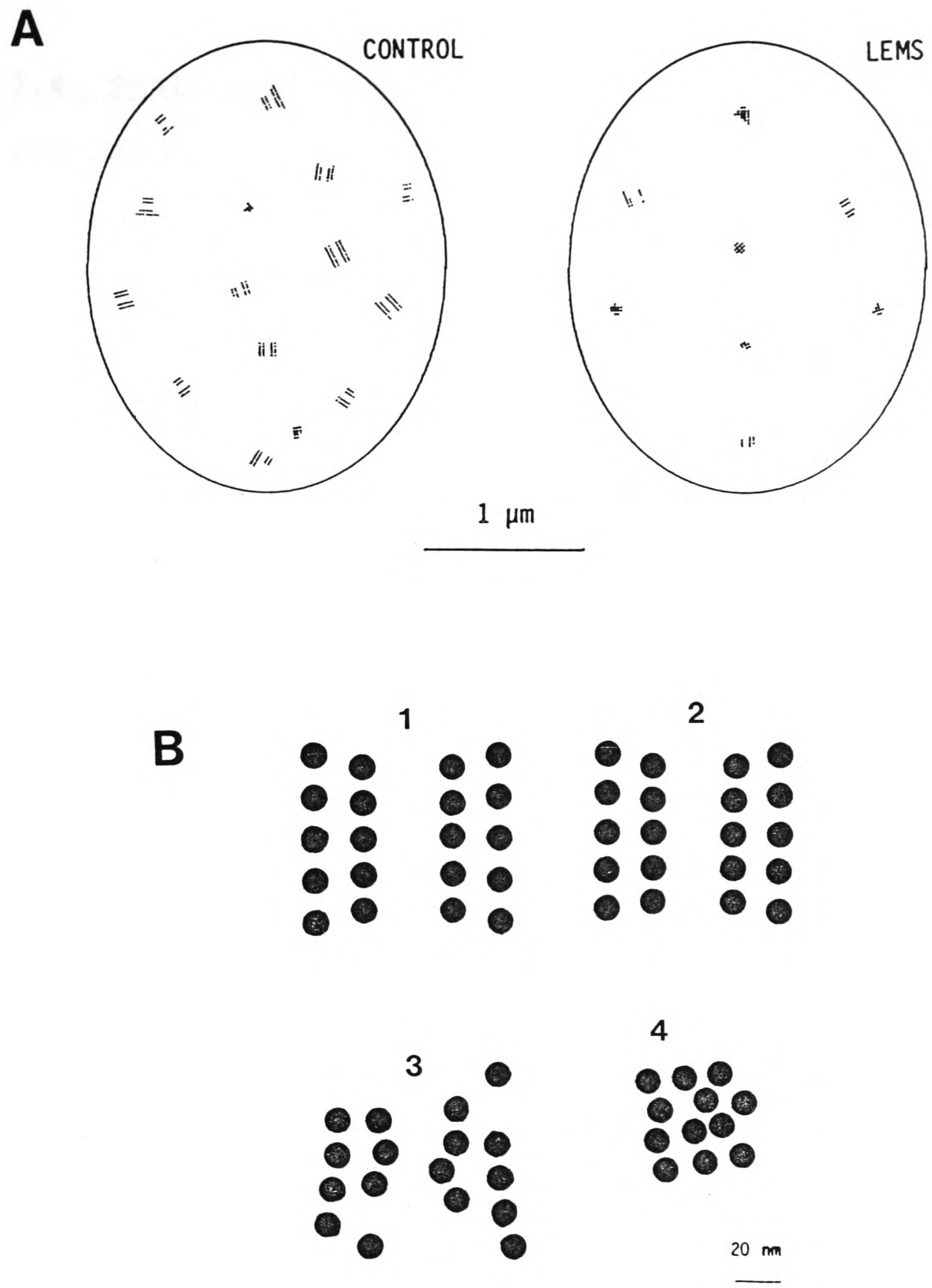


Figure 1.2: Modulation of VGCCs by LEMS IgG

(A) Reconstruction of control and LEMS presynaptic membranes showing disorganisation and paucity of active zone particles (Fukunaga et al 1982).

(B) Arrangement of AZPs in control mice (1) and mice treated with LEMS IgG (2-4). (2) shows a slight reduction of particle spacing, (3) shows a more pronounced aggregation and (4) shows a cluster (Fukuoka et al 1987).

1.2.4. Small cell lung carcinoma

The diagnosis of SCLC in 60% of LEMS patients is confirmed by histological analysis, revealing small, lymphocyte-like cells with characteristic large, granular nuclei and little cytoplasm. The cells contain dense neurosecretory vesicles which release peptides such as antidiuretic hormone, adrenocorticotrophic hormone, bombesin and neurone-specific enolase. They possess mechanisms for the uptake and decarboxylation of amine precursors (the APUD system), a characteristic of cells thought to be of neuroectodermal origin (Pearse 1969). They are also stained by the monoclonal antibody marker specific for human neuroectodermal tissue, UJ13A (Allan et al 1983).

The electrical excitability of cultured SCLC was demonstrated by the generation of short-duration action potentials (Tischler et al 1977, McCann et al 1981). The action potentials were inhibited by $MnCl_2$, an antagonist of calcium channels (McCann et al 1981). The presence of VGCCs in a cultured SCLC line was confirmed by Roberts et al (1985) who showed that depolarising the cells with potassium caused calcium influx that could be inhibited by the calcium antagonists nifedipine and methoxyverapamil.

The presence of SCLC in almost two thirds of LEMS patients implies an important role for this tumour in the pathogenesis of the disease. The neural characteristics of the tumour suggest that there may be crossreactive autoimmunity between neural antigens of the SCLC and the neuromuscular junction. It is possible that the immune response is triggered by tumour VGCCs and that the antibodies produced react with similar determinants at the motor nerve terminal. In support of this it has been shown that excision

or x-irradiation of the tumour in SCLC-LEMS results in improvement or remission of the neurological syndrome (Chalk et al 1990). The stimulus for the autoimmune response in LEMS patients with no detectable SCLC remains unknown.

1.2.5. Calcium flux studies

The demonstration of K^+-stimulated Ca^{2+} flux into cultured SCLC and other neuronal cell lines has provided a convenient model with which to study the effect of LEMS antibodies. When cells from the human SCLC line, MAR, were grown in the presence of IgG purified from the plasma of LEMS patients, the amount of K^+-stimulated Ca^{2+} flux was significantly reduced (Roberts et al 1985). This finding has been confirmed in other SCLC lines, some from patients with LEMS (De Aizpurua et al 1988), and in rodent neuronal cell lines (Lang et al 1989a). Further, it has been shown that the extent of inhibition of Ca^{2+} flux correlates with the disease severity of the LEMS patient (Lang et al 1989b). No inhibition of Ca^{2+} flux was detected until 24 hours after exposure of the cells to IgG and a maximum effect was seen after four days (De Aizpurua et al 1988). The results are consistent with the proposed modulatory effect of LEMS antibodies, causing a reduction in the number of functional VGCCs.

1.3. Voltage-gated calcium channels

VGCCs are activated in response to changes in membrane potential. They are found in most excitable tissues including cardiac muscle, smooth muscle, skeletal muscle and neurones. They are also present on secretory cells such as anterior pituitary cells, and 'non-excitable cells' such as glial cells. It has long been recognised that multiple VGCC subtypes exist, sometimes within a single cell. The evidence has predominantly been provided by electrophysiological measurements including whole cell or single channel recordings using the patch clamp technique.

1.3.1. Classification of VGCCs

Two types of VGCC have been described in smooth muscle, skeletal muscle and cardiac tissue (Bean 1989a). One type, activated by small membrane depolarisations and rapidly inactivating, has been termed the 'T' (transient) channel, low threshold or low voltage-activated (LVA) channel. The second type requires larger depolarisations and has a higher conductance and is known as the 'L'(long-lasting) channel, high threshold or high voltage-activated (HVA) channel. L channels are inhibited by the dihydropyridine (DHP) calcium channel blockers such as nifedipine and nitrendipine, whilst T channels are unaffected by these drugs. There may be differences in the characteristics of VGCCs between tissues; for instance, L channels in vascular smooth muscle are several times more sensitive to DHP calcium antagonists than those in cardiac cells.

A third VGCC subtype has been described in neuronal tissue. Whole cell voltage recordings showed the existence of LVA and HVA

calcium channels in mammalian CNS neurones (Llinas and Yarom 1981) and in chick dorsal root ganglion (DRG) neurones (Carbone and Lux 1984). With single channel recordings of barium currents in chick DRG neurones it was possible to distinguish between two types of HVA channels, which were termed L and N (N for neither T nor L, or neuronal channels, Nowycky et al 1985). Differences between the three types of VGCC in DRG neurones are based on both their electrical and pharmacological properties (summarised by Miller 1987 and Tsien et al 1988) and can be described as follows:

L-type channels

These carry large currents and contribute to a long-lasting current that is activated by strong depolarisations from relatively depolarised holding potentials. They are DHP-sensitive and are also blocked by the 27-amino acid peptide ω-conotoxin (ωCgTx) from the marine fish-eating snail, conus geographus, although this block is sometimes incomplete.

T-type channels

T channels carry small, transient currents that are elicited only from negative holding potentials. They require only weak depolarisations for activation. They are DHP-resistant and only weakly and reversibly blocked by ωCgTx.

N-type channels

These are favoured by negative holding potentials but require strong depolarisations for activation. They are intermediate in channel conductance and inactivation rate between T and L channels. They are DHP-resistant but persistently blocked by ωCgTx.

Table 1.1 summarises the electrical and pharmacological properties of T, L and N channels in chick DRG neurones, although the precise properties of these channel subtypes vary between preparations. Their properties may also be different in other cell types, for example HVA channels in cultured human neuroblastoma cells have been subdivided on the basis of their sensitivity to DHPs and ωCgTx, but electrophysiologically they were indistinguishable (Carbone et al 1990). The DHP-sensitive component of the calcium current in these cells was not affected by ωCgTx, thus suggesting that ωCgTx does not act on L channels in all neurones.

Table 1.1

Electrical and pharmacological properties of VGCC subtypes in chick DRG neurones (from Tsien et al 1988).

	Channel type		
	T	N	L
Single channel conductance	8pS	13pS	25pS
Relative conductance	$Ba^{2+} = Ca^{2+}$	$Ba^{2+} > Ca^{2+}$	$Ba^{2+} > Ca^{2+}$
Cation block	$Ni^{2+} > Cd^{2+}$	$Cd^{2+} > Ni^{2+}$	$Cd^{2+} > Ni^{2+}$
ωCgTx block	Weak	Persistent	Persistent
DHP sensitivity	Resistant	Resistant	Sensitive
Activation (mV)	+ve to -70	+ve to -20	+ve to -10
Inactivation (mV)	-100 to -60	-120 to -30	-60 to -10
Inactivation rate	Rapid (20-50 ms)	Moderate (50-80 ms)	Very slow (>500 ms)

1.3.2. Function of neuronal VGCCs

Attempts have been made to associate the subtypes of neuronal VGCC with particular biological functions. Some studies have suggested that N-type channels may play a dominant role in neurotransmitter release. For example, potassium-evoked noradrenaline release in rat sympathetic neurones was reduced by ωCgTx but not by the DHP nitrendipine (Hirning et al 1988). Also, ωCgTx-labelled channels have been localised at transmitter release sites of frog neuromuscular synapses (Robitaille et al 1990). However, another DHP, nicarpidine, has been shown to suppress potassium-induced transmitter release from cultured neuronal cells (chick embryonic neural retina and rat pheochromocytoma, Takahashi and Ogura 1983). Miller (1987) has observed that in sympathetic neurones from the rat superior cervical ganglion, neurotransmitter release is not normally blocked by DHPs. However transmitter release can be enhanced by the agonist DHP, BAY K 8644. This extra release could be inhibited by nitrendipine. Miller suggested that there are clusters of VGCCs at active zones of neurotransmitter release on the nerve terminal and that these channels are of N-type. L-channels located elsewhere, such as on the cell soma, would only play a part in transmitter release in certain circumstances, such as after enhancement by an agonist. 'Hot spots' of calcium channels of one particular subtype have been reported, for example N channels in DRG neurones (Fox et al 1985). Such clustering may imply a specific function for those channels. Calcium influx through L channel hot spots near the neural growth cones of cultured neuroblastoma cells has been shown to cause local morphological changes, suggesting the involvement of L

channels in growth and development of neurites (Silver et al 1990).

The defect in LEMS appears to be due to a loss of VGCCs involved in neurotransmitter release. Whole-cell patch clamp recordings of calcium currents in a rodent cell line demonstrated that LEMS IgG selectively blocked L-type channels whilst having no effect on T channels (Peers et al 1990). The same technique has shown that LEMS IgG inhibits VGCCs in isolated bovine adrenal chromaffin cells, which are also thought to be L-type (Kim and Neher 1988). However, the presence of N-type VGCCs was not demonstrated in these preparations and therefore the effect of LEMS IgG on N channels has not been determined.

1.3.3. The dihydropyridine receptor

The highest concentration of calcium channels in any tissue is to be found in the transverse tubules (t-tubules) of skeletal muscle. These are DHP-sensitive and mediate very slowly activated, long-lasting calcium currents and are, therefore, of L type. A fast-activated T-type current has also been demonstrated in intact mammalian and frog muscle fibres (Beaty et al 1987). However most biochemical studies of the properties of VGCCs have used the L channels of skeletal muscle due to their high density and availability for purification.

The high affinity and specificity of DHPs for their binding sites has made them suitable molecular probes for the purification of calcium channels. The solubilisation of DHP receptors from rabbit skeletal muscle membranes has been performed using [^{3}H]-nitrendipine (Borsotto et al 1984, Curtis and Catterall 1984)

and its analogue [^{3}H]-PN200-110 (Borsotto et al 1985). After purification by anion exchange, lectin affinity and sucrose gradient sedimentation, followed by analysis by gel electrophoresis, it was found that the DHP-receptor complex was composed of at least three noncovalently linked polypeptides (α,ß,γ; approximate molecular weights 170, 50 and 30 kDa respectively). It has since been found that there are two distinct high molecular weight polypeptides, one of which is a disulphide-linked complex of two subunits which were previously thought to be breakdown products (Takahashi et al 1987, Vaghy et al 1987). An oligomeric structure for the t-tubule calcium channel was, therefore, proposed by Takahashi et al (1987) comprising the α_1 subunit (175 kDa), α_2 (143 kDa), δ (27kDa), ß (54kDa) and γ (30kDa) (see Figure 1.3). The α_2 and δ subunits are linked by a disulphide bond and thus appear on non-reducing gel electrophoresis as a larger single polypeptide of 170 kDa. The α_1 subunit, which contains the largest hydrophobic domains, was proposed to be the central ion channel-forming component of the complex, by analogy with the α subunit of the sodium channel. The α_1 subunit contains the binding sites for the DHPs (Takahashi et al 1987) and also for the other major calcium antagonists, the phenylalkylamines such as verapamil, the benzothiazepine diltiazem, and bepridil (Galizzi et al 1986, Vandaele et al 1987). Radioligand binding studies show that there are separate binding sites for DHPs, verapamil and diltiazem, but that there are allosteric interactions between them (Goll et al 1983, Borsotto et al 1984). Thus verapamil and diltiazem inhibit and stimulate DHP binding respectively, but there is no direct competition between these drugs for binding site occupancy.

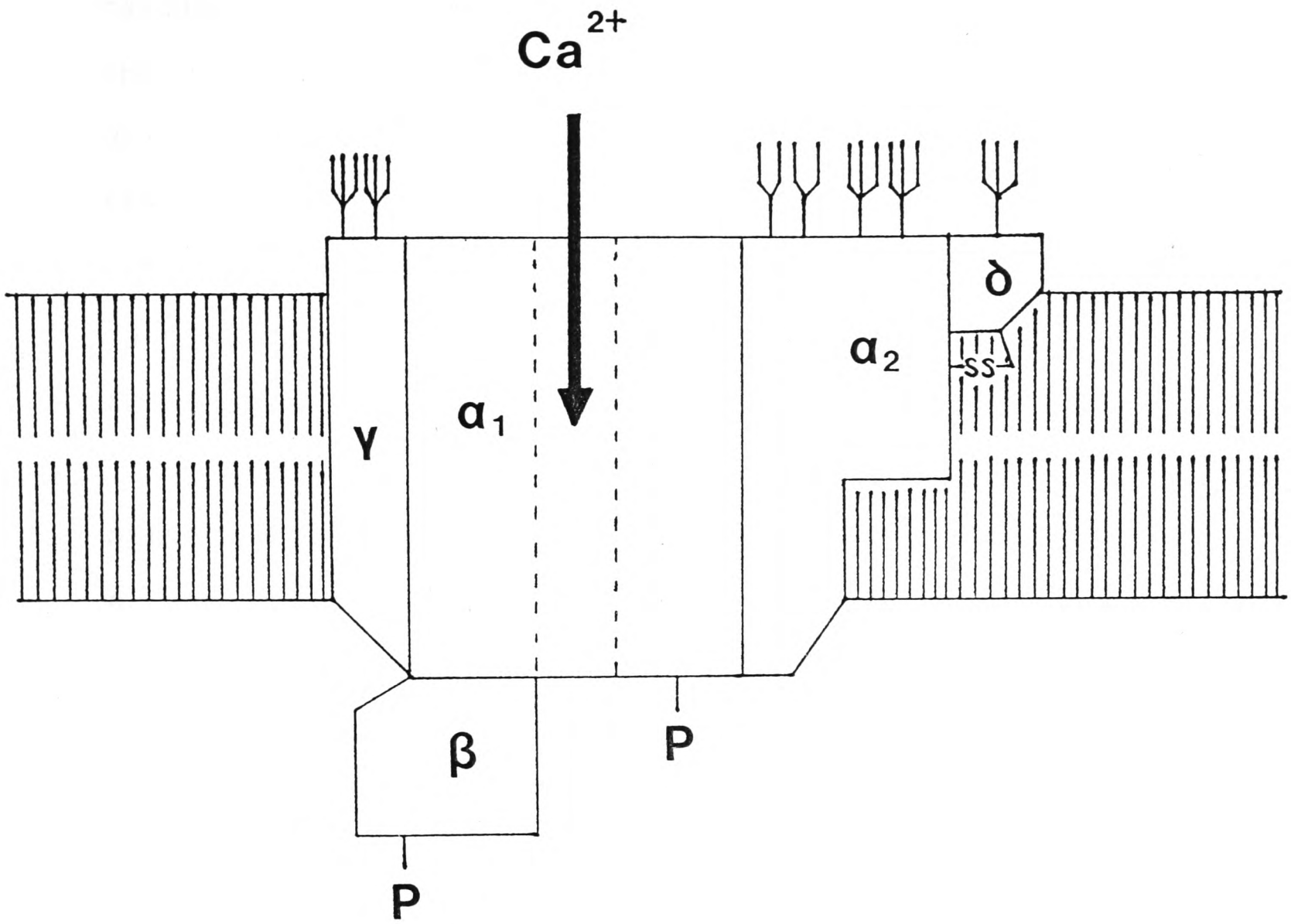


Figure 1.3: Subunit structure of the skeletal muscle VGCC

Representation of the subunit structure and transmembrane organisation of calcium channels purified from t-tubules of rabbit skeletal muscle (adapted from Takahashi et al 1987).

Ψ = glycosylation sites, P = phosphorylation sites,

-SS- = disulphide bond.

Polyclonal antibodies raised against purified skeletal muscle calcium channels were shown to be specifically directed against the α subunits, but the ß and γ subunits were coprecipitated, demonstrating the specific association of these polypeptides in the purified channel (Takahashi and Catterall 1987a). Furthermore, there was some immunoreactivity with these antibodies for purified cardiac calcium channels, indicating that the L channels of these two tissues have some epitopes in common.

Complementary DNA clones have been used to deduce the primary structure of the DHP-sensitive channel of skeletal muscle (Tanabe et al 1987, Ellis et al 1988). The α_1 subunit shows structural and sequence homology with other voltage-dependent ion channels. It has four domains containing multiple hydrophobic areas, thought to correspond to four transmembrane regions as in the sodium channel (Figure 1.4). By contrast, the α_2 subunit shows no homology to other known protein sequences and is predominantly hydrophilic. mRNA hybridisation studies suggest that the α_1 subunit is relatively specific to skeletal muscle, whereas the α_2 transcript could be detected in heart, smooth muscle and brain (Ellis et al 1988). Recent cloning of the cardiac DHP receptor, however, has shown 66% sequence homology with its skeletal muscle counterpart and suggests a similar transmembrane structure (Mikami et al 1989).

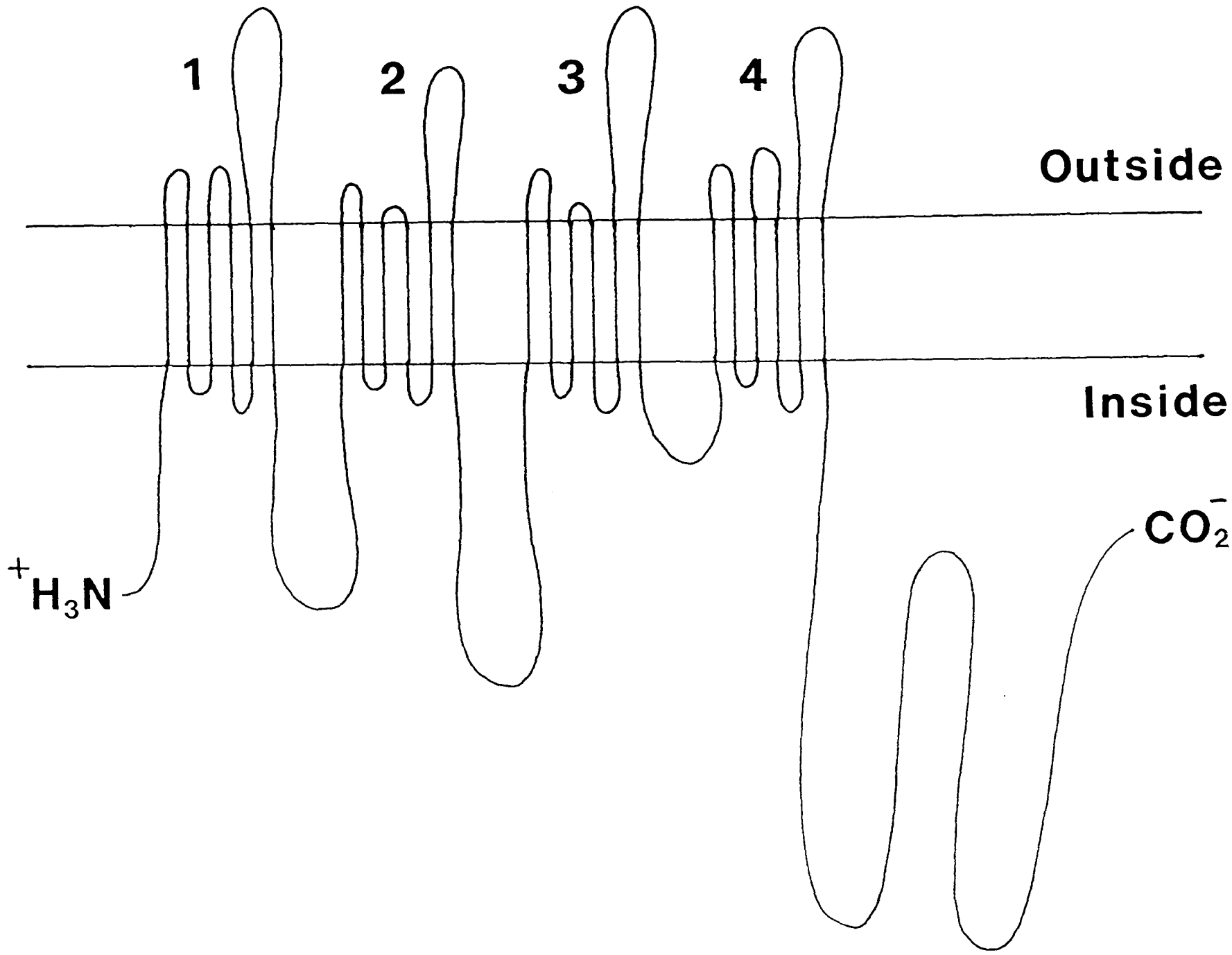


Figure 1.4: Primary structure of the calcium channel α_1 subunit

Proposed structure of the α_1 subunit of the rabbit skeletal muscle calcium channel showing the four transmembrane regions (adapted from Catterall 1988).

Expression studies suggest that the α_1 subunit of both skeletal muscle and heart can function as an ion channel without the presence of the other calcium channel subunits (Perez-Reyes et al 1989, Mikami et al 1989). However transfection of the α_1 subunit cDNA alone into murine cells produced a larger protein than the skeletal muscle protein and resulted in much slower calcium currents (Perez-Reyes et al 1989). This suggests that the α_1 subunit must associate with one or more of the other subunits for correct expression. Co-transfection of the α_2 subunit cDNA in Xenopus oocytes increased the level of calcium channel activity (Mikami et al 1989), indicating a modulatory role for the α_2 subunit.

High affinity binding sites for [^{3}H]-nitrendipine and [^{3}H]-PN200-110 have been described in several neuronal tissues including rat brain (Lee et al 1984, Weiland and Oswald 1985), chick brain (Cruz et al 1987), rat pheochromocytoma cells (Takahashi and Ogura 1983) and bovine chromaffin cells (Ballesta et al 1989). However, due to the relatively low density of neuronal DHP receptors their purification and characterisation has proved more difficult than for the skeletal muscle DHP receptor. Table 1.2 compares the levels of DHP binding in neurones with skeletal muscle and other tissues.

Polyclonal antibodies against the α subunits of rabbit skeletal muscle L channels immunoprecipitated DHP-labelled calcium channels of both muscle and brain (Takahashi and Catterall 1987b) suggesting some similarities in the calcium channels of these tissues. The antibodies specifically recognised a large peptide

from rabbit brain membranes of molecular weight 169 kDa (140 kDa after reduction of disulphide bonds) that resembled the α_2 subunit of skeletal muscle. A monoclonal antibody raised against chick synaptic membranes has identified two polypeptides of 193kDa and 130kDa as the main components of the neuronal DHP-sensitive calcium channel (Takahashi and Fujimoto 1989). These may be analogous to the α_1 and α_2 subunits respectively of the skeletal muscle L channel. A full characterisation, however, of all the subunits of the neuronal L channel has yet to be carried out.

Table 1.2

Comparison of DHP binding parameters in different tissues

DHP	Species	Tissue	B_{max} (fmol/mg)	K_D (nM)
[^{3}H]-nimodipine	Guinea pig	Sk. muscle	80,000	3.6[a]
	Guinea pig	Heart	350	0.26[a]
	Rat	Heart	400	0.24[a]
	Human	Heart	100	0.28[a]
	Guinea pig	Brain	570	0.62[b]
[^{3}H]-nitrendipine	Rabbit	Sk. muscle	56,000	1.7[b]
	Guinea pig	Ileum	1,100	0.16[b]
	Rabbit	Heart	335	0.14[b]
	Guinea pig	Heart	122	0.29[b]
	Rat	Heart	176	0.76[c]
	Rat	Brain	255	0.37[c]
[^{3}H]-PN200-110	Guinea pig	Sk. muscle	20,600	1.4[a]
	Guinea pig	Ileum	820	0.04[b]
	Rat	Heart	144	0.06[c]
	Rat	Brain	209	0.03[c]

[a] = Glossman et al 1984

[b] = Triggle and Janis 1987

[c] = Lee et al 1984

1.3.4. The ω-conotoxin receptor

The conotoxins are a group of small peptides found in the venom of the predatory marine cone snails, Conus. There are approximately 500 members of the Conus species and each uses a diverse array of toxins with which to paralyse and capture its prey. Only a few of these toxins have been characterised but they all seem to be targeted to ion channels and receptors in the neuromuscular system (reviewed by Olivera et al 1985 and 1990). Conotoxins are cysteine rich peptides and have a very high density of disulphide bonds, providing them with rigid conformations necessary for targeting to specific receptors with very high affinity (Woodward et al 1990).

The venom of the fish-hunting cone snail, Conus geographus, contains peptides that act on voltage-gated calcium channels (ω-conotoxins), sodium channels (μ-conotoxins), acetylcholine receptors (α-conotoxins), NMDA receptors ('sleeper' peptides), vasopressin receptors and many more with unknown targets (Olivera et al 1990). ω-conotoxin GVIA (ωCgTx) was purified and sequenced by Olivera et al (1984) and is a basic 27 amino acid peptide with three disulphide bridges. Its sequence is as follows:

Cys-Lys-Ser-Hyp-Gly-Ser-Ser-Cys-Ser-Hyp-
Thr-Ser-Tyr-Asn-Cys-Cys-Arg-Ser-Cys-Asn-
Hyp-Tyr-Thr-Lys-Arg-Cys-Tyr

ωCgTx was shown to block irreversibly stimulus-evoked transmitter release at the frog skeletal neuromuscular junction and to block calcium entry into chick DRG neurones (Kerr and Yoshikami 1984). The specificity of ωCgTx for neuronal VGCCs is demonstrated by the inhibition of HVA channels in sensory,

sympathetic and hippocampal neurones of vertebrates but not in cardiac, skeletal or smooth muscle cells (McCleskey et al 1987) (Table 1.3). This specificity and the virtual irreversibility of action of ωCgTx has provided a powerful tool for the biochemical study of neuronal calcium channels.

Table 1.3

The sensitivity of VGCCs to ωCgTx in different tissues

(from McCleskey et al 1987)

Cell type	VGCC type	DHP block	ωCgTx block
Chick DRG	L	+	Persistent
	N	-	Persistent
	T	-	Weak, reversible
Rat hippocampal	L	+	Persistent
Rat sympathetic	L	+	Persistent
	N	-	Persistent
Frog atrial	L	+	None
	T	-	Weak, reversible
Frog ventricular	L	+	None
Guinea pig ventricular	L	+	None
Rabbit smooth muscle	L	+	None

High affinity and irreversible ^{125}I-ωCgTx binding has been described in chick brain (Cruz and Olivera 1986, Barhanin et al 1988), rat brain (Barhanin et al 1988, Marqueze et al 1988), cultured rat neurones (Marqueze et al 1988), bovine chromaffin cells (Ballesta et al 1989) and rat pheochromocytoma and human neuroblastoma cell lines (Sher et al 1988). There is no competition between ωCgTx and either nitrendipine or verapamil binding, suggesting that ωCgTx binds to a site separate from both the DHP and phenylalkylamine target sites.

^{125}I-ωCgTx binding could not be detected in chick cardiac or skeletal muscle, both of which had demonstrable [^{3}H]-nitrendipine binding (Cruz et al 1987). Combined with the electrophysiological data of McCleskey et al(1987), this implies a difference between the L channels of muscle and nerve. Cruz et al(1987) proposed to call the ωCgTx-sensitive channels in neurones L_n, and the ωCgTx-insensitive channels in muscle L_m. There are more binding sites for ωCgTx than for DHPs in chick brain due to the combination of binding to L_n and N channels. However, as mentioned above, ωCgTx does not affect L channels in all neurones, therefore this subdivision may not always be appropriate.

ωCgTx receptors have been solubilised and purified from brain membranes and attempts made to identify the proteins associated with this receptor. In rat brain, polypeptides of 300kDa (Rosenberg et al 1989), 222 and 25-35kDa (Marqueze et al 1988) and 310, 230 and 34kDa (Abe and Saisu 1987) have been described in association with the ωCgTx binding site. In chick brain a polypeptide of 135kDa was labelled by ωCgTx (Cruz et al 1987). Another study identified a polypeptide of 210-220kDa and another

of 170kDa which was reduced to two components (140 and 30kDa) after breakage of disulphide bonds (Barhanin et al 1988). This last finding is reminiscent of the α_2 subunit of the skeletal muscle L channel, and may be a component of the neuronal L channel, while the larger component may be part of the N-type channel. No subunit structure to link all of the above findings has yet been postulated for neuronal ωCgTx-sensitive calcium channels.

In addition to the effects on neuronal VGCCs mentioned above, ωCgTx has been found to inhibit K^+-stimulated Ca^{2+} uptake in SCLC lines (De Aizpurua et al 1988). The properties of ωCgTx binding, in particular its irreversibility, have led to its recent application in serological tests for the detection of LEMS antibodies. It has been reported that some LEMS sera immunoprecipitate ωCgTx-labelled VGCCs solubilised from human SCLC lines (Lennon and Lambert 1989) and human neuroblastoma cell lines (Sher et al 1989, Leys et al 1989 and 1991). These reports provide the first direct evidence that the target of some LEMS antibodies is the neuronal VGCC.

1.4. Aims of project

1.4.1. Potassium-stimulated calcium flux in neuronal cell lines

The uptake of radiolabelled calcium in cultured cells after depolarisation of the membrane by high potassium concentrations provides a useful system for the study of voltage-gated calcium channels. It has already been mentioned that LEMS IgG reduces the amount of K^+-stimulated Ca^{2+} influx in various cell lines, probably by down-regulating the number of functional VGCCs. However, very little pharmacological analysis of the VGCC subtypes present on these cells has been carried out. The first part of this project was concerned with establishing the presence of VGCCs on several cell lines, all thought to be of neural origin, using the technique of K^+-stimulated Ca^{2+} influx. Calcium antagonists were then used to investigate the VGCC subtypes involved in the Ca^{2+} flux thus measured.

1.4.2. Calcium antagonist binding to neuronal cell membranes

Receptor binding studies with radiolabelled calcium antagonists offered an alternative method of detecting the presence of VGCCs on the neuronal cell lines studied. The radioligands [^{3}H]-PN200-110 and ^{125}I-ωCgTx were, therefore, used to measure the level of expression of DHP and ωCgTx binding sites, respectively. The effect of LEMS IgG on the number of ^{125}I-ωCgTx binding sites was studied in order to confirm that VGCCs are the target of attack in LEMS.

1.4.3. Immunoprecipitation of VGCCs by LEMS serum

The Ca^{2+} flux assay is impractical for the routine detection of LEMS antibodies in individual patients. It was, therefore, decided to use solubilised ^{125}I-ωCgTx-labelled VGCCs from a suitable neuronal cell line as the basis for an immunoprecipitation assay to detect anti-VGCC antibody activity. The aim was to study sera from a large number of LEMS patients and to compare the results with those from a wide range of controls, including healthy individuals and patients with other neurological or immunological disorders. The potential use of such an assay as a diagnostic test for LEMS is discussed.

Summary The aims of this project were:

(1) to investigate the VGCC subtypes present on neuronal cells by Ca^{2+} influx studies and radioligand binding (2) to study the effect of LEMS IgG on these channels and (3) to develop an immunoprecipitation assay to detect the presence of anti-VGCC antibodies in LEMS serum.

CHAPTER 2

MATERIALS AND GENERAL METHODS

2.1 Materials

All cell culture media, trypsin/ethylenediaminetetraacetic acid (EDTA) solution, hypoxanthine-aminopterin-thymidine (HAT) supplement, L-glutamine, penicillin, streptomycin, newborn calf serum, horse serum, Hepes buffer, culture flasks and plates were from Gibco (Life Technologies Ltd). Foetal calf serum (FCS) was from Imperial Laboratories (Europe) Ltd, poly-L-lysine from Sigma Chemical Co. Ltd and phosphate buffered saline (PBS Dulbecco 'A') from Oxoid Ltd. $^{45}CaCl_2$ (18.4 mCi/mg Ca), [^{3}H]-PN200-110 (85 Ci/mmol), ^{125}I-ωCgTx (2000 Ci/mmol) and the enzyme-linked immunosorbent assay (ELISA) kit were obtained from Amersham International Plc, standard human IgG and sheep anti-human IgG from Seward Laboratories and goat anti-human IgG from Lawrence Laboratories. Unlabelled ωCgTx was from Peninsula Laboratories.

Trizma base, Tween 20, 6,9-diamino-2-ethoxy-acridine lactate (Rivanol reagent), bovine serum albumin (BSA), pepstatin, leupeptin, phenylmethylsulphonylfluoride (PMSF), soybean trypsin inhibitor, polyethyleneimine (PEI), verapamil, methoxyverapamil (D600), diltiazem, dibutyryl cyclic AMP and $CoCl_2$ were from Sigma. Nitrendipine and nifedipine were gifts from Bayer UK Ltd. $MnCl_2$ was from Fluka Chemicals Ltd. Hartmanns solution (102mM NaCl, 29mM sodium lactate, 5mM KCl, 2mM $CaCl_2$) was from the hospital pharmacy. Folin and Ciocalteu's phenol reagent and all other chemicals were from BDH Ltd.

Scintillation fluid was obtained from Pharmacia LKB, scintillation tubes from L.I.P. Ltd, LP4 tubes from Luckham Ltd and GF/C filters from Whatman.

2.2 Methods

2.2.1 Cell culture

Details of the origin and culture of the cell lines used in these studies are summarised in Table 2.1. All of the cell lines, with the exception of the MAR5 line, grew as adherent monolayers and were routinely grown in 800ml (surface area 175cm^2) tissue culture flasks containing 50mls of the relevant culture medium. Flasks of cells were grown to confluence before passaging. At confluence, the cells were transferred to new flasks at a ratio of one confluent flask to between 3 and 6 new flasks. The NG108, F21D1 and PC12 cultures were removed from the old flasks manually with a jet of medium from a syringe, while the SKNSH, Kelly and IMR32 cells were dispersed chemically by incubation with 10mls Trypsin (0.05%)/EDTA (0.02%) solution in phosphate buffered saline (PBS). After 5 minutes incubation these cells were diluted with 10mls culture medium to neutralise the effects of the trypsin-EDTA solution. The cells were then transferred into 50ml centrifuge tubes and spun down at 1000rpm for 5 minutes (MSE Centaur 2). Cells were resuspended in 10-20mls fresh medium and divided into the new flasks. Cells that had been exposed to trypsin tended to clump at this stage and were dispersed into single cell suspensions by passing through a 21 gauge (0.8mm) needle and then aliquoted into the new flasks. The medium in each flask was made up to 50mls and the flasks placed in an incubator. The MAR5 cells,

Table 2.1

Origin and culture conditons of cell lines studied

Cell line	Origin	Culture medium[a]	Subculture	Reference	Source
SKNSH	Human neuroblastoma	RPM1 1640 with L-glutamine (300 mg/l) 10% FCS 5% CO_2/37°C	1:3 every 3-4 days Dispersed with Trypsin (0.05%)/ EDTA (0.02%)	Biedler et al 1973	Dr L. Lashford Institute of Child Health, London
IMR32	Human neuroblastoma	Eagle's MEM with non-essential amino acids and Earle's BSS 10% FCS 5% CO_2/37°C	1:3 every 3-4 days Dispersed with Trypsin/EDTA	Tumilowicz et al 1970	American Type Culture Collection
KELLY	Human neuroblastoma	RPMI 1640 with L-glutamine 10% FCS 5% CO_2/37°C	1:3 every 3-4 days Dispersed with Trypsin/EDTA	Schwab et al 1983	Dr L. Lashford Institute of Child Health, London
NG108	Mouse neuroblastoma/ rat glioma hybrid	Dulbecco's MEM with 25mM Hepes and 4500mg/1 glucose 10% FCS 2mM L-glutamine HAT supplement 10% CO_2/37°C	1:3 every 3-4 days Dispersed manually	Nelson et al 1976	Dr F. Walsh Institute of Neurology Queen's Square, London

Cell line	Origin	Culture medium[a]	Subculture	Reference	Source
F21D1	Mouse neuroblastoma/ human dorsal root ganglion hybrid	Dulbecco's MEM with 25mM Hepes and 4500mg/l glucose 10% FCS 2mM L-glutamine HAT supplement 10% CO_2/37°C	1:3 every 3-4 days Dispersed manually	Dickson et al 1983	Dr F. Walsh Institute of Neurology, Queen's Square, London
PC12	Rat adrenal pheochro-mocytoma	Dulbecco's MEM 10% Newborn calf serum 10% Horse serum 2mM L-glutamine 0.3% glucose 5% CO_2/37°C	1:3 every 4-5 days Dispersed manually	Greene and Tischler 1976	American Type Culture Collection
MAR5	Human small cell lung carcinoma	RPMI 1640 with L-glutamine 10% FCS 5% CO_2/37°C	1:2 every 4 days Dispersed with 0.02% EDTA	Ellison et al 1976	Dr M. Ellison Ludwig Institute, London

[a] Each culture medium additionally contained 50U/ml penicillin and 50µg/ml streptomycin.

RPMI = Roswell Park Memorial Institute media.

MEM = minimum essential medium

BSS = balanced salt solution

HAT = hypoxanthine (100 µM), aminopterin (0.4 µM) and thymidine (16 µM)

used for binding and immunoprecipitation assays, were kindly provided by Irene Johnston, Institute for Molecular Medicine, Oxford.

At the beginning of each series of experiments several aliquots of cells were frozen in culture medium containing 20% FCS and 10% dimethylsulphoxide (DMSO) by the following procedure. Confluent flasks of cells were spun down as above, the culture medium removed and the tubes placed on ice. Each cell pellet was resuspended in 0.5mls cold medium containing 20% FCS. Medium containing 20% FCS and 20% DMSO was prepared at room temperature, 0.5mls added to each tube and the contents mixed. The cells were then placed in freezing vials and frozen slowly by placing them in a polystyrene box at -70°C for 24 hours. They were then stored under liquid nitrogen until required. Cells were thawed by immersion in a water bath at 37°C and transferred to a culture flask to which warmed medium was added slowly. They were then cultured as described above. Experiments were carried out with cells from the third passage after freezing onwards. Cells were discarded after 20 passages and a further aliquot from the same batch of frozen cells was used.

2.2.2. Measurement of protein concentration

Protein concentration was determined by an adaptation of the method of Lowry et al (1951) using BSA as the standard protein. Tubes were set up containing 250µl BSA (between 25 and 200 µg/ml) and several dilutions of each test sample. A solution composed of 1ml 1% copper sulphate, 1ml 2% sodium potassium tartrate and 98mls 2% sodium carbonate in 0.1M NaOH was freshly prepared. 1ml of this

solution was added to each tube, mixed and left for 10 minutes. 50µl of Folin and Ciocalteu's phenol reagent was then added, mixed and left for a further 30 minutes. The absorbance of each sample was measured at 550nm in a digital ultraviolet spectrophotometer (Cecil, CE292) and a standard curve constructed by plotting concentration of BSA against absorbance. The concentrations of the test samples were read directly from this standard curve.

2.2.3. Preparation of IgG from plasma by the Rivanol method

Plasma from known LEMS patients and those with other neurological or immunological diseases was obtained after therapeutic plasma exchange and stored at -20°C until use. Immunoglobulin was prepared as described elsewhere (Horejsi and Smetana 1956). Plasma was filtered and mixed with distilled H_2O and 3% Rivanol reagent in the ratio 1 litre plasma to 690mls dH_2O and 650mls Rivanol. Also added were 2-3 drops octanol to prevent frothing. After 2 hours a large precipitate was formed which was removed by filtration. NaCl (5% w/v) was then added to the filtrate and stirred overnight at 4°C. This solution was filtered, solid ammonium sulphate was added (50% w/v), stirred for 2 hours and spun at 12,000rpm (MSE Europa 24M) for 45 minutes. The pellet was redissolved in dH_2O to the original volume. Ammonium sulphate (45% w/v) was added, the solution stirred for 2 hours and recentrifuged. The final pellet was then dissolved in the minimum amount of dH_2O and dialysed at 4°C against 4 litres Hartmanns solution (p43); this was changed twice over 3 days. The dialysate was spun at 12,000rpm for 1 hour, sterilised by filtration through 0.45µm filters and stored in aliquots at -20°C.

2.2.4. Measurement of IgG concentration

IgG concentration was estimated using an enzyme-linked immunosorbent assay (ELISA). 96-well microtitre plates were coated with 100µl/well sheep anti-human IgG, diluted 1:1000 with 0.1M Tris buffer pH 10, and left overnight at 4°C. The plate was washed 3 times with PBS-Tween (0.1% v/v Tween 20 in PBS, pH 7.5). Non-specific sites were blocked by incubating with 1% BSA in PBS (100µl/well) for 1 hour at room temperature.

After washing as before, 50µl/well standard IgG diluted in PBS-Tween was added to give a concentration range of 0-100ng/well. Test IgGs at appropriate dilutions were also added, and the plate incubated for 2 hours at 37°C.

The plate was washed and 50µl/well beta-galactosidase-linked sheep anti-human Ig was added (diluted 1 in 500 in PBS containing 0.1% v/v Tween 20, 10mM $MgCl_2$ and 1mM 2-mercaptoethanol). This was incubated for 1 hour at 37°C.

After washing, 100µl/well of the substrate, ortho-nitrophenyl-beta-D-galactopyranoside (1mg/ml in PBS containing 10mM $MgCl_2$ and 0.1M 2-mercaptoethanol) was added and incubated at 37°C until a yellow colour had developed (usually 1-2 hours). The reaction was stopped by the addition of 50µl/well 1M Na_2CO_3 and the absorbance read at 410nm.

Each ELISA contained 4 dilutions of each test IgG and a known IgG standard (10mg/ml) as an internal control.

2.2.5. Membrane preparation

Cells were cultured and harvested at confluence as described above. After centrifugation for 5 minutes at 1000rpm, culture

medium was removed and the cells were resuspended in PBS. They were recentrifuged and the final cell pellet stored at -70°C until required. Batches of membranes were prepared from the cells of 25-30 confluent flasks. They were thawed and resuspended in 10mls ice-cold buffer (25mM Tris-HCl, 5mM Hepes, 0.32M sucrose, 1µM pepstatin, 2µM leupeptin, 0.1mM PMSF, 20µg/ml soybean trypsin inhibitor, pH 7.4). The cells were homogenised with a Polytron PT10-35 homogeniser (Kinematica GmbH Littau, Switzerland) at setting 6 for 10 seconds, the volume made up to 50mls with buffer and the homogenate spun at 18,000rpm for 20 minutes (Beckman J2-21). The pellet was rehomogenised and centrifuged as before. The final membrane pellet was resuspended at a protein concentration of 10-20mg/ml, determined by the method of Lowry as described above. 200-500µl aliquots were stored at -70°C until required.

Binding assays were standardised using rat brain membranes. Whole brains from adult male Sprague-Dawley rats were homogenised, centrifuged at 1000rpm for 10 minutes to remove debris and the supernatant spun at 18,000rpm for 20 minutes. Membranes were washed and resuspended as above.

2.2.6. Patients

The diagnosis of LEMS was made on the basis of clinical features (O'Neill et al 1988) and electrophysiological recordings using surface electrodes. The resting compound muscle action potential (CMAP) in abductor digiti minimi was reduced in amplitude (<8.5mV) following supramaximal stimulation of the ulnar nerve. The percentage increment in CMAP amplitude after 15 seconds maximum

voluntary contraction of the muscle was abnormally high (% increment = 100 x (maximum CMAP amplitude - initial CMAP amplitude) / initial CMAP amplitude; upper limit of normal is 25% (Newsom-Davis and Murray 1984)).

The LEMS patients were divided into 3 groups: those with biopsy-proven SCLC (SCLC-LEMS), those with no cancer detected (NCD-LEMS) and those whose status was uncertain (SU-LEMS). The patients in the NCD-LEMS group had been followed for at least 5 years and were,therefore,unlikely to have SCLC (O'Neill 1988). The SU-LEMS group included patients followed for less than 5 years, patients with suspected lung cancer where histology was not available, one patient with a lymphoma and one with carcinoma of the breast. Serum was obtained from a total of 78 LEMS patients, aliquoted and stored at -20°C until required.

Serum was also obtained from 88 control individuals who were divided into 6 groups:

1. Healthy laboratory volunteers (n = 18).
2. SCLC with no symptoms of LEMS (n = 17).
3. Myasthenia gravis with detectable anti-AChR antibodies (n = 12).
4. Myasthenia gravis with no detectable anti-AChR antibodies (n = 10).
5. Other neurological disorders (OND) including Guillain-Barré syndrome, chronic inflammatory demyelinating polyneuropathy, chronic neuropathy, neuromyotonia and motor neurone disease (n = 15).
6. Non-organ specific autoimmune disorders including rheumatoid arthritis (RA) and systemic lupus erythematosus (SLE) (n = 16).

2.2.7. Statistical methods

Statistical analysis was performed using Oxstat II (Microsoft Corporation).

Student's t test for paired samples was used to investigate the effect of dibutyryl cAMP on K^+-stimulated calcium flux by comparing the amount of stimulated flux measured in treated and untreated cells grown in parallel. Student's t tests were also used to analyse the effect of pooled IgG (paired samples) and single IgG preparations (unpaired samples) on calcium flux and the number of ^{125}I-ωCgTx binding sites.

The mean anti-VGCC antibody titres obtained for each group of LEMS patients in the radioimmunoassay were compared using the Wilcoxon rank sum test for unpaired data. The use of a non-parametric test was necessary as the titres were not normally distributed, being skewed toward zero.

The incidence of positive results in a particular group was compared with the incidence in the healthy control group by the chi-square test with Yates correction. The tests were carried out using the numbers of positive titres in each group rather than the percentages. A positive titre was defined as greater than 2 standard deviations above the mean titre for the healthy controls. A titre higher than this value is significantly different from the healthy control population at the 5% level.

The titres obtained using 2 sources of antigen were compared using Spearman's method of rank correlation for non-parametric data.

CHAPTER 3

CALCIUM FLUX STUDIES

3.1. Introduction

The characteristics of VGCCs on neuronal cells have been investigated using a number of complex electrophysiological techniques. However, a simpler method for the study of calcium channels on cultured cells has been developed, involving the uptake of $^{45}Ca^{2+}$ following membrane depolarisation. This can be achieved by the elevation of extracellular K^+ concentrations. The clonal cell line, PC12, derived from a rat adrenal pheochromocytoma, has provided a model for such K^+-stimulated Ca^{2+} influx (Chalfie et al 1976), which could be blocked by the calcium channel inhibitors Mn^{2+} and Co^{2+} (Stallcup 1979). Further studies with PC12 cells have demonstrated the sensitivity of this Ca^{2+} uptake to VGCC antagonists such as dihydropyridines (Toll 1982, Takahashi and Ogura 1983).

Calcium flux assays have been used to investigate the effect of LEMS antibodies on VGCCs. The reduction of K^+-stimulated Ca^{2+} uptake following exposure to LEMS IgG was first demonstrated in the SCLC line, MAR (Roberts et al 1985), and confirmed in other SCLC lines (De Aizpurua et al 1988) and PC12, NG108 and F21D1 cell lines (Lang et al 1989a,b). The inhibition of K^+-stimulated Ca^{2+} uptake in SCLC lines by DHPs and ω-conotoxin was shown by De Aizpurua et al (1988). However, the sensitivity of Ca^{2+} influx to antagonists in other cell lines has not been fully investigated. The purpose of these experiments was to study the effects of

calcium channel antagonists on K^+-stimulated Ca^{2+} flux in several cell lines of neuronal origin (see Table 2.1) and to investigate the effect of LEMS IgG on calcium flux in the human neuroblastoma lines, SKNSH and Kelly.

3.2. Methods

At confluence, cells were harvested from culture flasks and an aliquot counted in a haemocytometer. They were then plated out in 6-well culture plates (well diameter = 35mm) at a density of 0.2-1.0 x 10^6 cells/well. Plates coated with poly-L-lysine (10µg/well) were used for the NG108 and F21D1 cells in order to promote adherence. After 3-4 days, when confluent monolayers were formed, the culture medium was removed and the cells washed once with PBS containing 1.5mM $CaCl_2$. 3 wells of each plate were incubated for 60 seconds with Hepes-Locke buffer (144mM NaCl, 1.8mM $CaCl_2$, 1.8mM $MgCl_2$, 10mM Hepes, 5mM glucose, pH 7.4) containing a physiological concentration of potassium (2.7mM) in order to measure basal flux. The remaining 3 wells were incubated with Hepes-Locke buffer in which KCl was substituted for NaCl on an equimolar basis (144mM KCl, 2.7mM NaCl) in order to measure calcium influx after membrane depolarisation. A known amount of $^{45}Ca^{2+}$ (0.5µM) (0.75µCi/ml) was added to both solutions. Preliminary experiments determined the time of incubation and K^+ concentration necessary for depolarisation. After removal of the Hepes-Locke buffers the cells were washed three times with PBS. Triton X 100 (0.5%) was added to each well for 20 minutes to permeabilise the cells. Aliquots were taken from representative wells to measure protein concentration (Methods 2.2) and the remainder transferred to 6ml polypropylene tubes. 4mls scintillation fluid (Optiphase "Safe") were added to each tube and the samples were thouroughly mixed and counted in a Beckman LS1701 liquid scintillation counter at 40% efficiency. $^{45}Ca^{2+}$ influx in cpm was converted into nmoles by comparison with the cpm measured in a sample of Hepes-Locke buffer

containing a known concentration of Ca^{2+} ions. Results from individual wells were standardised by expressing calcium influx as nmoles/mg protein. Net stimulated Ca^{2+} influx was calculated by subtracting the mean basal flux from the mean depolarised flux in each plate of cells.

The effect of antagonists on calcium influx was studied by preincubating cells for 5-10 minutes either with PBS alone or with PBS containing increasing amounts of the antagonist. All experiments using DHPs were carried out under sodium light to prevent degradation. Ca^{2+} is necessary for DHP binding but has an inhibitory effect on ωCgTx binding. Therefore, when studying the additive effect of antagonists the cells were incubated for 5 minutes with ωCgTx in PBS followed by 5 minutes with nitrendipine in PBS + 1.5mM $CaCl_2$. A separate plate of cells was used for each different concentration of antagonist so that both basal and depolarised fluxes were measured. The antagonist was also present at a corresponding concentration in the Hepes-Locke incubation buffers, but not in the final three PBS washes. IC_{50} values (the concentration at which 50% of the stimulated flux was inhibited) were calculated by non-linear regression (Elsevier Biosoft).

To induce cell differentiation 1mM dibutyryl cAMP was added to the culture medium at the time of plating out. K^+-stimulated $^{45}Ca^{2+}$ flux was measured after 3 days in these and untreated cells grown in parallel.

The effect of IgG on calcium flux was studied by adding 2mg/ml IgG to the culture medium 24 hours after plating out. $^{45}Ca^{2+}$ influx was assayed after a further 2-3 days. IgG was not present during the calcium flux assay.

In all the above experiments cells were kept in culture conditions until the time of assay. Plates were removed from the incubator in pairs and assayed immediately. The buffers were added to and removed from the wells at timed 5 or 10 second intervals thus incubating each well for the same length of time. The assays took place at room temperature.

3.3 Results

3.3.1. Voltage dependency of K^+-stimulated calcium flux

The relationship of calcium influx to membrane potential was studied in SKNSH and Kelly cells by increasing the K^+ concentration in the depolarising buffer. Basal flux was determined in the presence of 2.7mM KCl, while depolarised flux was determined for the range 25-144mM KCl. Figure 3.1 shows that in SKNSH cells the depolarised Ca^{2+} flux increased over this concentration range, reaching maximum levels at about 125mM KCl. A similar effect is shown in Figure 3.2 for the Kelly cell line, although maximum Ca^{2+} influx was achieved at about 90mM KCl. Membrane potential (Vm) can be calculated from the Nernst equation, taking the intracellular K^+ concentration ($[K^+]ic$) as 155mM (Hille 1984):

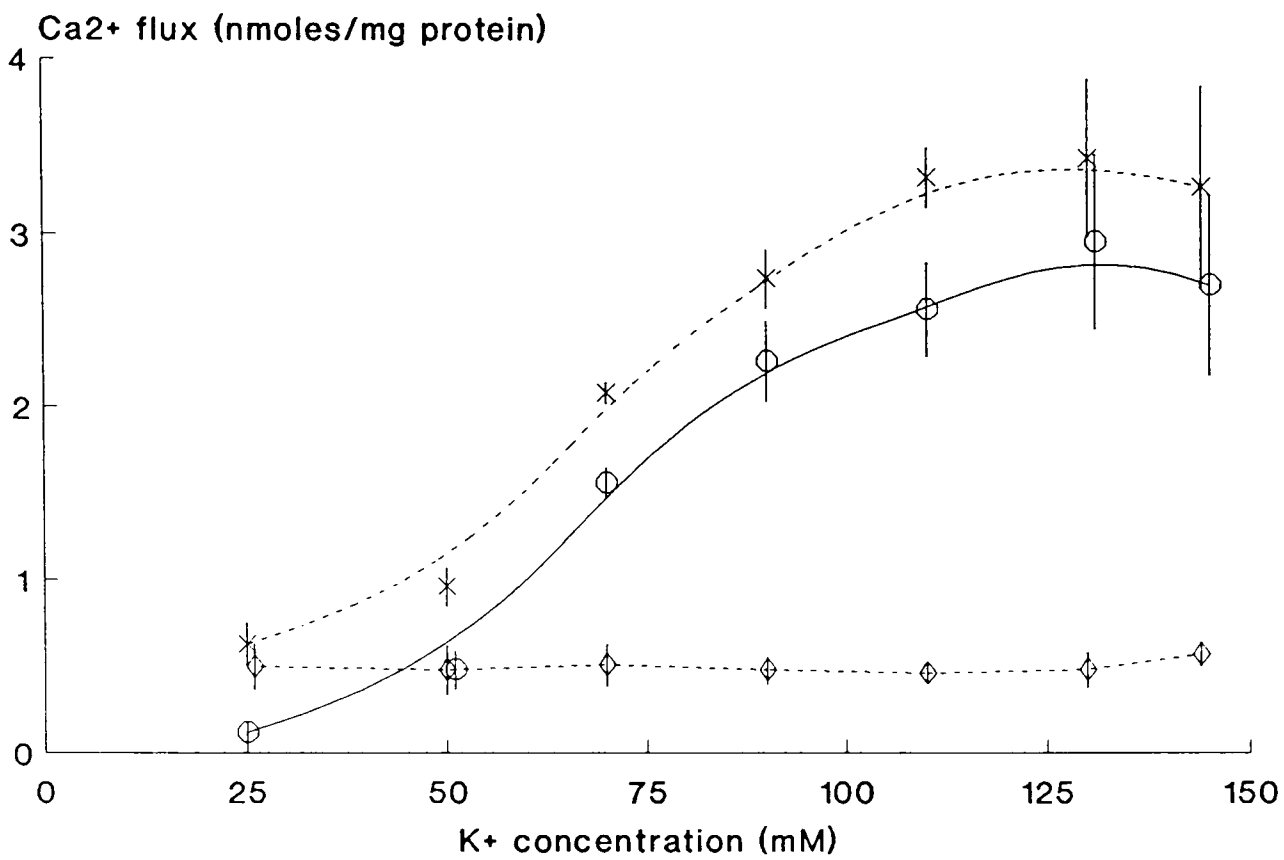
$$Vm = 59.8 \log ([K^+]ec / [K^+]ic)$$

where $[K^+]ec$ = extracellular K^+ concentration, ie. that of the depolarising buffer.

The concentration range studied thus corresponds to a membrane potential of -50mV to -2mV, with maximum effects at approximately -5mV (SKNSH) or -15mV (Kelly) and very little flux seen below -30mV. Patch-clamp recordings in human neuroblastoma cells show that transient, low threshold (LVA,T) calcium currents activate at membrane potentials positive to -50mV, while high threshold (HVA) currents activate at membrane potentials positive to -30mV (Carbone et al 1990). Therefore, it seems likely that the K^+-stimulated Ca^{2+} flux measured here was due to the activation of HVA channels, composed of L and N types. 144mM K^+ was used in all further experiments in order to study these HVA channels.

Figure 3.1: Voltage dependency of calcium influx in SKNSH cells. SKNSH cells were incubated with increasing concentrations of potassium for 60 seconds in order to measure the depolarised calcium influx (X, dotted line). Net stimulated calcium influx (O, solid line) was calculated by subtracting the basal flux determined in the presence of 2.7mM KCl (◇, dotted line). Means and SEMs of 3 experiments performed in triplicate are shown.

Figure 3.2: Voltage dependency of calcium influx in Kelly cells. The above measurements repeated with the Kelly cell line. Means and SEMs of 4 triplicate determinations.


Ca2+ flux (nmoles/mg protein)
4
3
2
1
0
0
25
50
75
100
125
150
K+ concentration (mM)

Ca2+ flux (nmoles/mg protein)
3.5
3
2.5
2
1.5
1
0.5
0
0
25
50
75
100
125
150
K+ concentration (mM)
-50
-25
-10
0
Membrane potential (mV)

3.3.2. Time course of K^+-stimulated calcium flux

The time course of Ca^{2+} uptake from 15 to 90 seconds was investigated. The results for the SKNSH cell line are shown in Figure 3.3. The basal flux remained constant over this period while the depolarised flux increased, reaching maximum levels at 60 seconds. The time course of Ca^{2+} flux for the Kelly cell line was more rapid, reaching a maximum value at 45 seconds (Figure 3.4). Similar studies in the other cell lines showed that maximum K^+-stimulated Ca^{2+} uptake was achieved by 30-60 seconds. In order to standardise the assay, Ca^{2+} uptake over 60 seconds was used for all cell lines.

3.3.3. Net K^+-stimulated calcium flux in neuronal cell lines

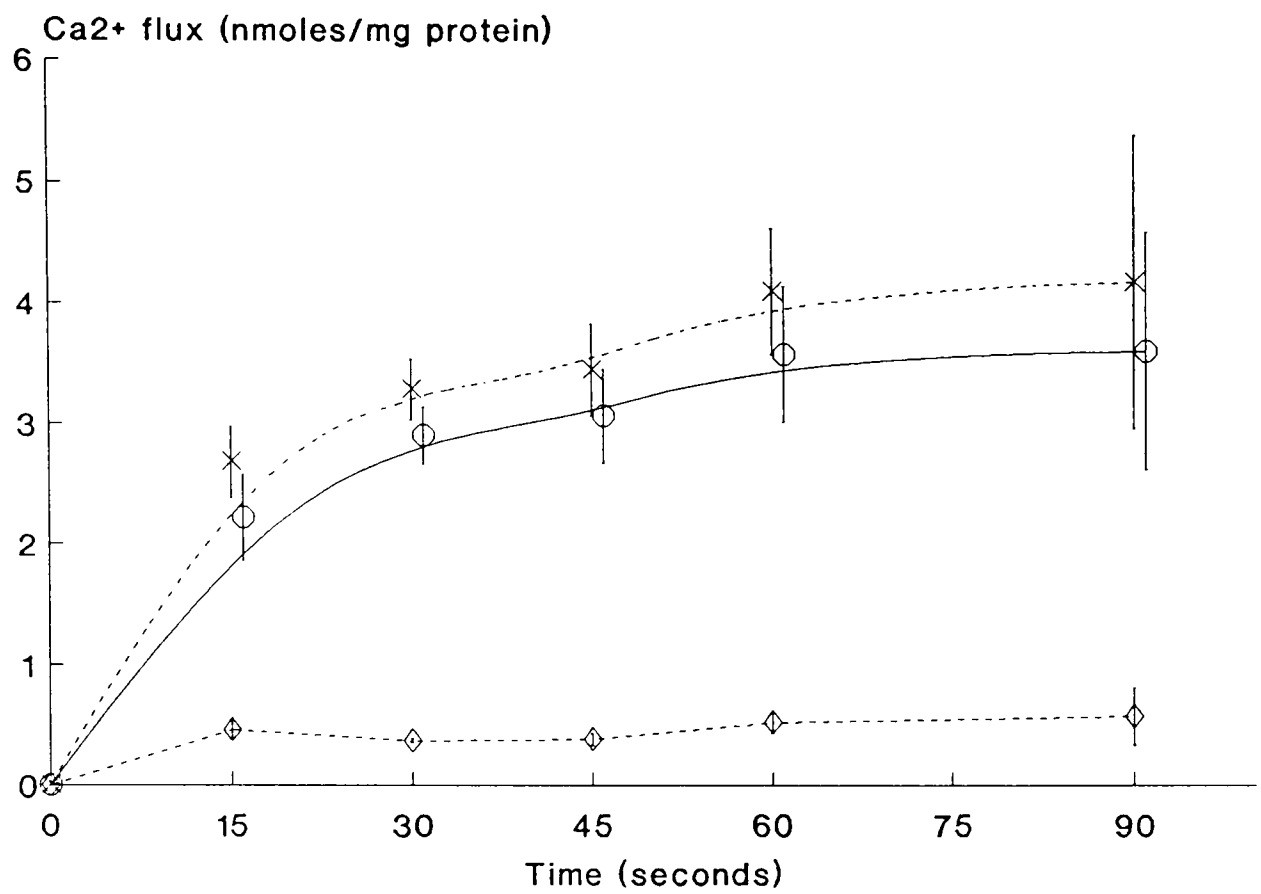
Figure 3.5 shows the levels of stimulated (ie. depolarised - basal) Ca^{2+} flux achieved using the above conditions for the six neuronal cell lines studied. The amount of stimulated flux varied widely between the cell lines, but for a given line the value was consistant over multiple estimations. Of particular note is the different amounts of calcium flux measured in the three human neuroblastoma lines SKNSH, Kelly and IMR32. The two hybrid lines (NG108 and F21D1) and the IMR32 cells showed the lowest levels of stimulated uptake and also the highest levels of basal flux (as a proportion of depolarised flux). Mean levels of basal, depolarised and stimulated Ca^{2+} flux are listed in Table 3.1.

Figure 3.3: Time course of K^+-stimulated calcium flux in SKNSH cells

Depolarised (K^+=144mM) (X) and basal (K^+=2.7mM) (◇) calcium fluxes were measured in SKNSH cells from 15 to 90 seconds. Net stimulated influx is indicated with the solid line. Means and SEMs are shown for 3 triplicate determinations.

Figure 3.4: Time course of K^+-stimulated calcium flux in Kelly cells.

The above measurements repeated with the Kelly cell line. Means and SEMs of 3 triplicate determinations.


Ca2+ flux (nmoles/mg protein)
6
5
4
3
2
1
0
0
15
30
45
60
75
90
Time (seconds)

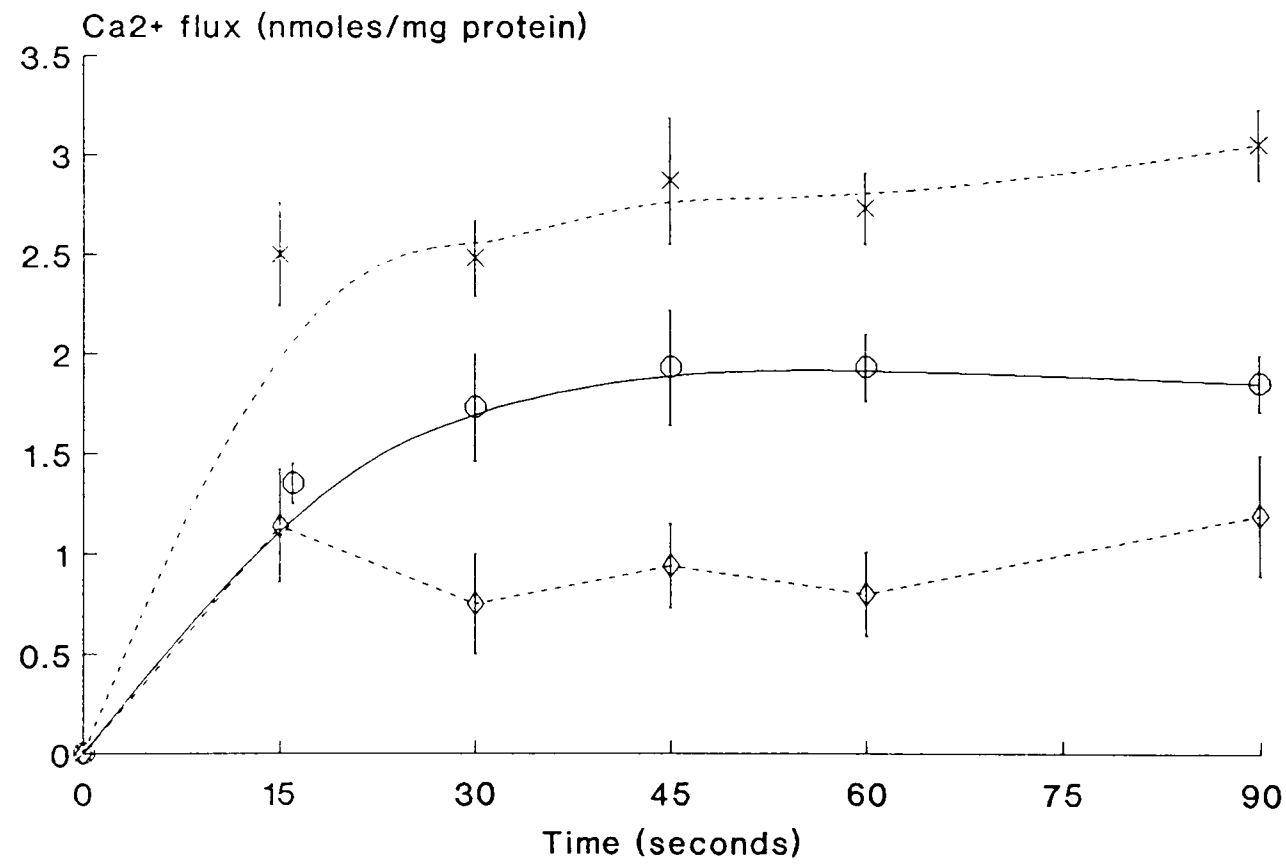

Ca2+ flux (nmoles/mg protein)
3.5
3
2.5
2
1.5
1
0.5
0
0
15
30
45
60
75
90
Time (seconds)

Figure 3.5: Net K^+-stimulated calcium flux in 6 neuronal cell lines.

Depolarised and basal fluxes were measured using the conditions described in Methods 3.2. Net stimulated flux was calculated by subtracting basal from depolarised flux. Means and SEMs are shown for the number of determinations indicated.

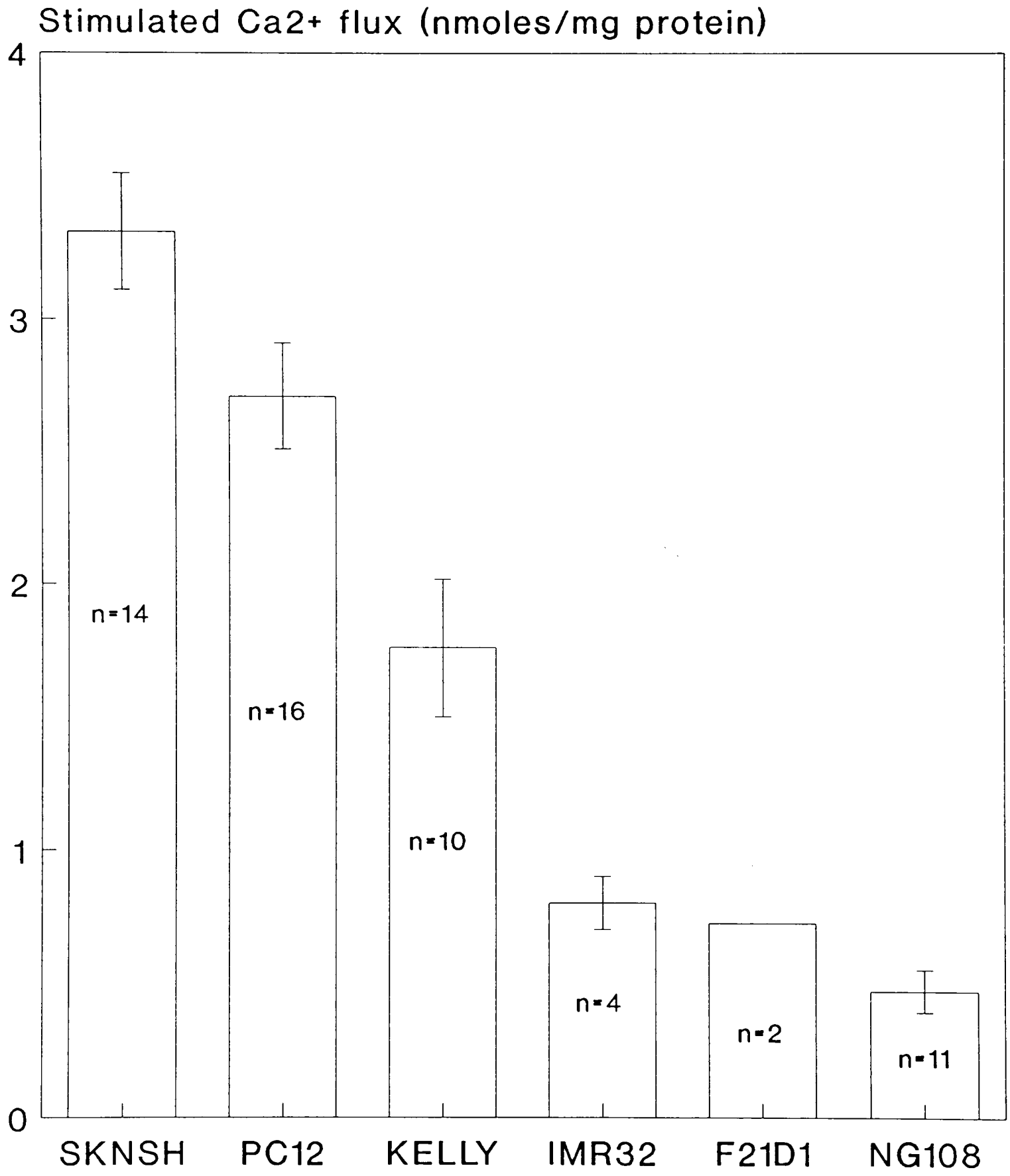

Stimulated Ca2+ flux (nmoles/mg protein)
4
3
2
1
0
n=14
n=16
n=10
n=4
n=2
n=11
SKNSH
PC12
KELLY
IMR32
F21D1
NG108

Table 3.1

K^+-stimulated calcium flux in neuronal cell lines

Cell line	n	Uptake of $^{45}Ca^{2+}$ (nmoles/mg protein) Basal (2.7mMKCl)	Depolarised (144mM KCl)	Stimulated
SKNSH	14	0.57±0.03	3.89±0.24	3.32±0.22
KELLY	10	0.67±0.08	2.40±0.29	1.73±0.24
IMR32	4	0.90±0.04	1.71±0.08	0.81±0.10
PC12	16	0.77±0.11	3.48±0.30	2.71±0.20
NG108	11	0.67±0.11	1.14±0.19	0.47±0.08
F21D1	2	1.12	1.85	0.73

n = number of determinations, each performed in triplicate. Means and SEMs are shown, apart from the data for F21D1 cells (mean of two determinations).

3.3.4. The effect of antagonists on K^+-stimulated calcium flux

(i) Nitrendipine

Dose-response curves for nitrendipine (0.1nM-10μM) were constructed for SKNSH, Kelly, NG108 and PC12 cells (Figure 3.6). The effect of high concentrations only were studied in the IMR32 and F21D1 cells. Nitrendipine inhibited K^+-stimulated Ca^{2+} uptake in a dose-related manner. In PC12 cells there was almost total abolition of stimulated flux (95% at 1μM, IC_{50} = 4.5nM). In the other cell lines the inhibition by nitrendipine was incomplete at 10μM and, in the NG108 cells, at 100μM.

(ii) Methoxyverapamil

The effect of methoxyverapamil (D600) was compared in the PC12 and NG108 cell lines (Figure 3.7). In agreement with the effect of nitrendipine, the inhibition of Ca^{2+} uptake was complete in the PC12 cells (100% at 100μM, IC_{50} = 1.4μM) but only partial inhibition was seen in NG108 cells at this concentration (62%).

(iii) ω-Conotoxin

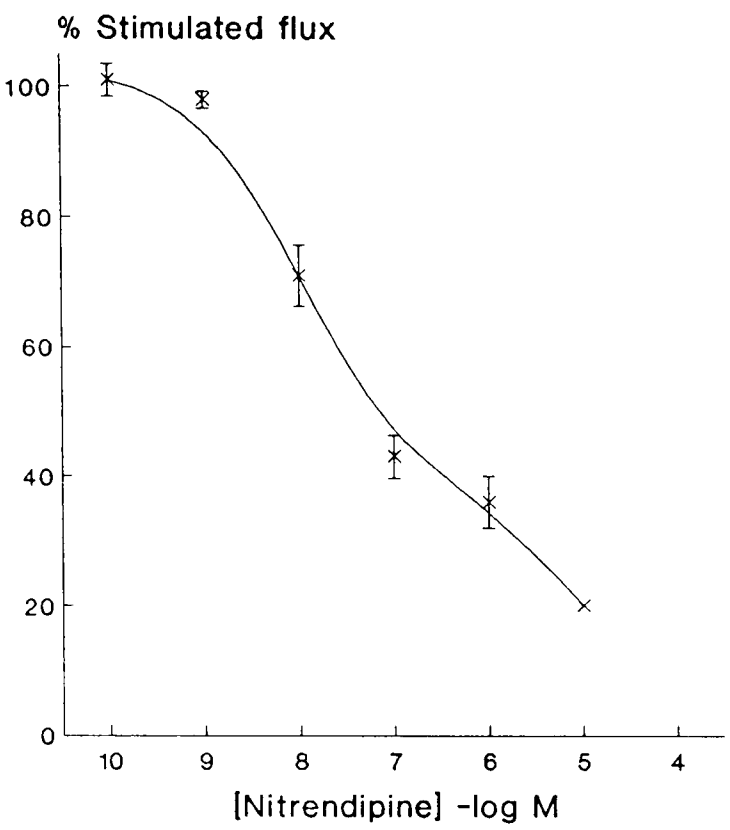
Dose-response curves for ω-conotoxin are shown in Figure 3.8. In the neuroblastoma cell lines there was little effect of ωCgTx on stimulated Ca^{2+} flux except at high concentrations and then only partial inhibition was found. In NG108 cells the inhibition was still incomplete at 1μM, but some inhibition was seen at lower concentrations. In contrast to the effects of nitrendipine and D600, there was no effect of ωCgTx in PC12 cells, even at high concentrations.

Table 3.2 summarises the effects of the above calcium antagonists on stimulated Ca^{2+} flux in the cell lines studied.

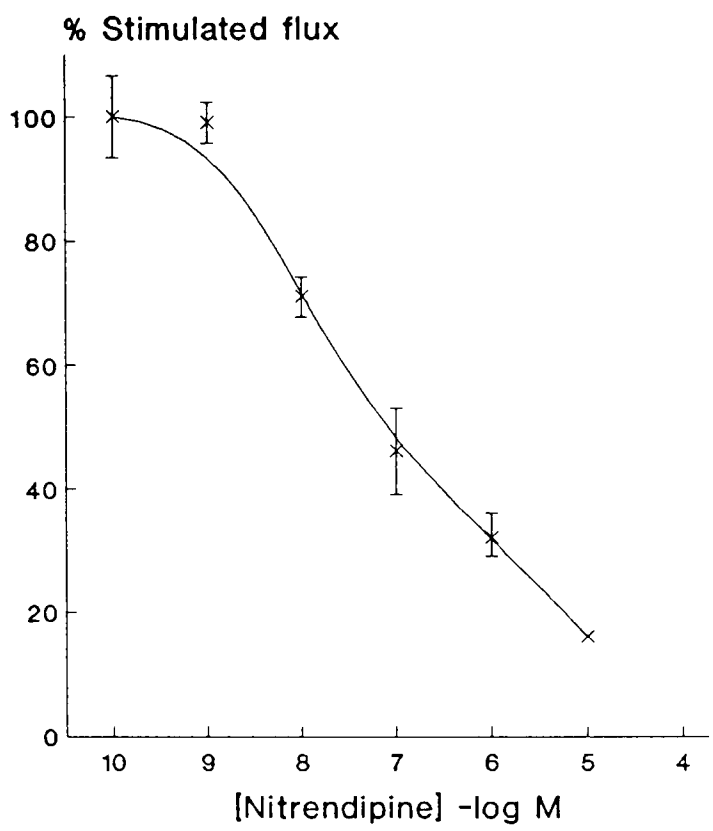
Figure 3.6: Inhibition of K^+-stimulated calcium flux by nitrendipine.

K^+-stimulated flux was determined in 4 cell lines after incubation with increasing concentrations of nitrendipine. Results are expressed as a percentage of the stimulated flux measured in the absence of antagonist. Means and SEMs are shown for 3-7 determinations (n = 2 where no error bars are shown).

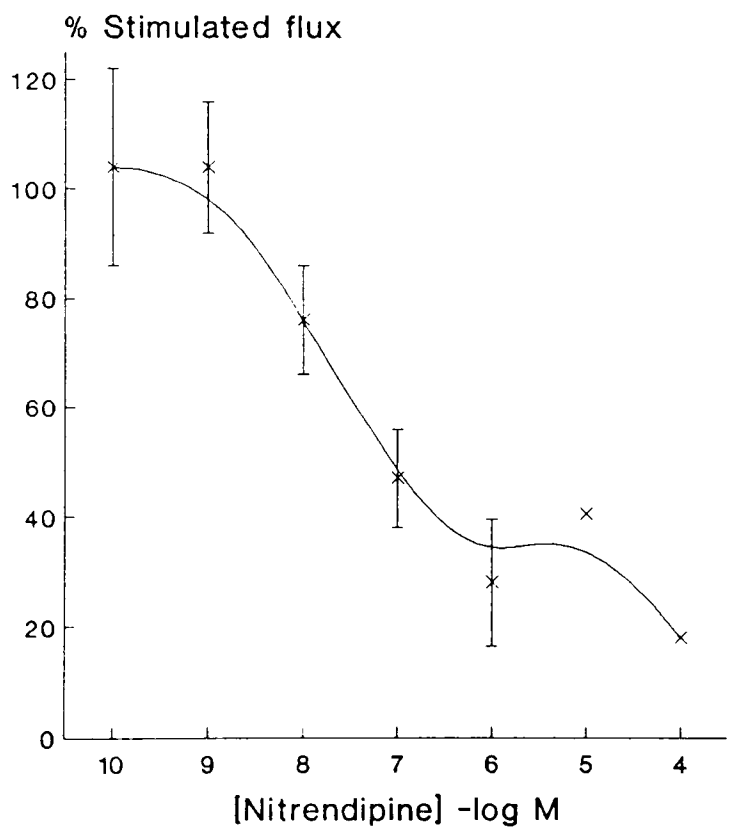
(a) SKNSH



(a) KELLY



(c) NG108



(d) PC12

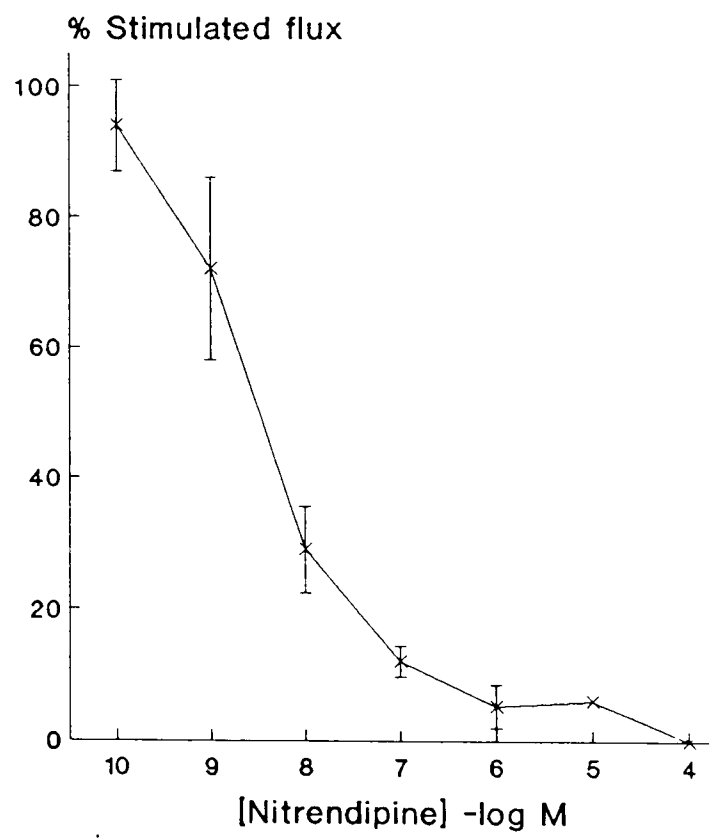
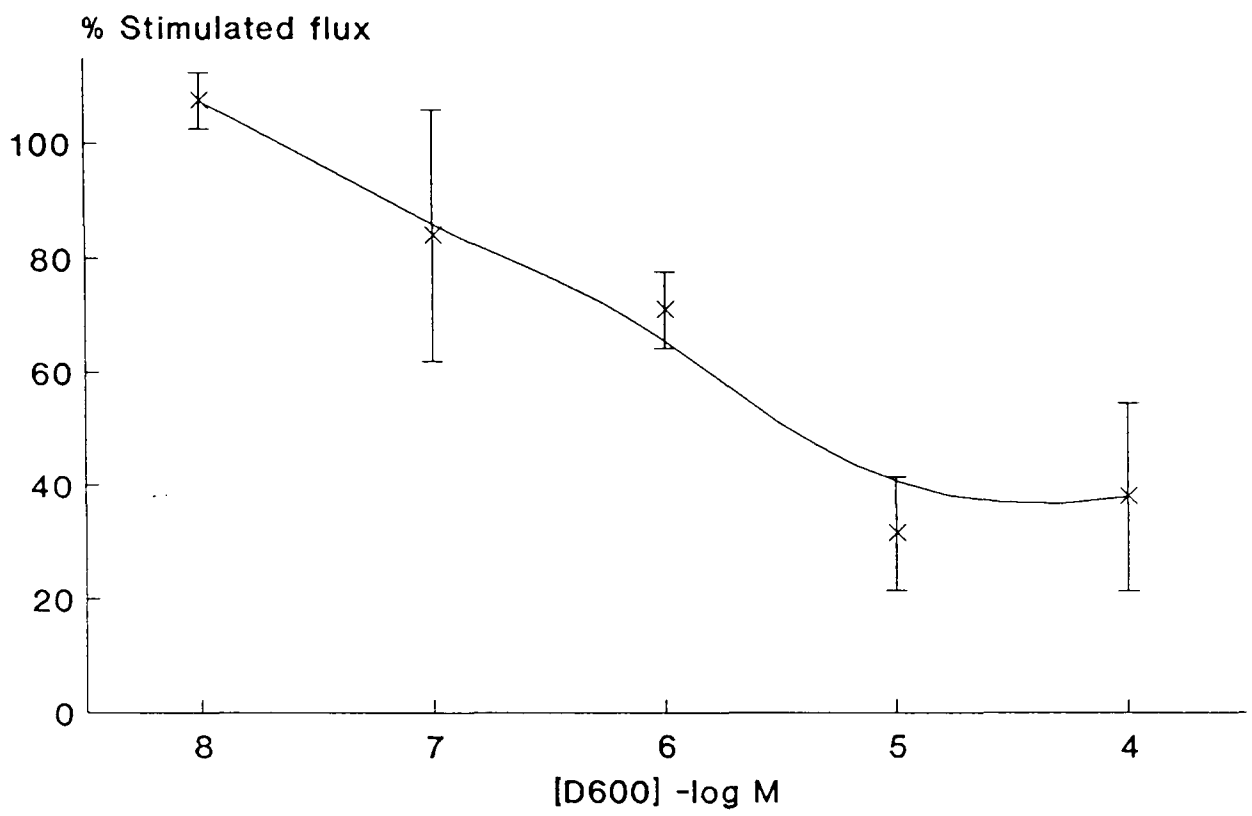


Figure 3.7: Inhibition of K^+-stimulated calcium flux by methoxyverapamil.

K^+-stimulated flux was measured in NG108 and PC12 cells after incubation with 0.01-100μM methoxyverapamil (D600). Results are expressed as a percentage of the stimulated flux measured in the absence of antagonist. Means and SEMs are shown for 3-4 determinations.

(a) NG108



(b) PC12

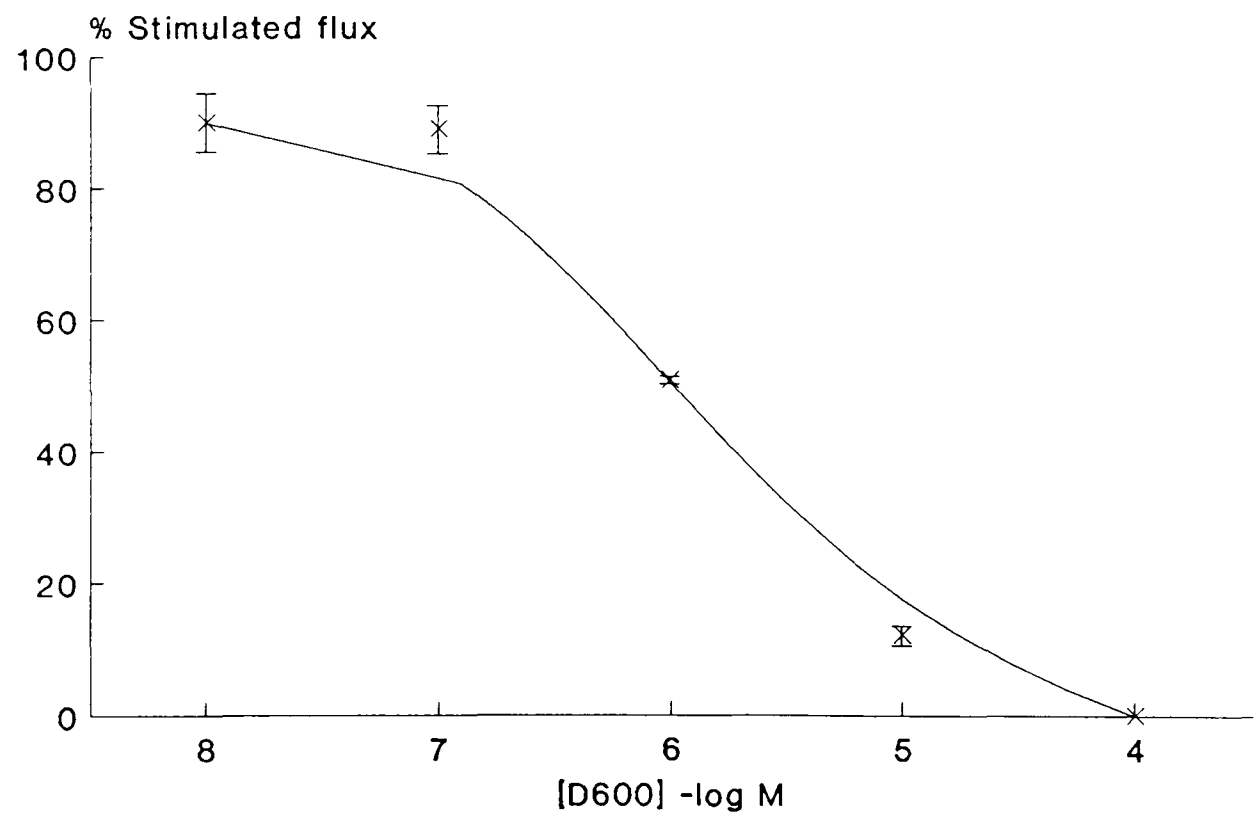
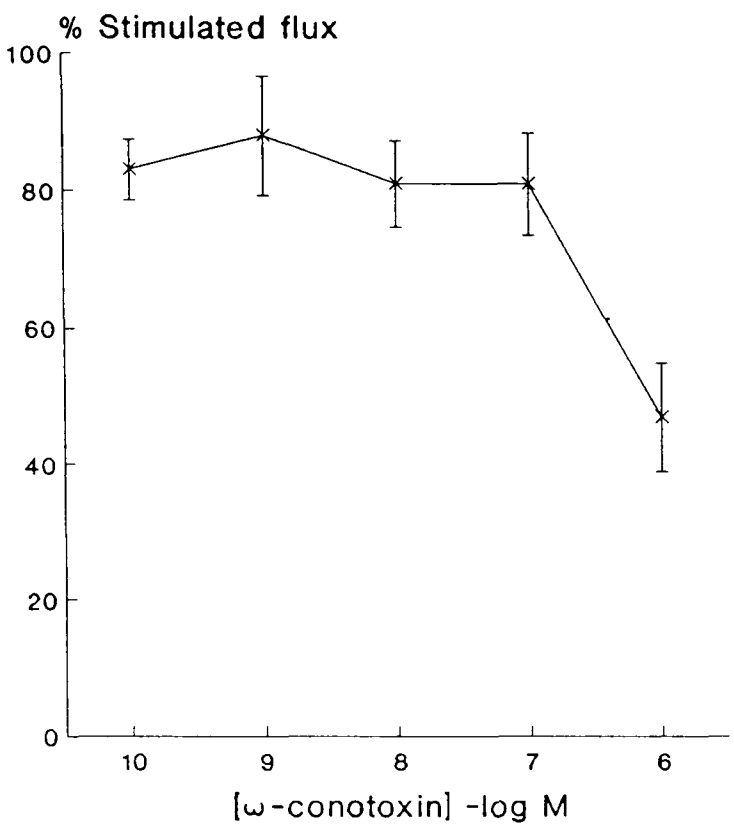


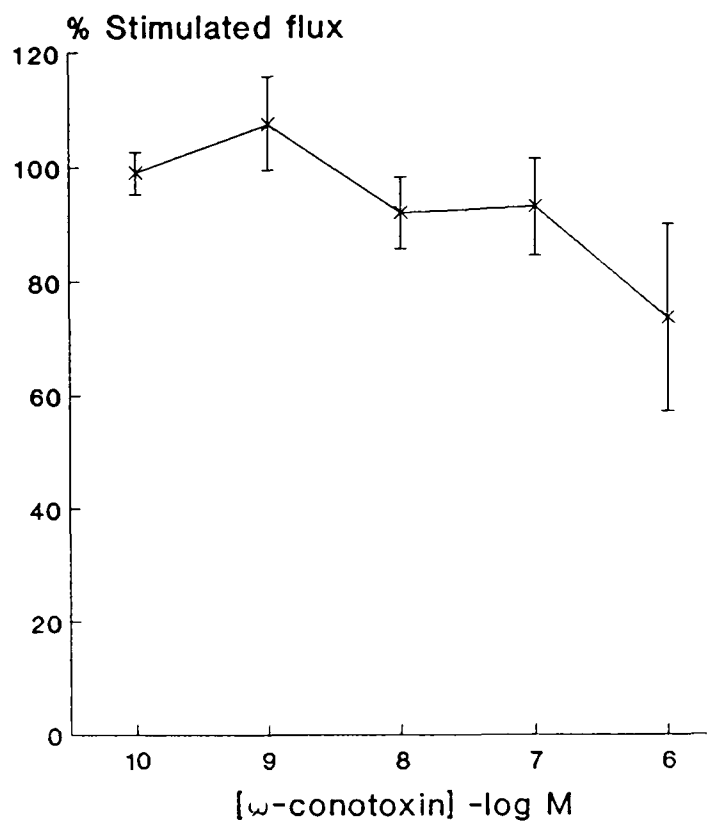
Figure 3.8: Inhibition of K^+-stimulated calcium flux by ω-conotoxin.

K^+-stimulated flux was measured in 4 cell lines after incubation with 0.1nM-1μM ωCgTx. Results are expressed as a percentage of the stimulated flux measured in the absence of antagonist. Means and SEMs are shown for 3-4 determinations.

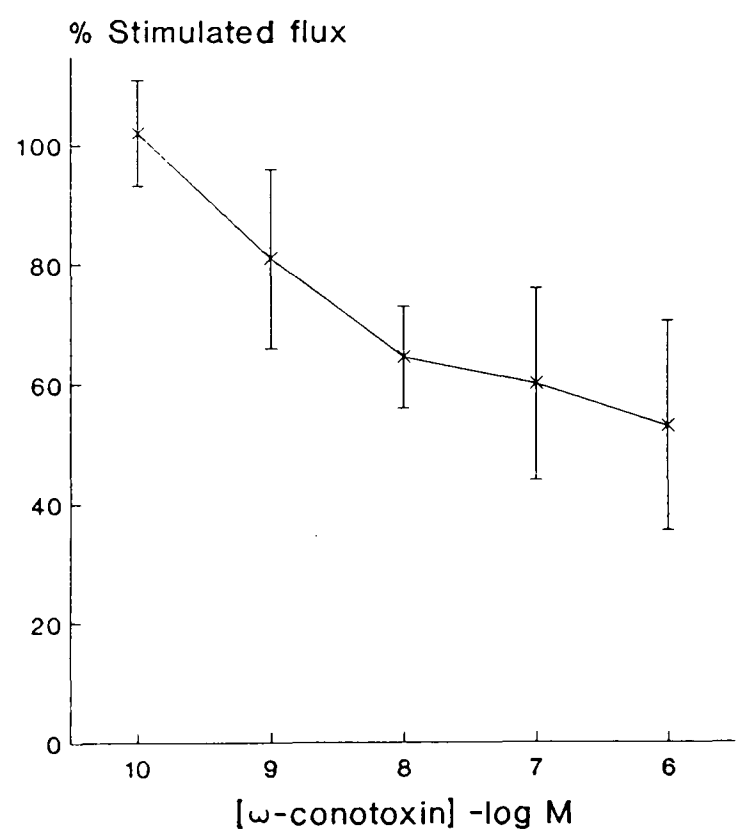
(a) SKNSH



(b) KELLY



(c) NG108



(d) PC12

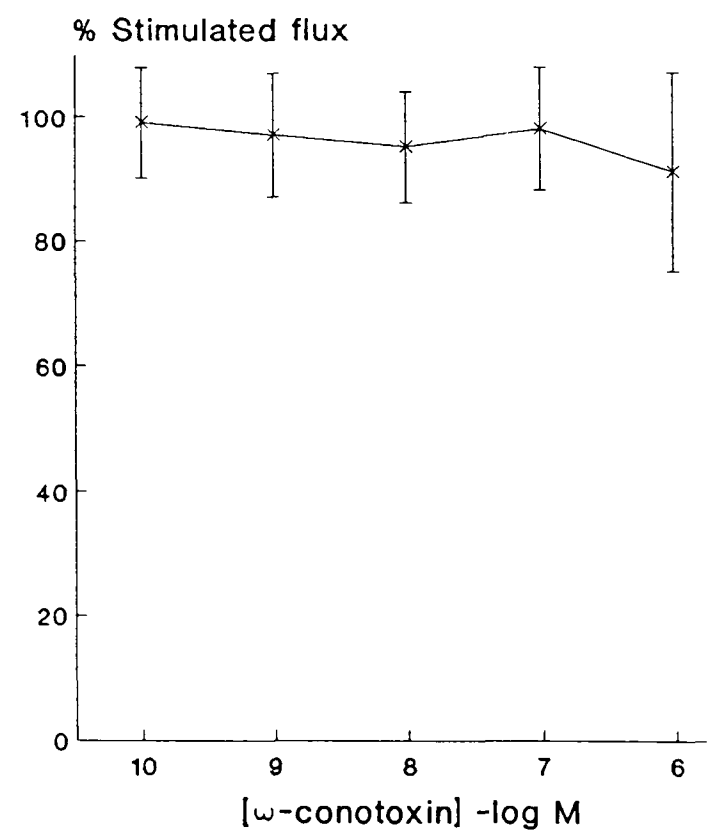


Table 3.2

Inhibition of K^+-stimulated calcium flux by antagonists

Cell line	% Inhibition		
	Nitrendipine (1μM)	D600 (100μM)	ωCgTx (1μM)
SKNSH	64±4 (7)	ND	53±8 (7)
Kelly	68±3 (6)	ND	26±17 (6)
IMR-32	87 (2)	ND	16 (2)
PC12	95±3 (5)	100±1 (3)	9±16 (3)
NG108	72±12 (7)	62±17 (4)	47±18 (4)
F21D1	44 (2)	ND	42 (2)

Figures in brackets indicate number of determinations.

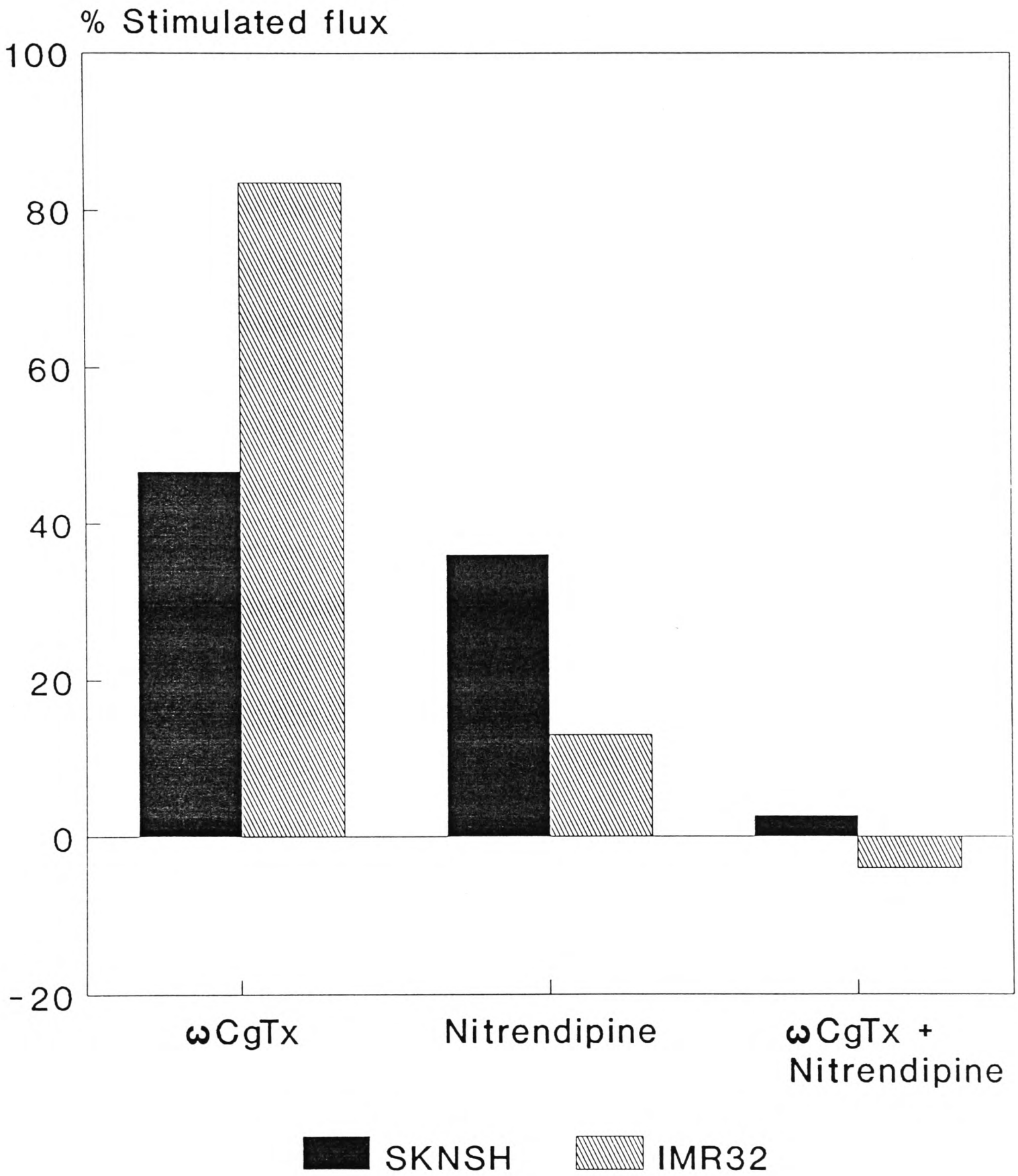
ND = not determined.

(iv) Nitrendipine and ω-Conotoxin together

Two cell lines with different levels of inhibition by nitrendipine and ωCgTx were used to study the additive effect of these two antagonists. In both the SKNSH and IMR32 cells there was partial inhibition of stimulated flux with 1μM nitrendipine (64% and 87% respectively) and 1μM ωCgTx (53% and 16% respectively) (see Table 3.2). As the incubation conditions for the two antagonists were different, the cells were incubated with ωCgTx for 5 minutes before the addition of nitrendipine (see Methods 3.2). This resulted in the complete inhibition of K^+-stimulated Ca^{2+} flux in both cell lines (Figure 3.9).

Figure 3.9: The additive effect of nitrendipine and ω-conotoxin on K^+-stimulated calcium flux.

K^+-stimulated flux was measured in SKNSH and IMR32 cells after incubation with either ωCgTx (1μM) or nitrendipine (1μM) alone, or ωCgTx followed by nitrendipine (1μM of each, see Methods 3.2). Mean results of 2 triplicate analyses are shown.


% Stimulated flux
100
80
60
40
20
0
-20
ωCgTx
Nitrendipine
ωCgTx +
Nitrendipine
SKNSH
IMR32

3.3.5. The effect of dibutyryl cAMP on K^+-stimulated calcium flux

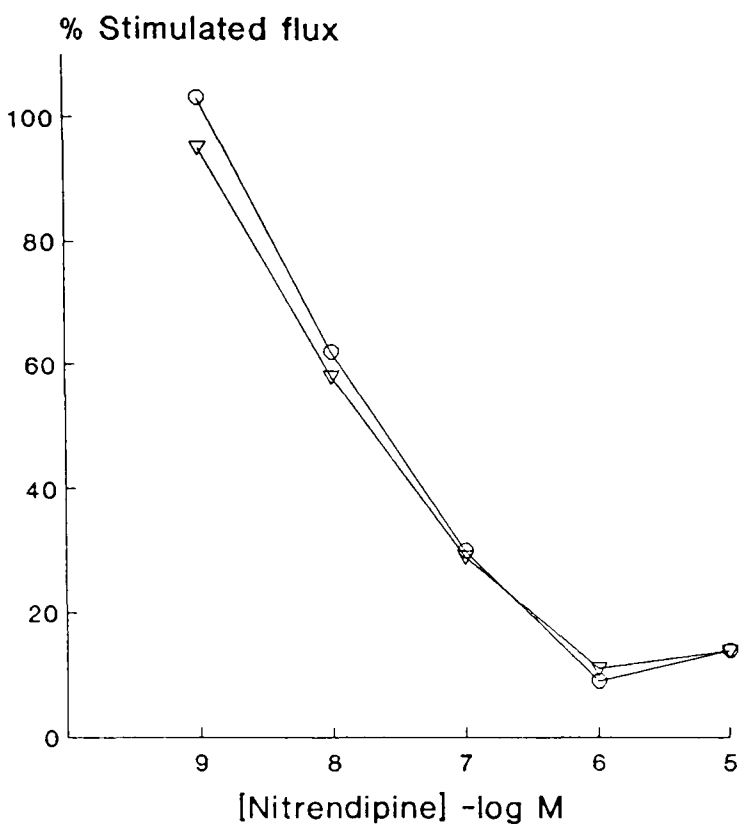
PC12 and NG108 cells have previously been shown to differentiate in response to raised intracellular cAMP concentrations (Plummer et al 1989, Docherty 1988). These two cell lines were, therefore, used to investigate the effect of dibutyryl cAMP on K^+-stimulated calcium flux. After 3 days in the presence of 1mM dibutyryl cAMP, the cells appeared to have differentiated due to the development of neurites and the lack of cell division. Stimulated flux was increased from 0.70±0.15 to 1.08±0.09 nmoles/mg protein in treated NG108 cells (mean±SEM, n=4). This increase was not significant (paired t-test). In the PC12 cells, stimulated flux was reduced from 1.57±0.40 to 1.37±0.36 nmoles/mg protein (p=0.05, paired t-test; n=5).

Inhibition curves with nitrendipine showed no difference in the effect of this antagonist between treated and untreated cells in either cell line (Figure 3.10). Similarly, no difference in the effect of ωCgTx on treated and untreated cells was detected in the PC12 line.

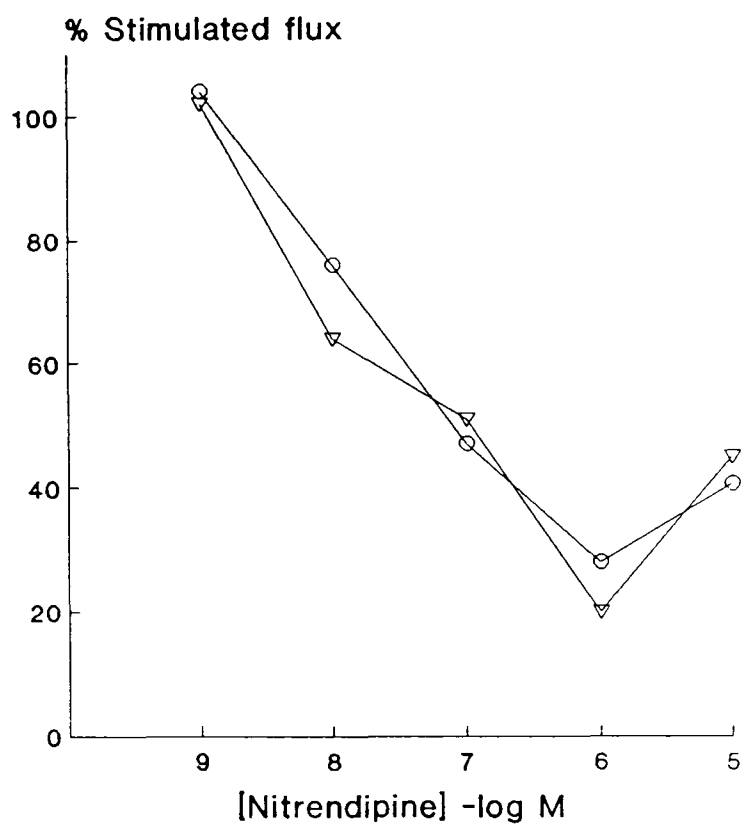
Figure 3.10: Inhibition of K^+-stimulated calcium flux by antagonists in dibutyryl cAMP-treated cells.

NG108 and PC12 cells were grown for 3 days in the presence of 1mM dibutyryl cAMP. K^+-stimulated flux was measured in dibutyryl cAMP-treated cells (▽) and cells grown in standard culture medium (○) after incubation with antagonist (n=2).

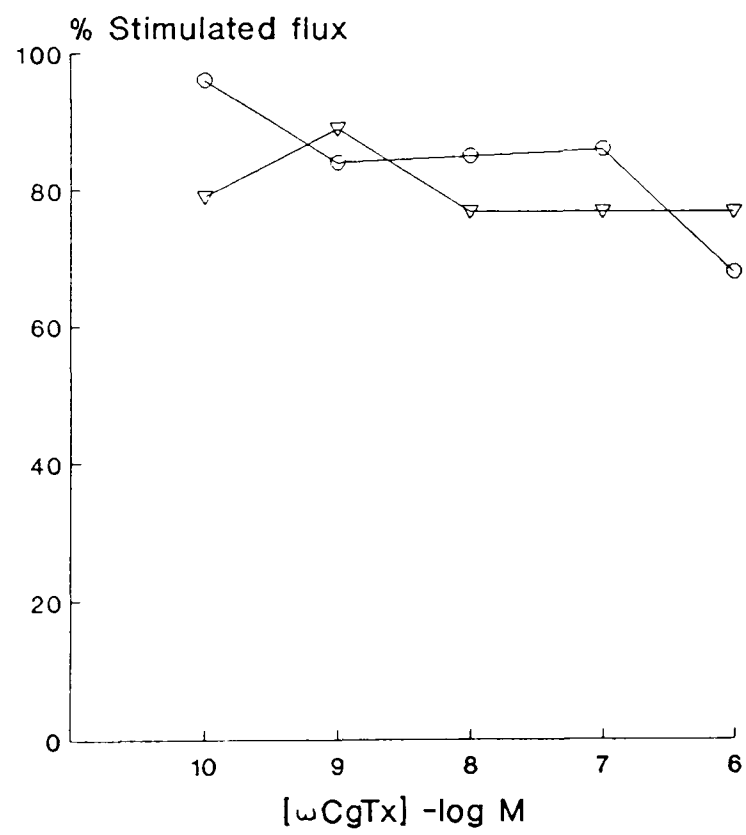
(a) PC12



(b) NG108



(c) PC12



3.3.6. The effect of LEMS IgG on K^+-stimulated calcium flux

IgG pools were prepared from the plasma of six LEMS patients or six patients with other neurological disorders (OND). The LEMS pool contained IgG from two patients with SCLC and four patients with no cancer detected, although in two of these cases the history was less than five years and an occult SCLC could not therefore be excluded. The OND pool was composed of IgG from three patients with myasthenia gravis, two with Guillain-Barré syndrome and one with chronic inflammatory demyelinating neuropathy. SKNSH and Kelly cells were grown for two days in culture medium containing 2mg/ml IgG. K^+-stimulated Ca^{2+} flux in SKNSH cells exposed to LEMS IgG was reduced to 65±6% of that seen in untreated cells, while cells exposed to OND IgG showed similar levels of flux to control cells (93±3%) (Figure 3.11). The difference between the effects of LEMS and OND IgG on stimulated flux was significant ($p=0.013$, paired t-test; $n=5$). There was no further effect when cells were cultured in the presence of 4mg/ml IgG (LEMS = 60±7%, OND = 90±9%; $n=6$).

In Kelly cells there was no change in K^+-stimulated flux after exposure to pooled IgG, either at 2mg/ml (LEMS = 92±5%, OND = 94±6%; $n=6$) or 4mg/ml (LEMS = 114±9%, OND = 120±11%; $n=5$).

K^+-stimulated Ca^{2+} flux was also measured after exposure to **IgG from individual LEMS or OND patients.** In SKNSH cells, 14 LEMS and 6 OND samples were tested. There was no significant difference (unpaired t-test) in the mean stimulated flux for the LEMS IgG treated cells (87±4% of control levels) and the OND IgG treated cells (91±5% of control levels). The LEMS samples tested

included those which comprised the IgG pool described above. However, when tested individually, these preparations did not affect K^+-stimulated Ca^{2+} flux (93±3% of control levels). There was no specific effect of LEMS IgG on stimulated flux in the Kelly cells, although the means for both LEMS and OND IgG were higher than control levels (128±9%, n=11 and 124±8%, n=6 respectively). Figure 3.12 shows the individual and mean results for single IgG preparations in both cell lines.

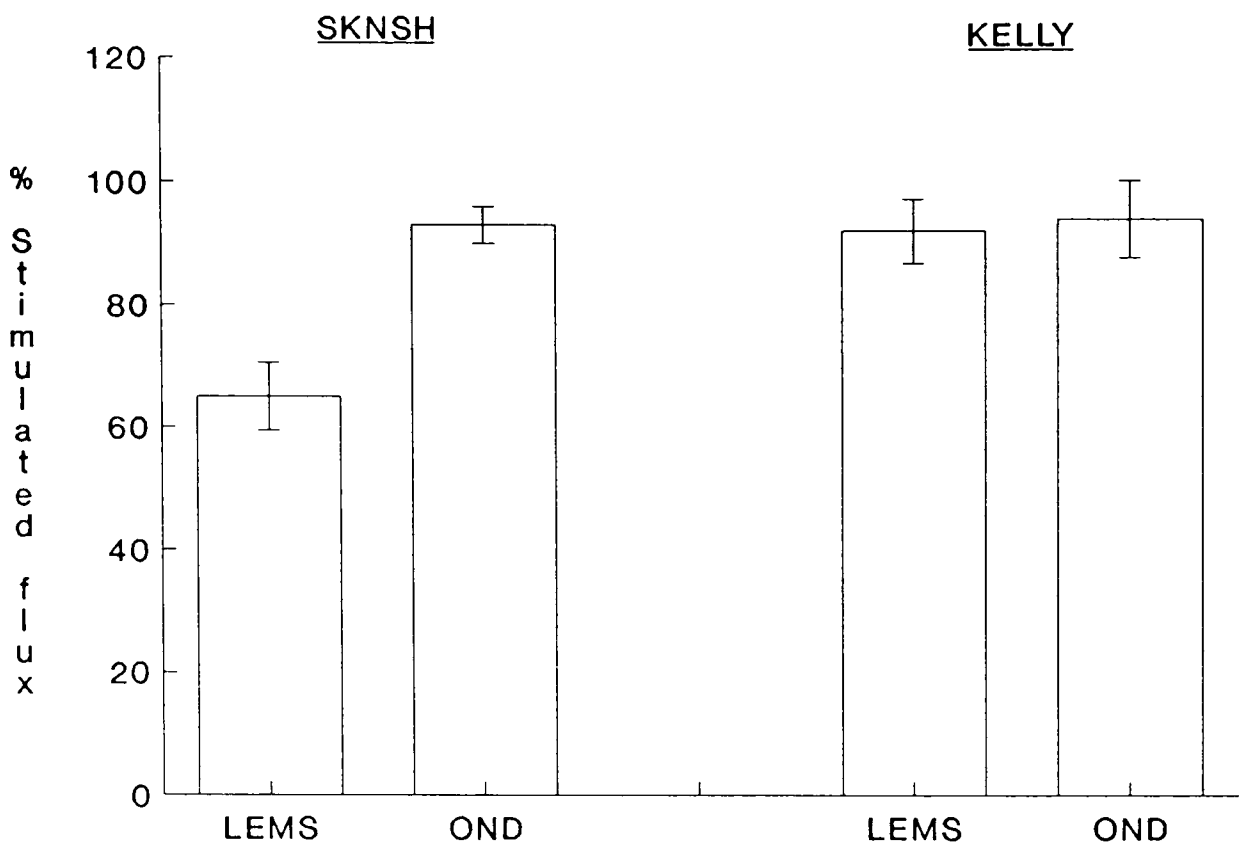
As SKNSH cells had reduced levels of K^+-stimulated Ca^{2+} flux after treatment with pooled LEMS IgG, this line was chosen to investigate the type of calcium channel affected by LEMS antibodies. Figure 3.13 shows that after the exposure of cells to LEMS IgG the decreased level of flux is still partially blocked by both nitrendipine (1μM) and ωCgTx (1μM), in approximately the same proportions as seen in control cells. Similarly, OND IgG had no effect on the proportion of flux blocked by these two antagonists.

Figure 3.11: The effect of pooled IgG on K^+-stimulated calcium flux.

SKNSH and Kelly cells were grown for 2 days in the presence of pooled LEMS or OND IgG (2mg/ml), each composed of 6 individual samples. The K^+-stimulated flux measured in treated cells is expressed as a percentage of that measured in cells grown in parallel in medium alone. Means and SEMs are shown for 5-6 separate analyses using the same IgG pools.

Figure 3.12: The effect of single IgG preparations on K^+-stimulated calcium flux

SKNSH and Kelly cells were grown for 2 days in culture medium containing 2mg/ml IgG, prepared from the plasma of individual LEMS or OND patients. K^+-stimulated flux is shown as a percentage of that measured in untreated cells. O = SCLC-LEMS, Δ = NCD-LEMS, ∇ = OND. The means and SEMs are shown adjacent to each group of individual results ($\Diamond$).


SKNSH
KELLY
120
100
80
60
40
20
0
% Stimulated flux
LEMS
OND
LEMS
OND

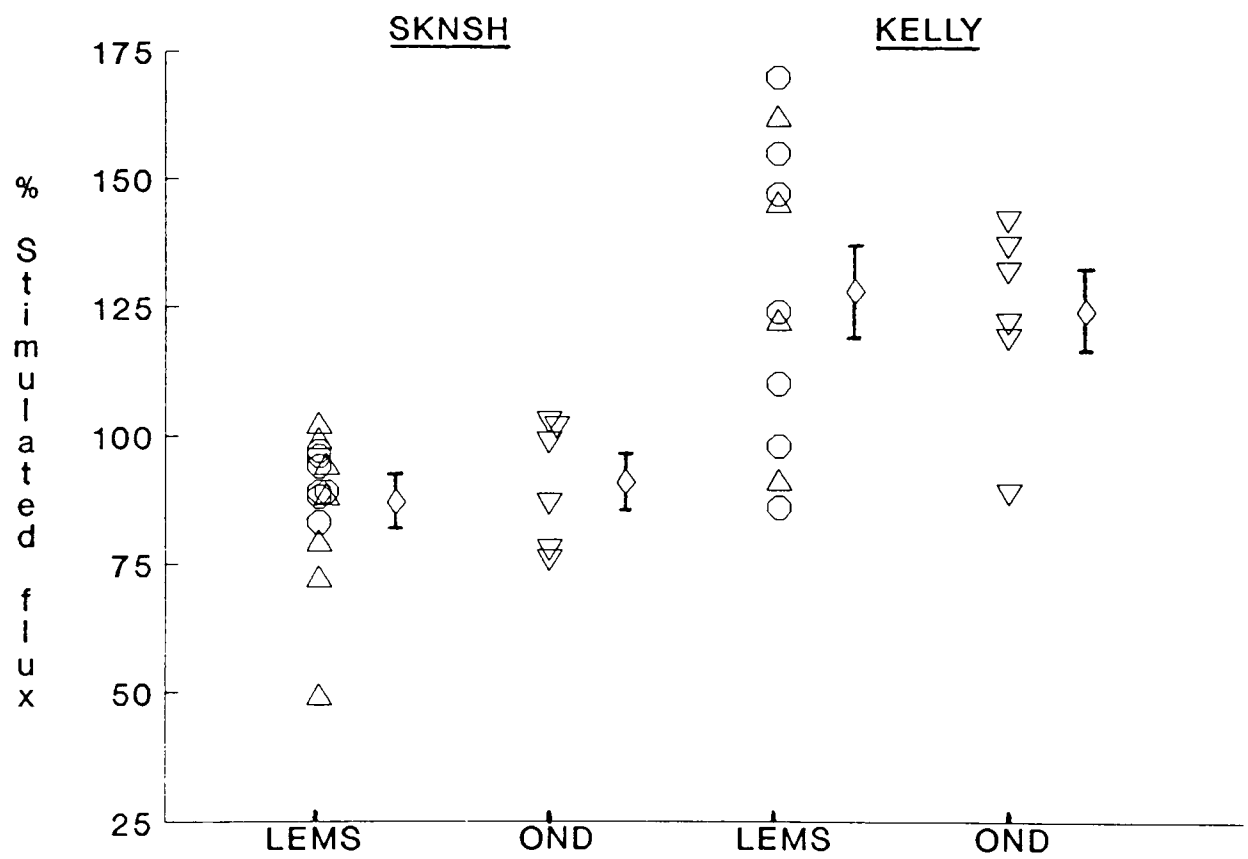
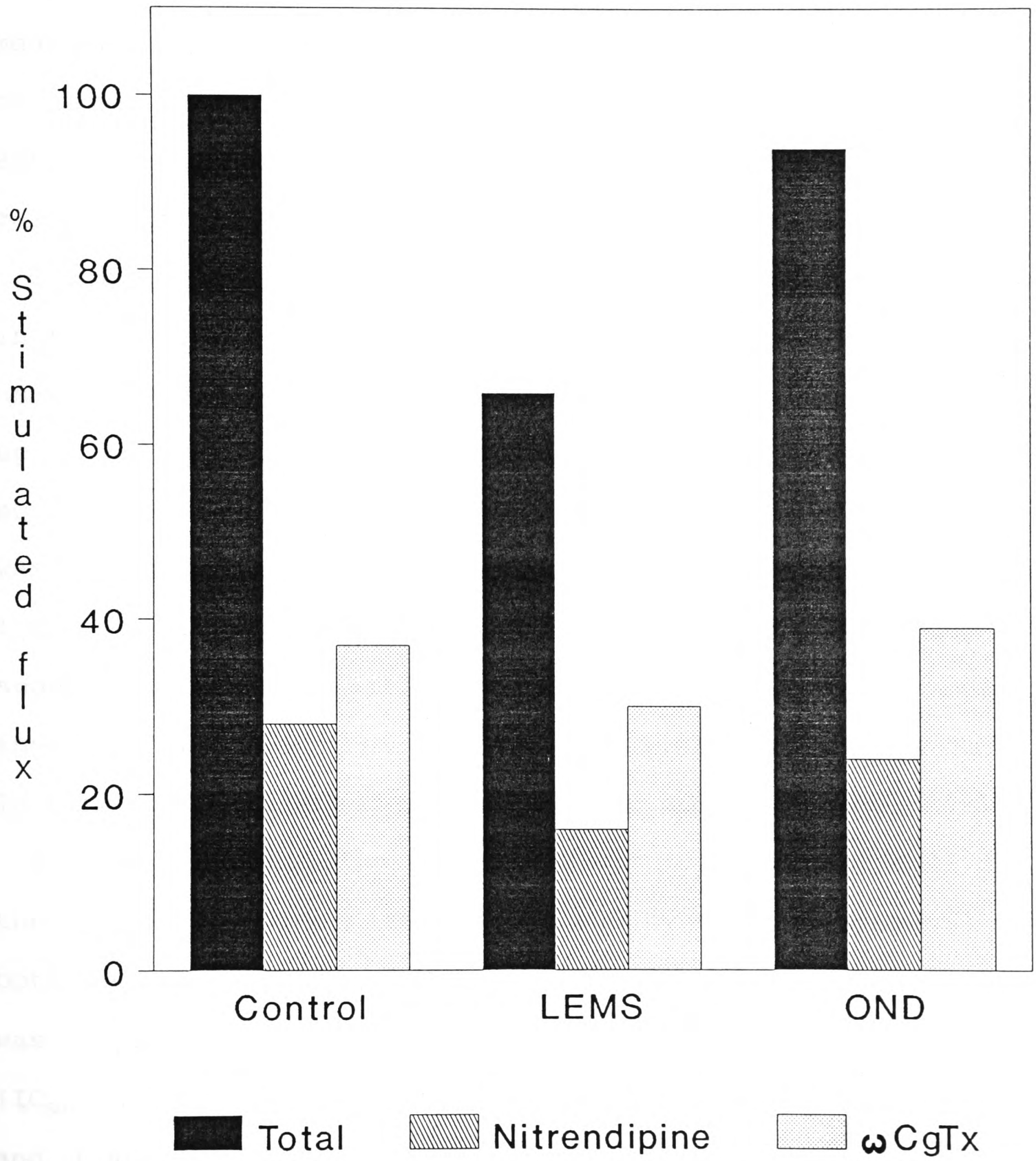

SKNSH
KELLY
175
150
125
100
75
50
25
% Stimulated flux
LEMS
OND
LEMS
OND

Figure 3.13: Inhibition of K^+-stimulated calcium flux by antagonists in IgG-treated cells.

SKNSH cells were grown for 2 days in the presence of pooled LEMS or OND IgG (2mg/ml), or in culture medium alone (control). K^+-stimulated flux was measured after incubation with PBS alone (total), or PBS containing nitrendipine (1μM) or ωCgTx (1μM). Results are expressed as a percentage of the flux measured in untreated cells in the absence of antagonist.

For comparison with control cells, the proportions of total flux in IgG treated cells measured after incubation with antagonist are included in the following table (in brackets):

	K^+-stimulated Ca^{2+} flux (% of control)		
	Total	Nitrendipine (1μM)	ωCgTx (1μM)
Control	100	28	37
LEMS	65	16 (25%)	30 (46%)
OND	93	24 (26%)	39 (42%)


100
80
60
40
20
0
% Stimulated flux
Control
LEMS
OND
Total
Nitrendipine
ωCgTx

3.4 Discussion

In these studies the presence of VGCCs was demonstrated in six cultured cell lines of neuronal origin using the technique of K^+-stimulated $^{45}Ca^{2+}$ influx. Stimulated flux was rapid, reaching a maximum level within 60 seconds. By contrast, the basal flux measured in the presence of low K^+ concentrations was independent of time. The time course of K^+-stimulated calcium flux was in agreement with previous studies in PC12 cells showing half-maximal calcium uptake within 30 seconds (Toll 1982).

Stimulated flux was dependent on the concentration of potassium in the depolarising buffer. Calcium uptake could not be detected using 25mM KCl, but increased with higher potassium concentrations up to a maximum level at around 100mM KCl. Using the Nernst equation (see 3.3.1) it is possible to deduce that calcium flux was detected at membrane potentials of greater than -30mV, indicating the activation of HVA channels. Stallcup (1979) suggests that calcium flux measured under these conditions involves channels that inactivate slowly or not at all. Long lasting currents are a characteristic of HVA channel activation.

K^+-stimulated calcium uptake was inhibited in all cell lines by the dihydropyridine nitrendipine and by methoxyverapamil (D600), both well-characterised VGCC antagonists. However, the inhibition was complete only in the PC12 cell line. Half maximal inhibition (IC_{50}) in this cell line was calculated as 4.5nM for nitrendipine and 1.4μM for D600. These values are in agreement with other studies in PC12 cells using similar methods, for example Toll (1982) reports IC_{50}s of 5.5nM for nitrendipine and 3.5μM for D600. In the other cell lines, the maximum inhibitory effect of

nitrendipine was not reached at 10μM, therefore IC_{50} values could not be calculated. It was technically difficult to increase the concentration of nitrendipine further owing to its insolubility in water. Also non-specific effects are likely to occur at very high concentrations.

The neuronal calcium channel blocker, ω-conotoxin, also produced only partial inhibition of K^+-stimulated calcium flux. With the exception of the NG108 cell line, micromolar concentrations of ω-conotoxin were required to produce an effect. The lack of inhibition by ωCgTx at lower concentrations may be due to the presence of low levels of Ca^{2+}, which was shown to inhibit ωCgTx binding (see Chapter 4). No inhibition at all was found in the PC12 cells. Added together, the amount of inhibition by nitrendipine and ω-conotoxin approximates to 100% in each cell line (see Table 3.2). This suggests the existence of two distinct channel subtypes: one DHP-sensitive and the other ω-conotoxin-sensitive, neither being affected by the other antagonist. PC12 cells appear to express a single class of calcium channel which is DHP-sensitive but not affected by ω-conotoxin. It is possible that nitrendipine and ω-conotoxin are acting on the same channel in the other cell lines, leaving a portion of calcium uptake that cannot be inhibited by either antagonist. However, when both antagonists were used together in the neuroblastoma lines SKNSH and Kelly, complete inhibition of K^+-stimulated flux was produced.

Patch-clamp recordings in chick dorsal root ganglia and rat hippocampal and sympathetic neurones suggest that ω-conotoxin inhibits both L (DHP-sensitive) channels and N (DHP-insensitive)

channels (Fox et al 1987, McCleskey et al 1987). If this were true for all neurones one would expect ω-conotoxin to completely abolish K^+-stimulated calcium flux in all of the cells studied here. However, further studies of calcium currents in DRG neurones have revealed a DHP-sensitive current that is resistant to ω-conotoxin (Aosaki and Kasai 1989). Also studies of other neuronal cells suggest that ω-conotoxin may act primarily on a subtype of VGCC that is DHP-resistant. Sher et al (1988) found that nitrendipine and ω-conotoxin affected different phases of the calcium current in cultured neuroblastoma and PC12 cells. Plummer et al (1989) reported that the major component of the calcium current seen in PC12 cells and rat superior cervical ganglia was carried by N-type channels that were sensitive to ω-conotoxin. The L channels in these cells were insensitive to ω-conotoxin. Finally, Carbone et al (1990) found that ω-conotoxin blocked only part of the current in IMR32 cells and that the remainder was DHP-sensitive. These reports, together with the present studies, suggest that nitrendipine and ω-conotoxin affect two distinct subtypes of calcium channel.

It has already been mentioned that some groups find calcium currents in PC12 cells which are partially inhibited by ω-conotoxin (Sher et al 1988, Plummer et al 1989). Plummer reports however that the density of N channels in PC12s increases more than five-fold during differentiation in the presence of nerve growth factor. Kongsamut and Miller (1986) show that neurotransmitter release in undifferentiated PC12 cells is extremely sensitive to DHPs, whereas after differentiation transmitter release is not affected by DHPs. It is possible,

therefore, that the undifferentiated PC12 cells used here show no detectable sensitivity to ω-conotoxin owing to a very low density or even a complete absence of N channels, and a predominant expression of L channels that are DHP but not ω-conotoxin-sensitive.

Differentiation is also thought to affect calcium channel expression in other cultured cell lines. For example T, N and L channels have been described in differentiated NG108 cells (Docherty 1988) but only T and L channels appear to be present on undifferentiated NG108 cells (Peers et al 1990).

An attempt was made to modify calcium channel expression in the PC12 and NG108 lines used here by supplementing the culture medium with 1mM dibutyryl cAMP. Treated cells developed neurites and became neuronal in appearance. Growth was also halted and the cells did not reach confluence. However, the amount of stimulated calcium flux in these cells was no higher than in untreated cells, and in the PC12 cells slightly reduced. Sensitivity to the antagonists nitrendipine and ω-conotoxin was also unchanged. It may be necessary to use alternative methods of differentiation to induce changes in channel type. Human neuroblastoma cells have previously been treated with dibutyryl cAMP for 12 days to induce differentiation (Sher et al 1989a). Other groups have used nerve growth factor (Plummer et al 1989), dibutyryl cAMP with nerve growth factor (Kongsamut and Miller 1986) and prostaglandin E1 with 3-isobutyl-1-methylxanthene (IBMX) which increases intracellular cAMP levels by 10-100 fold (Freedman and Miller 1984).

The presence of at least two subtypes of calcium channel in a

single cell type provides an interesting model with which to study the action of LEMS antibodies. Individual IgG preparations from LEMS patients have previously been shown to block calcium influx in SCLC lines (Roberts et al 1985, De Aizpurua et al 1988) and also PC12, NG108 and F21D1 lines (Lang et al 1989a,b). The extent of the inhibition varied considerably between patients and 5 of the 19 LEMS samples tested by De Aizpurua did not inhibit stimulated flux at all. However, the mean results for the LEMS patients in the published studies were significantly different from those for the controls. Similar effects of LEMS IgG have not been reported in neuroblastoma cell lines. IgG from individual patients was tested here in the neuroblastoma lines SKNSH and Kelly. The mean amount of K^+-stimulated calcium flux measured in cells treated with IgG from LEMS patients was not significantly different from the amount measured in control cells, in either cell line. However, in the SKNSH cells, pooled IgG from LEMS patients reduced the amount of K^+-stimulated flux compared to control levels, while a control IgG pool had no effect. No such effect was observed in the Kelly cell line. The lack of inhibition by individual LEMS samples was surprising as both cell lines are of human origin and thus may express calcium channels similar in structure to those at the human NMJ. It was, therefore, expected that LEMS IgG would have a greater and more consistent effect on these cells than on the rodent lines previously studied. The fact that there is inhibition by pooled LEMS IgG in the SKNSH cells suggests that there is some cross-reactivity between the NMJ and SKNSH calcium channels, but implies that binding to several epitopes by a mixture of antibodies is necessary to induce down-regulation. It is

questionable whether this is a physiologically relevant result as each individual patient has the antibody or antibodies necessary to produce the symptoms of LEMS.

Previous studies demonstrating the inhibition of K^+-stimulated calcium uptake by LEMS IgG have not provided any information on the type of calcium channel affected. In this study, K^+-stimulated calcium flux was reduced to 65% of control levels by pooled LEMS IgG in SKNSH cells, which contained both DHP-sensitive and ωCgTx-sensitive VGCCs. It was possible that the inhibition of calcium flux in SKNSH cells was due to a selective action of LEMS IgG on a particular VGCC subtype. This was investigated by the sensitivity to antagonists of the K^+-stimulated flux remaining after exposure to LEMS IgG. The proportions of K^+-stimulated calcium flux blocked by nitrendipine and ω-conotoxin in IgG-treated cells were similar to the proportions blocked in untreated cells. This suggests that pooled LEMS IgG acts on both DHP-sensitive and ωCgTx-sensitive subtypes of calcium channel in SKNSH cells.

3.5 Summary

The presence of VGCCs was demonstrated in six undifferentiated neuronal cell lines by the technique of K^+-induced $^{45}Ca^{2+}$ influx. Three human neuroblastoma cell lines, a rat-mouse hybrid, a human-mouse hybrid and a rat pheochromocytoma line (PC12) were studied. With the exception of the PC12 cells, each line seemed to express two distinct calcium channel subtypes: one DHP-sensitive and one ω-conotoxin-sensitive. The K^+-stimulated calcium flux measured in the PC12 cells was carried by DHP-sensitive channels only and ω-conotoxin was without effect.

Chemical differentiation with dibutyryl cAMP in two cell lines tested (NG108 and PC12) did not increase levels of calcium uptake or alter the antagonist sensitivity of the VGCCs expressed.

Down-regulation of VGCCs occurred in the human neuroblastoma line SKNSH after exposure to pooled LEMS IgG, while pooled IgG from OND patients was without effect. The LEMS antibodies appeared to affect both VGCC subtypes equally, as measured by antagonist sensitivity of the calcium flux remaining after IgG treatment. Inhibition of calcium flux was not detected after exposure to individual IgG preparations from LEMS patients.

CHAPTER 4

RADIOLIGAND BINDING STUDIES

4.1. Introduction

The use of radiolabelled ligands to detect the presence of specific binding sites complements the data obtained from functional studies, such as those discussed in the previous chapter. Labelled dihydropyridines have been the most widely used ligands for studying voltage gated calcium channels. Saturable, high-affinity binding has been described in smooth muscle, cardiac muscle and neuronal preparations. DHP binding to skeletal muscle is of lower affinity but binding site density is much higher (see Table 1.2). There is a high correlation between the affinity of DHPs for membrane binding sites and their effects on events such as depolarisation-induced contraction in smooth muscle (Triggle and Janis 1987) or neurotransmitter release from DRG cells (Miller 1987). It is, therefore, thought that high affinity DHP binding sites correspond to VGCCs, and that the binding assay represents ligand behaviour at functional VGCCs in intact tissue.

[^{3}H]-Nitrendipine has been extensively used to characterise the properties of the DHP binding site. However, its analogue [^{3}H]-PN200-110 has a 10-fold higher affinity for the binding site and a low degree of non-specific binding (Lee et al 1984). [^{3}H]-PN200-110 is thus suitable as an improved ligand for the detection of DHP binding sites.

Despite the presence of high affinity DHP binding sites in brain, some neuronal processes were found to be insensitive to

these agents. It is now clear that neurones contain a heterogeneous population of DHP-sensitive and DHP-insensitive VGCCs. The iodination of ω-conotoxin has provided a new radioligand of high specific activity with which to study neuronal VGCCs. ^{125}I-ωCgTx binds irreversibly and with high affinity to a site distinct from both the DHP and the verapamil target sites (Cruz and Olivera 1986).

In these studies, [^{3}H]-PN200-110 and ^{125}I-ωCgTx were used to confirm the presence and specificity of VGCCs in cultured neuronal cells. Membranes prepared from PC12, NG108, human neuroblastoma (SKNSH, Kelly and IMR32) and human small cell lung carcinoma (MAR5) lines were studied. Binding to rat brain membranes was performed to standardise the assay conditions and for a comparison with existing studies in the literature.

4.2. Methods

4.2.1. Binding of [^{3}H]-PN200-110 to cell membranes

These experiments were performed under sodium light. 100-400µg membrane protein was incubated with increasing amounts of [^{3}H]-PN200-110 (85 Curies/mmol) in 500µl buffer (50mM Tris-HCl, 10mM Hepes, 1.5mM $CaCl_2$, pH 7.4). Tubes were set up in triplicate for each concentration of [^{3}H]-PN200-110. Identical tubes were also set up containing 10µM nitrendipine in order to measure non-specific [^{3}H]-PN200-110 binding. Membranes were incubated for 1 hour at room temperature and then collected on glass fibre filters (GF/C) using a multiple membrane filtration apparatus (Linca Lamon Instrumentation Co. Ltd, Tel-Aviv). The filters were rapidly washed three times with 3mls cold 50mM Tris-HCl, pH 7.4, to remove unbound [^{3}H]-PN200-110. They were then counted in tubes containing 4mls scintillation fluid in a Beckman liquid scintillation counter at 40% efficiency. Specific binding was calculated by subtracting non-specific binding from the total binding obtained in the absence of nitrendipine. Maximum binding capacity (B_{max}) and affinity of [^{3}H]-PN200-110 for membranes (K_D) were determined by non-linear regression analysis of the binding curve.

The effect of the antagonists nitrendipine, nifedipine and methoxyverapamil (D600) on specific [^{3}H]-PN200-110 binding was studied by incubating increasing concentrations of antagonist with membranes 5 minutes prior to the addition of a constant amount (approximately the K_D concentration) of ligand. Incubation and filtration was then carried out as above. Inhibition curves were constructed and IC_{50} values (the concentration at which 50% specific binding is inhibited) determined by non-linear

regression. Inhibition constants (K_i) were calculated by the equation of Cheng and Prusoff (1973) assuming competitive inhibition kinetics:

$$K_i = \frac{IC_{50}}{1 + (S/K_D)}$$

Where S = concentration of [^{3}H]-PN200-110 used and K_D = affinity of [^{3}H]-PN200-110.

4.2.2. Binding of ^{125}I-ω-conotoxin to cell membranes

^{125}I-ωCgTx (approximately 2000Ci/mmole) was supplied as the lyophilized peptide and was reconstituted in 1% acetic acid at a concentration of 100μCi/ml. It was then stored in 1μCi (10μl) aliquots at -20°C. Unlabelled ω-conotoxin was handled similarly and stored at a concentration of 100μM. After thawing, ω-conotoxin was kept on ice and the acetic acid was neutralised with 1M NaOH immediately prior to use.

Approximately 25μg membrane protein was incubated with increasing concentrations of ^{125}I-ωCgTx in 250μl buffer (25mM Tris-HCl, 5mM Hepes, 0.32M sucrose, 1μM pepstatin, 2μM leupeptin, 0.1mM PMSF, 20μg/ml soybean trypsin inhibitor, 0.5% BSA, pH 7.4). Non-specific binding was determined by the presence of 0.5μM unlabelled ω-conotoxin. After 60 minutes at room temperature the membranes were collected on GF/C filters which were presoaked in 0.3% polyethyleneimine (PEI) to reduce non-specific ^{125}I-ωCgTx binding to filters. The filters were washed three times with 3mls cold buffer (50mM Tris-HCl, 1.5mM $CaCl_2$, 0.2% BSA, pH 7.4) and counted in a gamma counter (Packard autogamma 500C) at 80%

efficiency. B_{max} and apparent K_D values were calculated as described above.

Inhibition curves for unlabelled ω-conotoxin and various cations were constructed by incubating increasing concentrations of the inhibitor with membranes for 5-10 minutes before the addition of 25pM ^{125}I-ωCgTx to each tube.

To study the effect of IgG on the number of ^{125}I-ωCgTx binding sites, cells were grown for 2 days prior to harvesting in medium containing 2mg/ml IgG. Membranes were prepared and the amount of binding of a saturating concentration (150pM) of ^{125}I-ωCgTx was determined. The number of specific binding sites was expressed as a percentage of that found in cells grown simultaneously in medium alone.

4.3. Results

4.3.1. Time course of [^{3}H]-PN200-110 binding

The increase of specific [^{3}H]-PN200-110 binding with time is shown in Figure 4.1. An assay using PC12 membranes is illustrated, but the time course was similar for the other preparations tested. Specific binding reached a maximum level at 60 minutes at room temperature. Membranes were,therefore,incubated with ligand for 60 minutes in the following assays to represent binding at equilibrium.

4.3.2. [^{3}H]-PN200-110 binding to rat brain

The specific binding of [^{3}H]-PN200-110 to membranes prepared from rat brains was saturable and of high affinity (B_{max} = 98$\pm$8 fmoles/mg protein, K_D = 0.28$\pm$0.06 nM; means and SEMs of 12 analyses). Figure 4.2. shows the total, non-specific and specific binding curves for a typical assay using rat brain membranes. The Scatchard plot of the specific binding data shows a straight line, characteristic of one class of binding sites. The B_{max} and K_D values obtained from the Scatchard plot were similar to those obtained by non-linear regression analysis.

Specific binding was inhibited by the DHPs nitrendipine and nifedipine at low concentrations (K_is 4.66$\pm$1.65 nM, n=4, and 6.03 nM, n=2, respectively). By contrast, specific binding was not significantly affected by the antagonists verapamil and ω-conotoxin. Typical inhibition curves are shown in Figure 4.3.

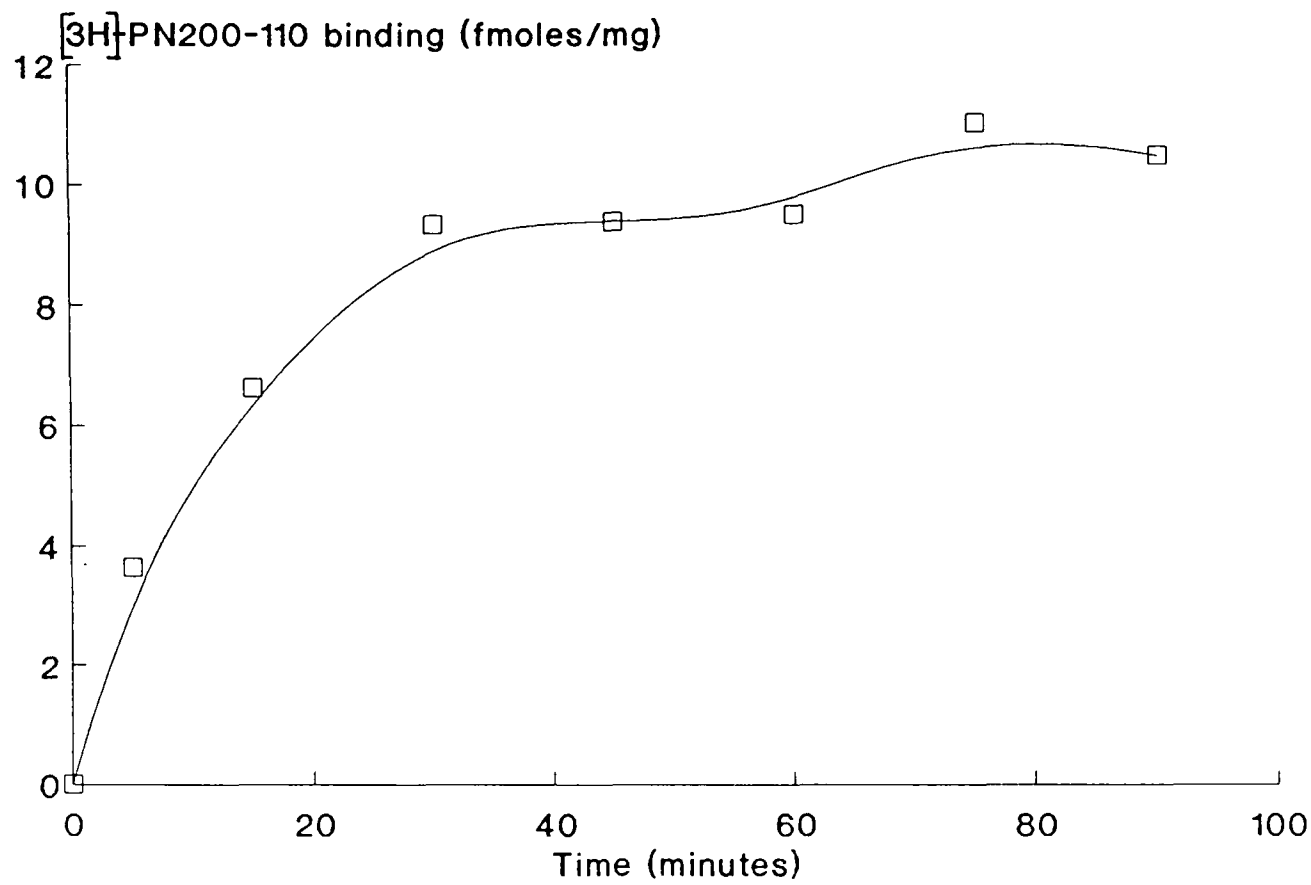


Figure 4.1: Time course of [^{3}H]-PN200-110 binding to PC12 membranes

Membranes were incubated with a saturating concentration of [^{3}H]-PN200-110 (1.5nM) at room temperature and the amount of specific binding (total - non-specific) was determined from 5 to 90 minutes. Non-specific binding was defined as the amount measured in the presence of 10μM nitrendipine.

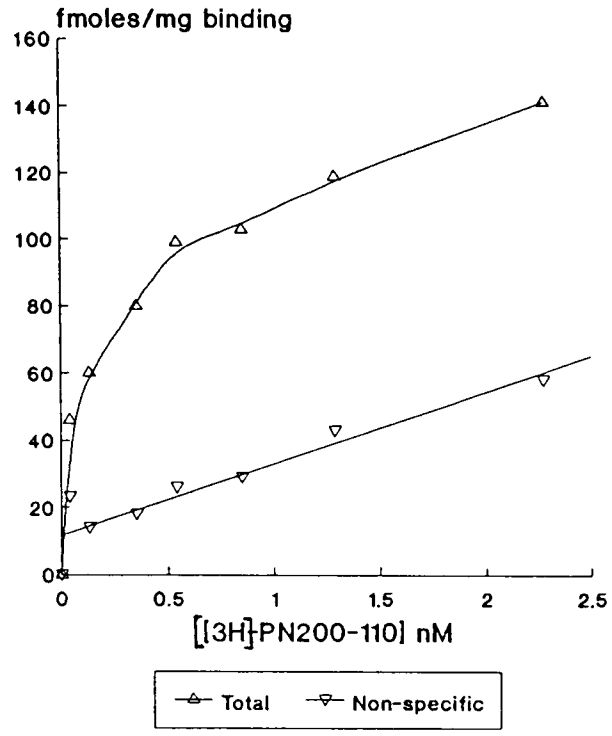
Figure 4.2: [^{3}H]-PN200-110 binding to rat brain membranes

(a) Total binding (Δ) was determined by incubating membranes with increasing amounts of [^{3}H]-PN200-110 for one hour at room temperature. Membranes were preincubated with 10μM nitrendipine before the addition of [^{3}H]-PN200-110 to determine non-specific binding (▽).

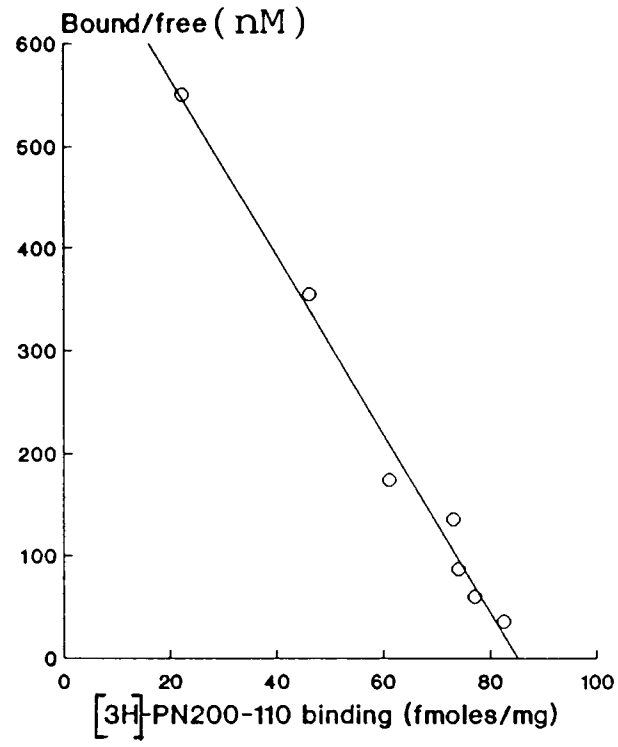
(b) Typical saturation binding curve of [^{3}H]-PN200-110 binding to rat brain membranes. Specific binding = total binding - non-specific binding. B_{max} and K_D values were calculated by non-linear regression. (B_{max} = 98±8 fmoles/mg protein, K_D = 0.28±0.06 nM, n=12.)

(c) Scatchard analysis of the specific binding data shown in (b). Abscissa = amount of specific binding. Ordinate = specific binding/unbound ligand concentration.

(a)


fmoles/mg binding
160
140
120
100
80
60
40
20
0
0
0.5
1
1.5
2
2.5
[[3H]-PN200-110] nM
Total
Non-specific

(c)


Bound/free (nM)
600
500
400
300
200
100
0
0
20
40
60
80
100
[3H]-PN200-110 binding (fmoles/mg)

(b)

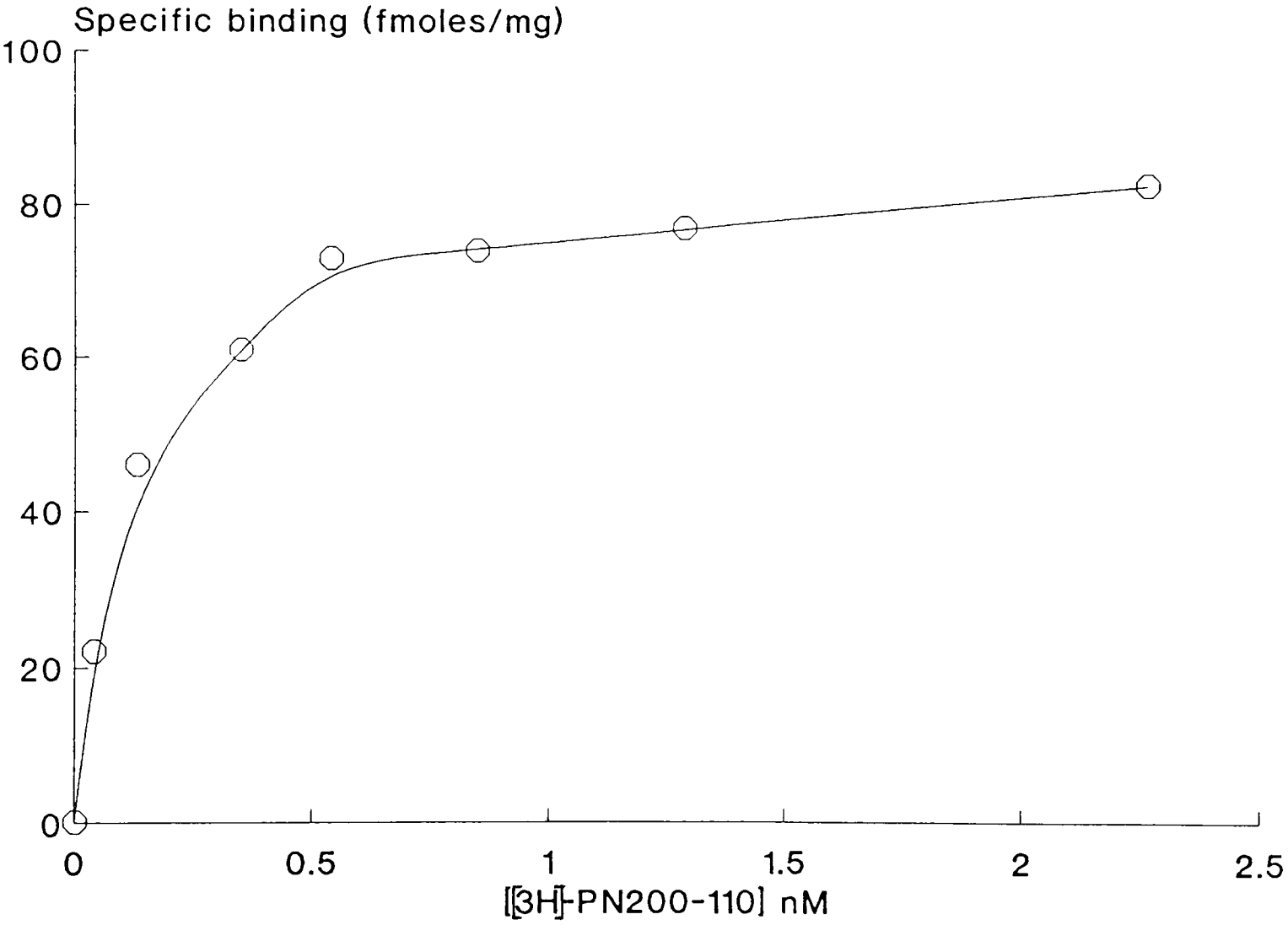
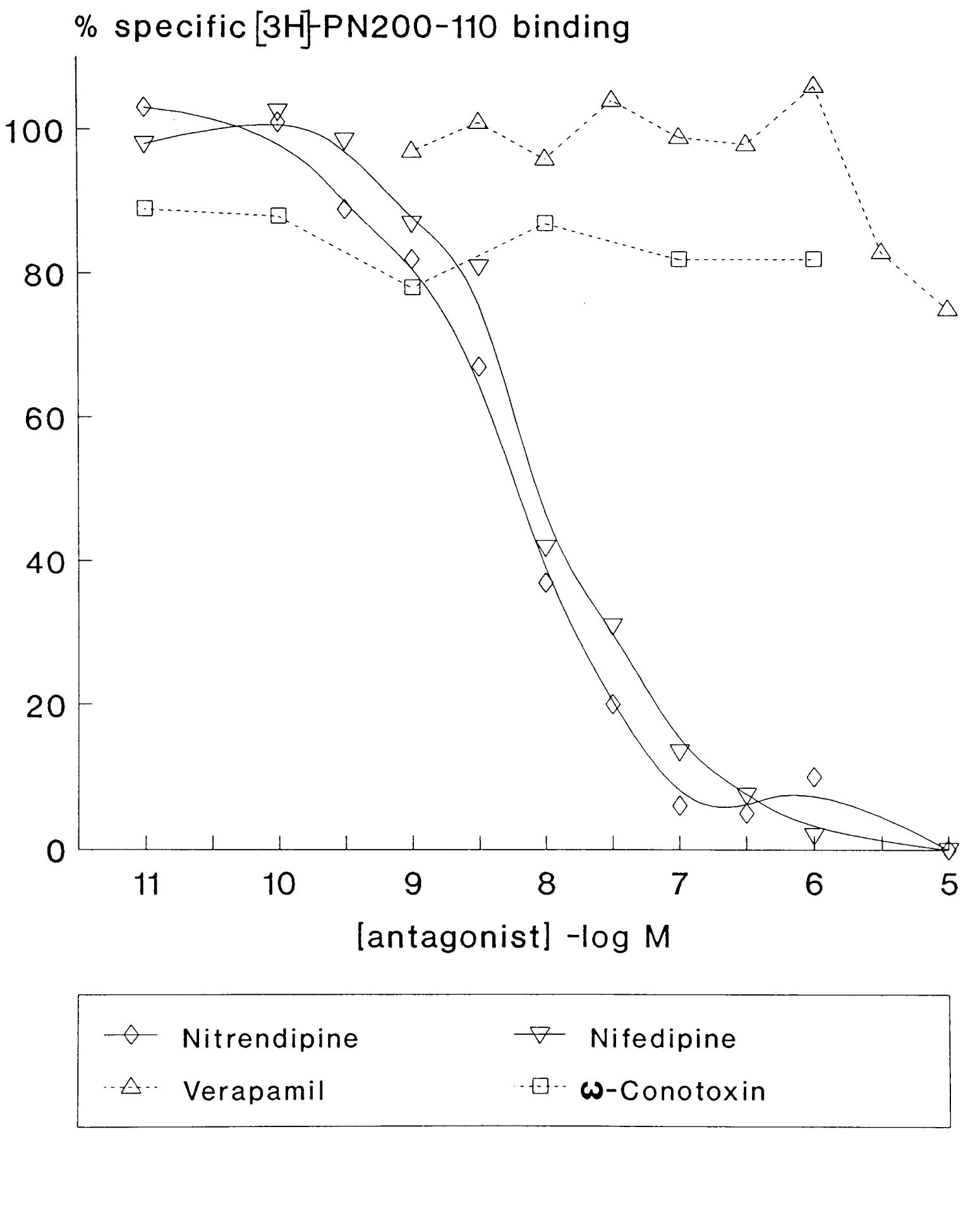

Specific binding (fmoles/mg)
100
80
60
40
20
0
0
0.5
1
1.5
2
2.5
[[3H]-PN200-110] nM

Figure 4.3: Inhibition of [^{3}H]-PN200-110 binding in rat brain membranes by antagonists

Membranes were incubated with increasing concentrations of antagonist before the addition of an approximate K_D concentration (0.2nM) of [^{3}H]-PN200-110. The data is expressed as the percentage of specific binding measured in the absence of antagonist. IC_{50} values for nitrendipine and nifedipine were calculated by non-linear regression and converted to K_i values by the equation of Cheng and Prusoff (see Methods). (K_i nitrendipine = 4.66$\pm$1.65 nM, n=4, K_i nifedipine = 6.03 nM, n=2.)


% specific [3H]-PN200-110 binding
100
80
60
40
20
0
11
10
9
8
7
6
5
[antagonist] -log M
Nitrendipine
Nifedipine
Verapamil
ω-Conotoxin

4.3.3. [^{3}H]-PN200-110 binding to neuronal cell membranes

A saturable population of specific binding sites was detected in PC12 membranes (Figure 4.4). The binding site density was low (B_{max} = 22.7±3.3 fmoles/mg protein, n=6) and the affinity of binding was lower than that found in rat brain, although still in the nanomolar range (K_D = 0.59±0.19 nM, n=6). The specificity of [^{3}H]-PN200-110 binding to PC12 membranes was demonstrated by antagonist inhibition studies (Figure 4.5). Specific binding was inhibited by nitrendipine and nifedipine (K_is 6.91±1.15 and 8.06±5.11 nM respectively, n=3) but only affected by methoxyverapamil (D600) at very high concentrations.

By contrast, saturable [^{3}H]-PN200-110 binding could not be demonstrated in MAR5, NG108, SKNSH or Kelly cell membranes. Figure 4.6 shows the binding data for a typical experiment using MAR5 membranes. Although there was some displacement of total binding by nitrendipine, the specific binding thus detected conformed to a straight line. The Scatchard plot was curvilinear, indicative of the presence of two classes of binding sites, one of very low affinity and therefore possibly a non-specific site. There was insufficient data to resolve the binding accurately into two sites, but there appeared to be less than 20 fmoles/mg protein of the high affinity site.

Similar binding properties were found in NG108, SKNSH and Kelly cell membranes. Specific [^{3}H]-PN200-110 binding was unsaturable and Scatchard analysis of the data indicated the presence of two binding sites, with less than 10 fmoles/mg protein of the high affinity site. Figure 4.7 illustrates the specific binding in NG108 membranes; similar binding curves were obtained for the

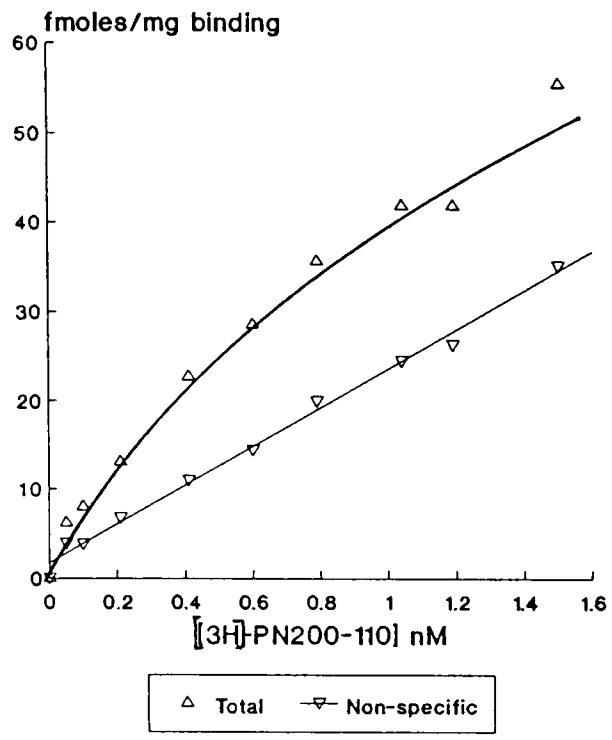
SKNSH and Kelly cells. The binding of low concentrations of ligand to NG108 membranes was inhibited by nitrendipine and nifedipine but not by D600 (Figure 4.8), thus providing further evidence for the presence of a high affinity DHP binding site. The K_i values obtained for nitrendipine and nifedipine in NG108s (8.3 and 7.1 nM respectively) were similar to those found for the inhibition of binding in PC12 membranes.

Low levels of a single high affinity binding site were detected in the IMR32 cell line (B_{max} = 6.1 fmoles/mg protein, K_D = 0.06 nM). The properties of [^{3}H]-PN200-110 binding to the membrane preparations tested are summarised in Table 4.1.

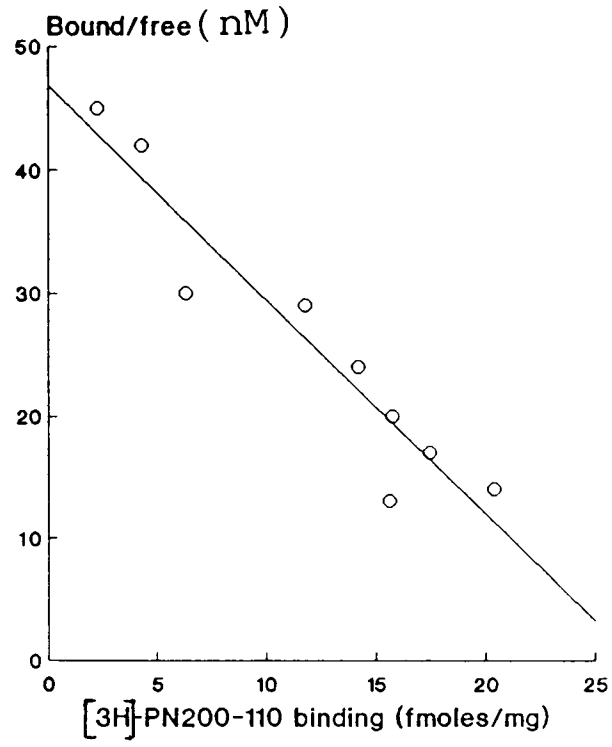
Figure 4.4: $[^3H]$-PN200-110 binding to PC12 membranes

(a) Total, non-specific and (b) specific binding of $[^3H]$-PN200-110 to membranes prepared from cultured PC12 cells. Non-specific binding was determined in the presence of 10μM nitrendipine. (B_{max} = 22.7±3.3 fmoles/mg protein, K_D = 0.59±0.19 nM, n=6.) (c) Scatchard analysis of the specific binding data shown in (b). Abscissa = specific $[^3H]$-PN200-110 binding. Ordinate = specific binding/ unbound ligand concentration.

(a)


fmoles/mg binding
60
50
40
30
20
10
0
0
0.2
0.4
0.6
0.8
1
1.2
1.4
1.6
[3H]-PN200-110] nM
Total
Non-specific

(c)


Bound/free (nM)
50
40
30
20
10
0
0
5
10
15
20
25
[3H]-PN200-110 binding (fmoles/mg)

(b)

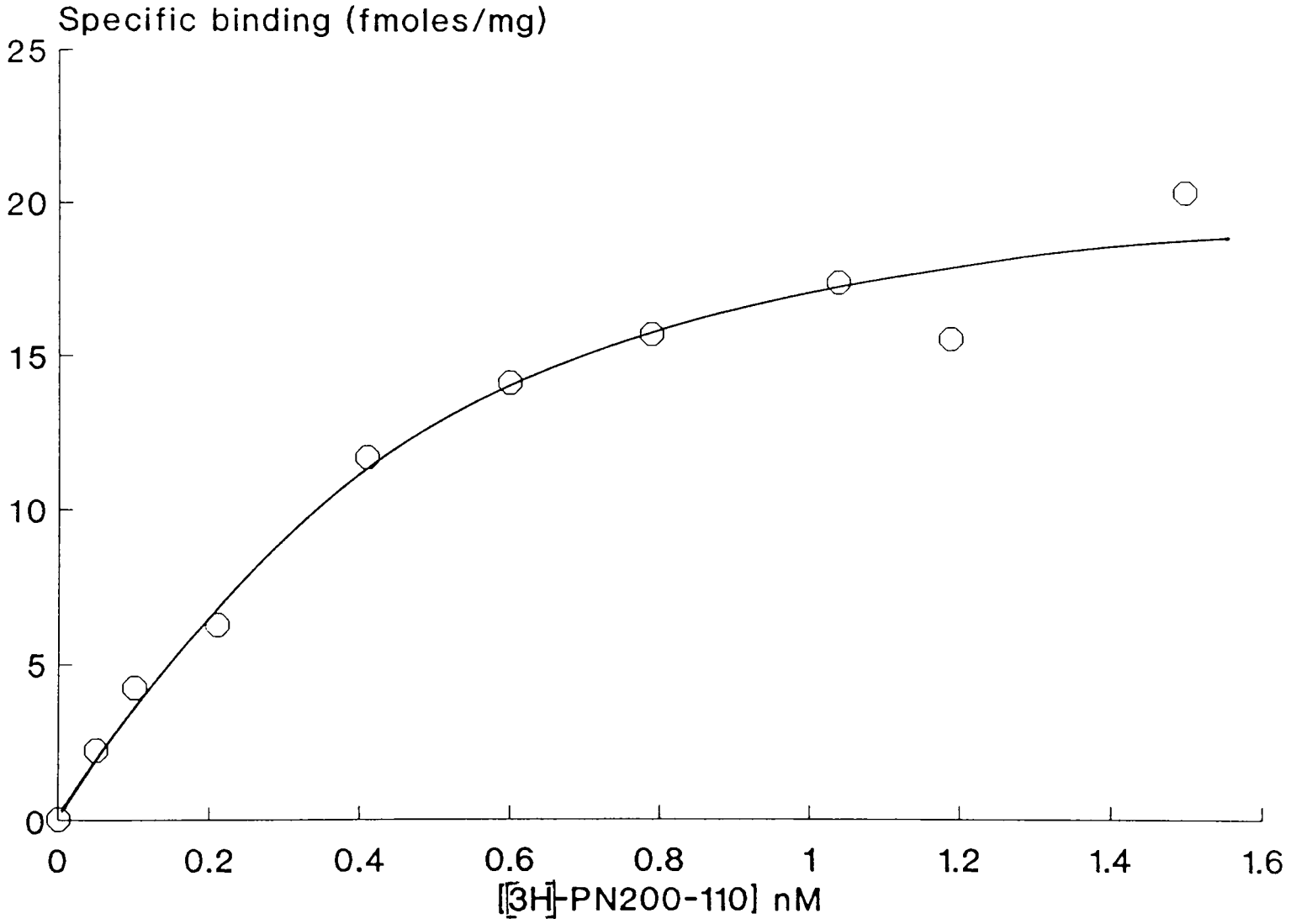

Specific binding (fmoles/mg)
25
20
15
10
5
0
0
0.2
0.4
0.6
0.8
1
1.2
1.4
1.6
[3H]-PN200-110] nM

Figure 4.5: Inhibition of [^{3}H]-PN200-110 binding to PC12 membranes by antagonists

Membranes were incubated with increasing concentrations of antagonist before the addition of an approximate K_D concentration (0.5nM) of [^{3}H]-PN200-110. Results are expressed as the percentage of specific binding measured in the absence of antagonist. (K_i nitrendipine = 6.91±1.15 nM, n=3, K_i nifedipine = 8.06±5.11 nM, n=3.)

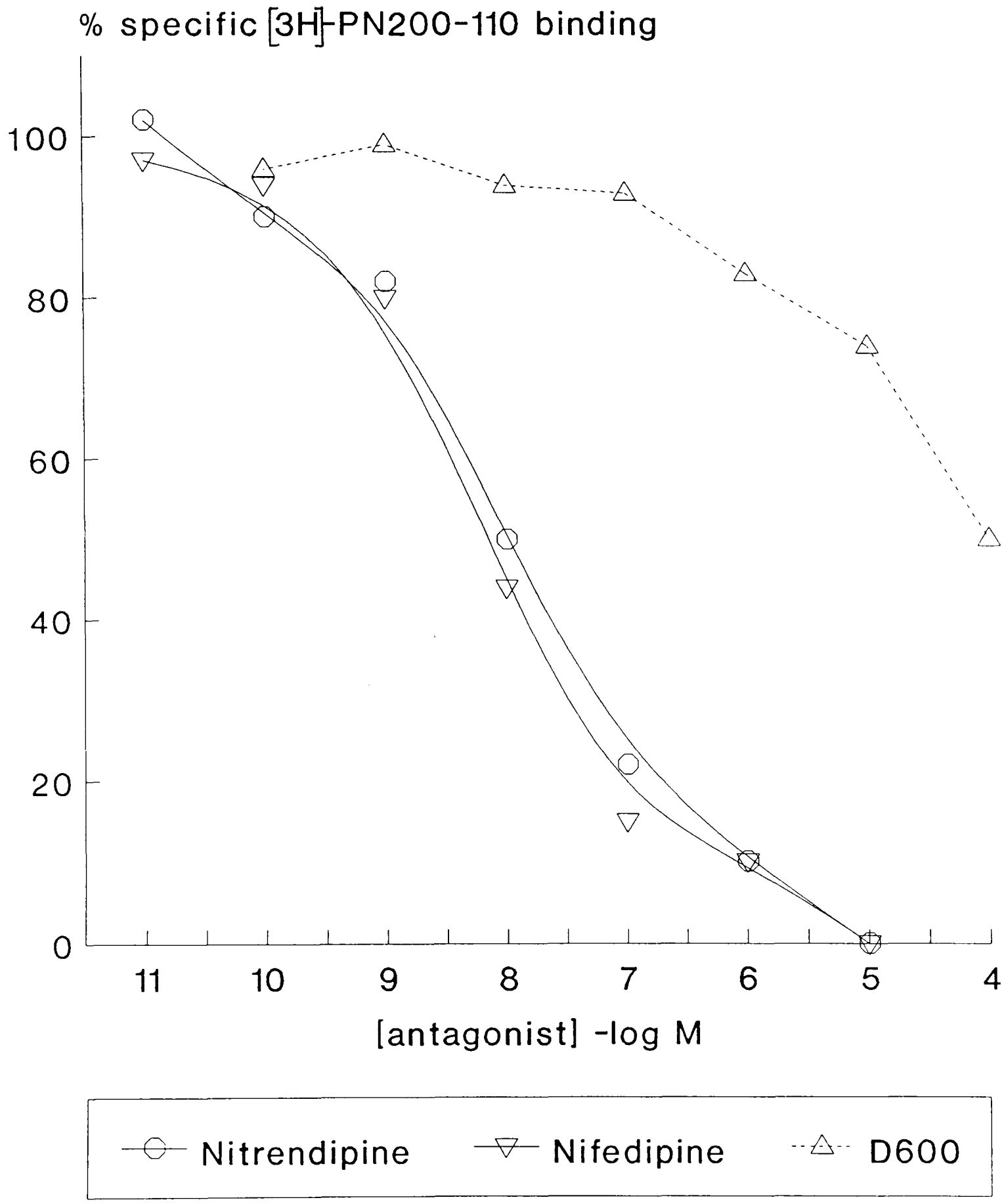
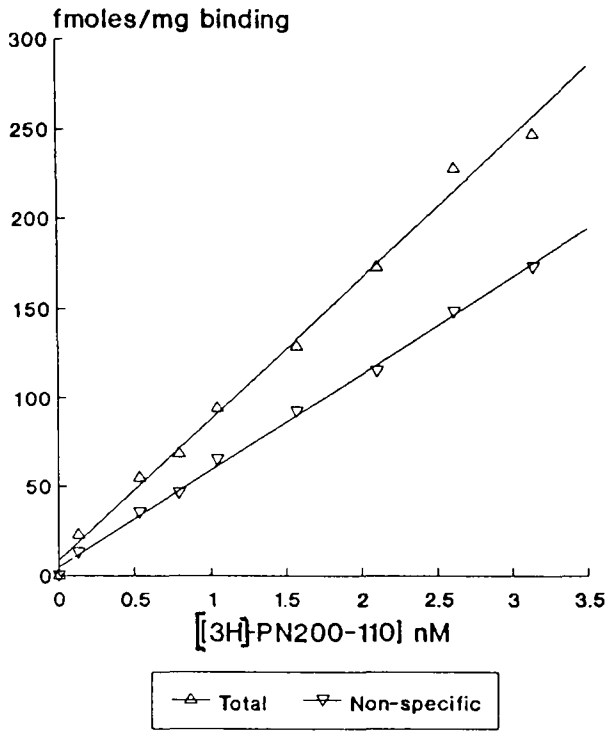

% specific [3H]-PN200-110 binding
100
80
60
40
20
0
11
10
9
8
7
6
5
4
[antagonist] -log M
Nitrendipine
Nifedipine
D600

Figure 4.6: [^{3}H]-PN200-110 binding to MAR5 membranes

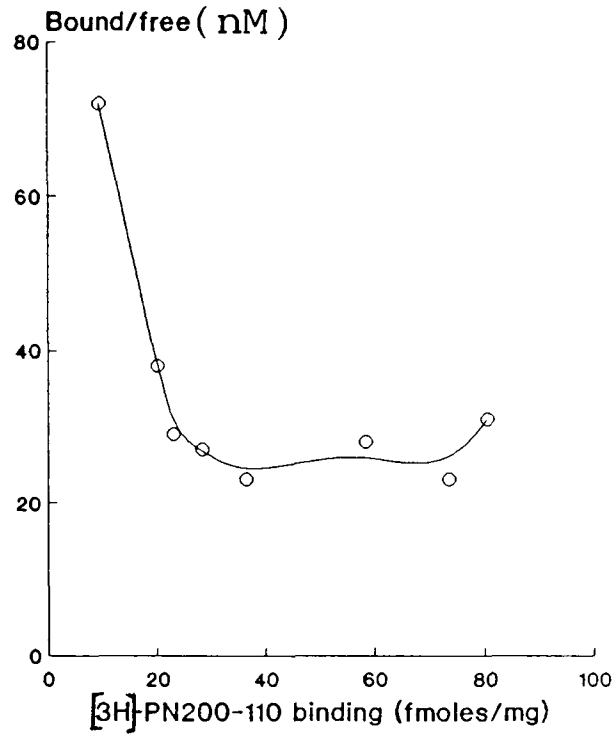
(a) Total, non-specific and (b) specific [^{3}H]-PN200-110 binding to membranes prepared from the human SCLC line, MAR5. Non-specific binding was determined in the presence of 10μM nitrendipine.

(c) Scatchard plot of the binding data. Abscissa = specific [^{3}H]-PN200-110 binding. Ordinate = specific binding/unbound ligand concentration.

(a)


fmoles/mg binding
300
250
200
150
100
50
0
0
0.5
1
1.5
2
2.5
3
3.5
[[3H]-PN200-110] nM
Total
Non-specific

(c)


Bound/free (nM)
80
60
40
20
0
0
20
40
60
80
100
[3H]-PN200-110 binding (fmoles/mg)

(b)

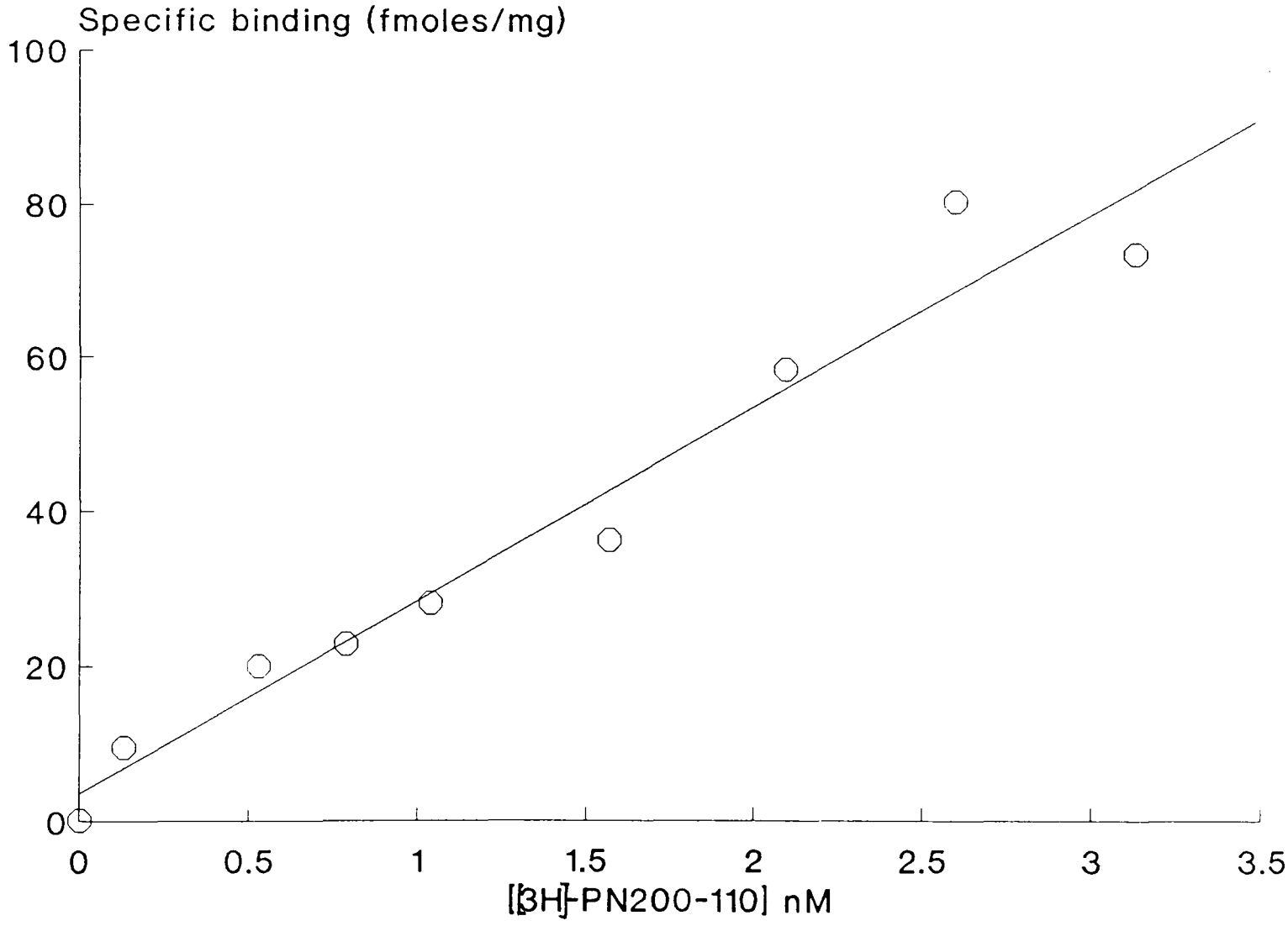
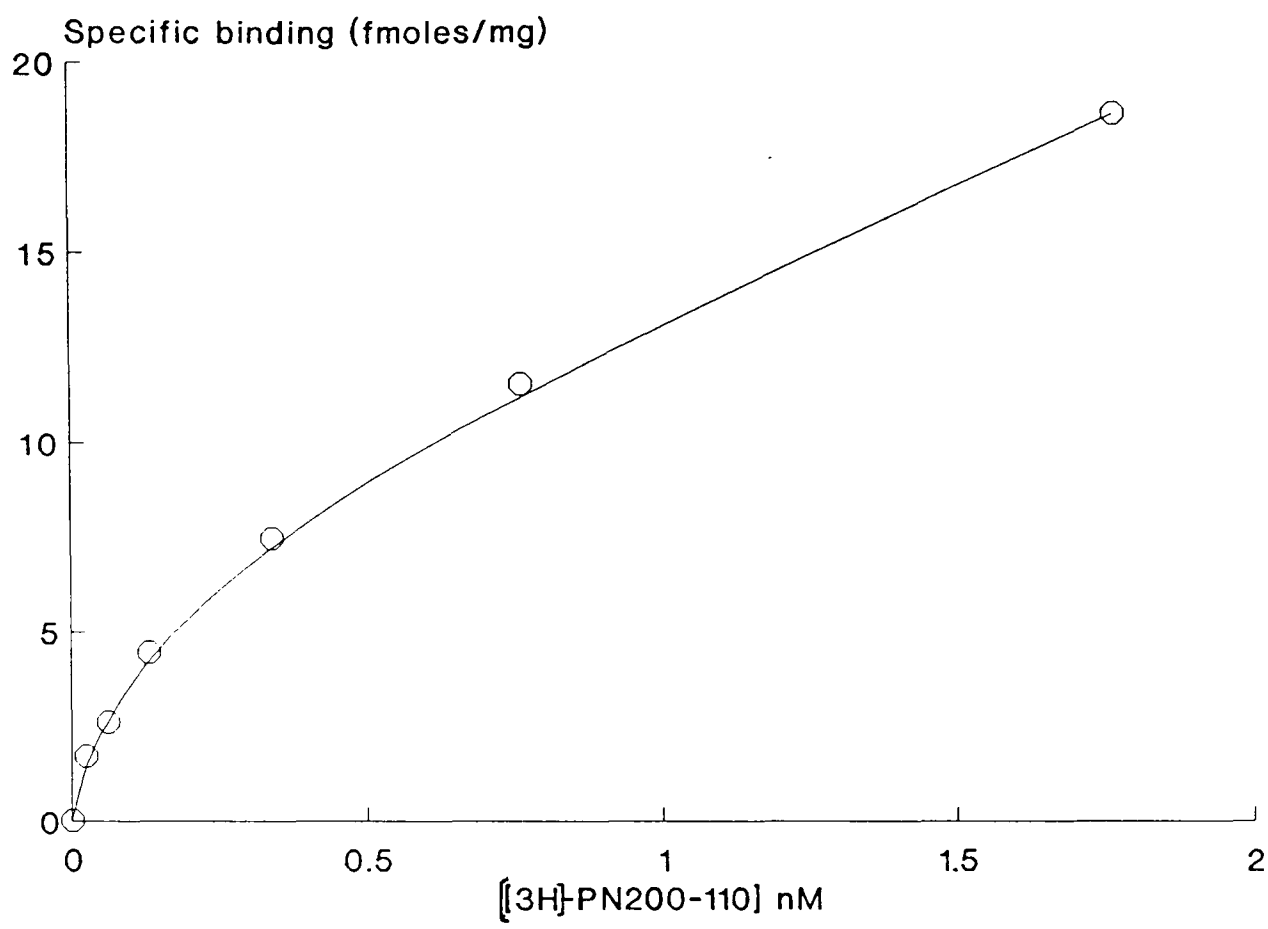

Specific binding (fmoles/mg)
100
80
60
40
20
0
0
0.5
1
1.5
2
2.5
3
3.5
[3H]-PN200-110] nM

Figure 4.7: [^{3}H]-PN200-110 binding to NG108 membranes

(a) Specific binding to membranes prepared from NG108 cells.

(b) Scatchard plot of the binding data. Abscissa = specific [^{3}H]-PN200-110 binding. Ordinate = specific binding/unbound ligand concentration.

(a)


Specific binding (fmoles/mg)
20
15
10
5
0
0
0.5
1
1.5
2
[3H]-PN200-110] nM

(b)

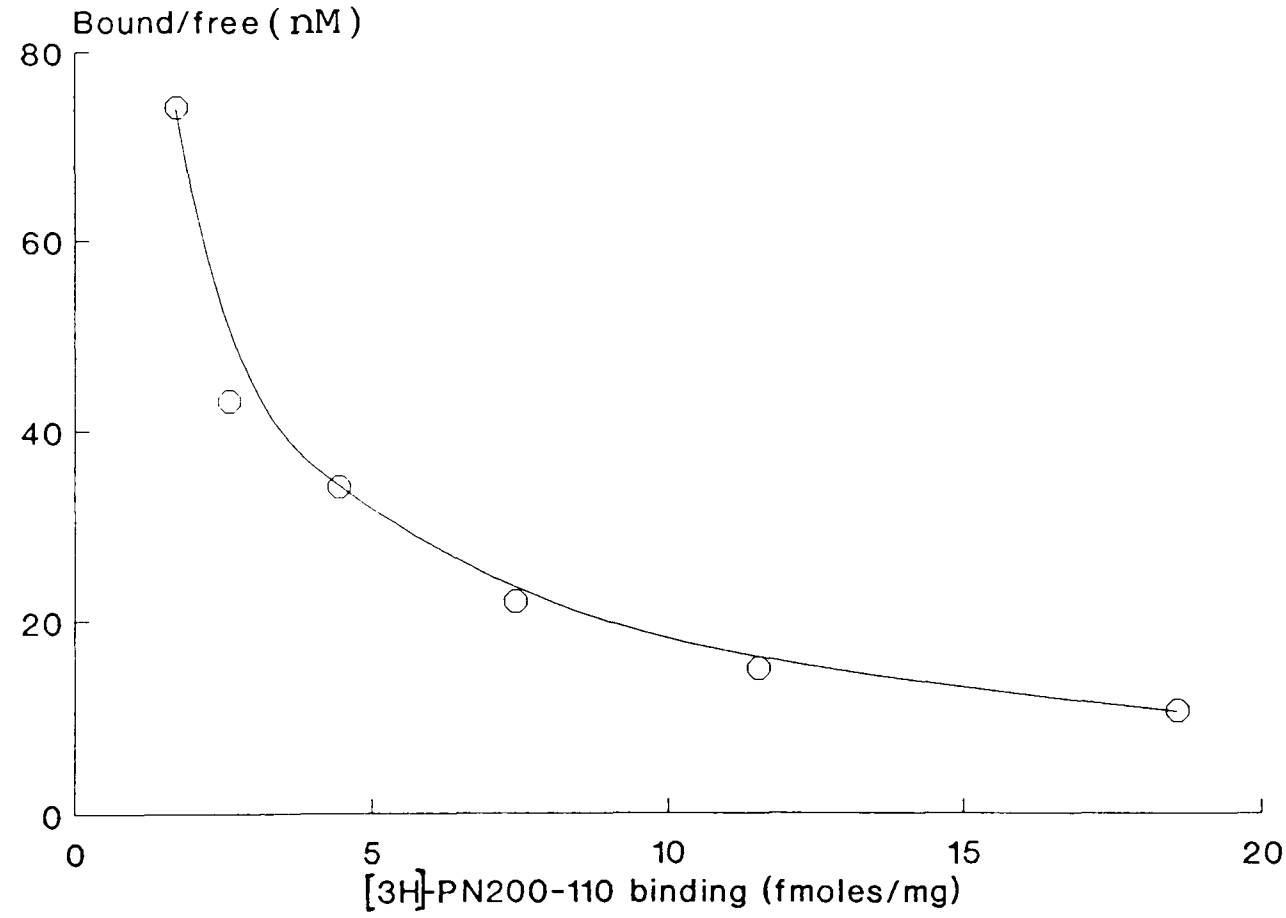

Bound/free (nM)
80
60
40
20
0
0
5
10
15
20
[3H]-PN200-110 binding (fmoles/mg)

Figure 4.8: Inhibition of [^{3}H]-PN200-110 binding to NG108 membranes by antagonists

Membranes were preincubated with increasing concentrations of antagonist before the addition of 0.5nM [^{3}H]-PN200-110. Results are expressed as the percentage of specific binding measured in the absence of antagonist. K_i nitrendipine = 8.3nM, K_i nifedipine = 7.1nM, n=1.

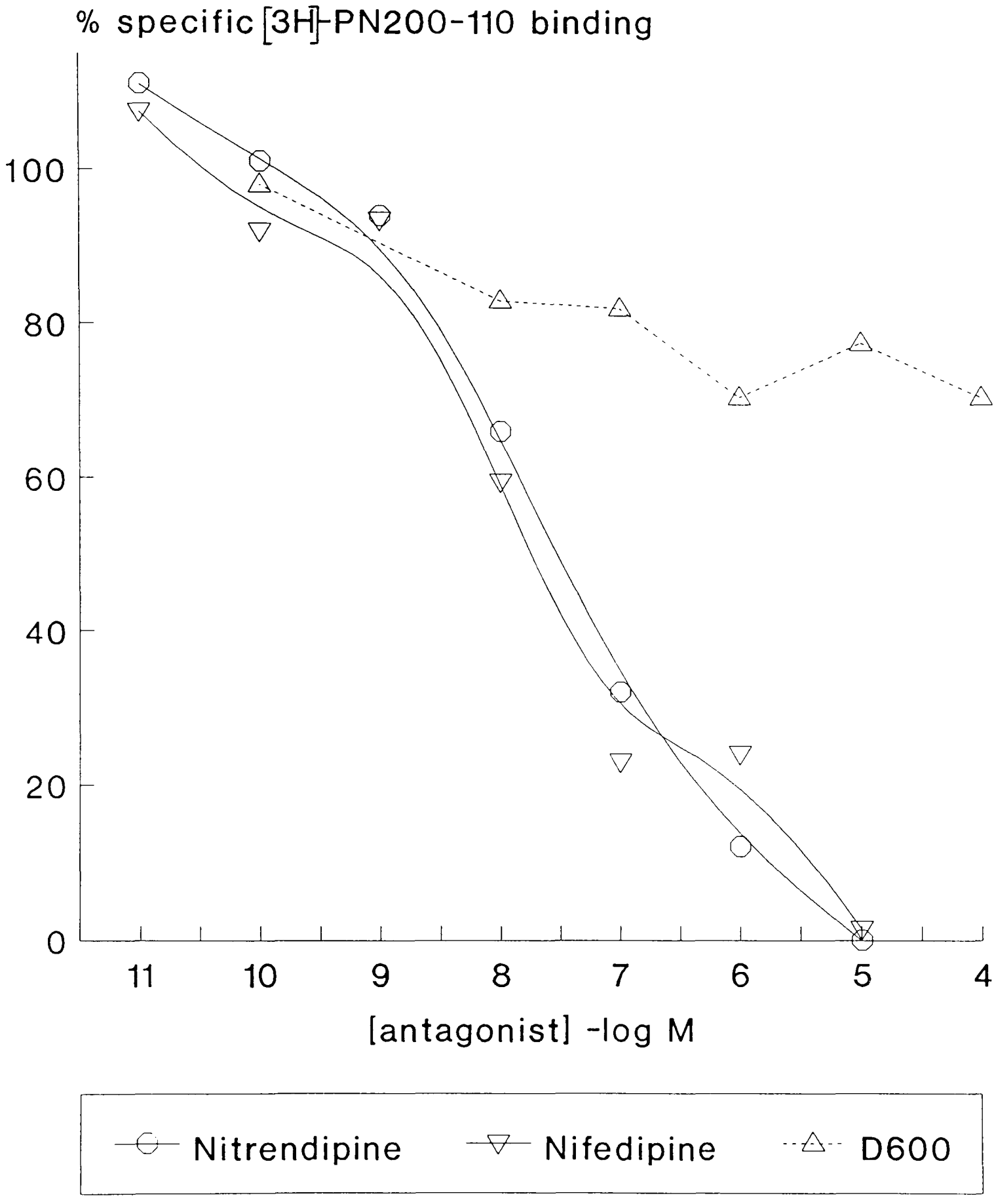

% specific [3H]-PN200-110 binding
100
80
60
40
20
0
11
10
9
8
7
6
5
4
[antagonist] -log M
Nitrendipine
Nifedipine
D600

Table 4.1

Properties of [^{3}H]-PN200-110 binding to neuronal membranes

Tissue/Cell line	B_{max} (fmol/mg protein)	K_D (nM)	Number of determinations
Rat brain	98±8	0.28±0.06	12
SKNSH	<10	-	2
Kelly	<10	-	2
IMR32	6.1	0.06	1
MAR5	<20	-	7
NG108	<10	-	7
PC12	23±3	0.59±0.19	6

4.3.4. Calcium dependency of [^{3}H]-PN200-110 binding

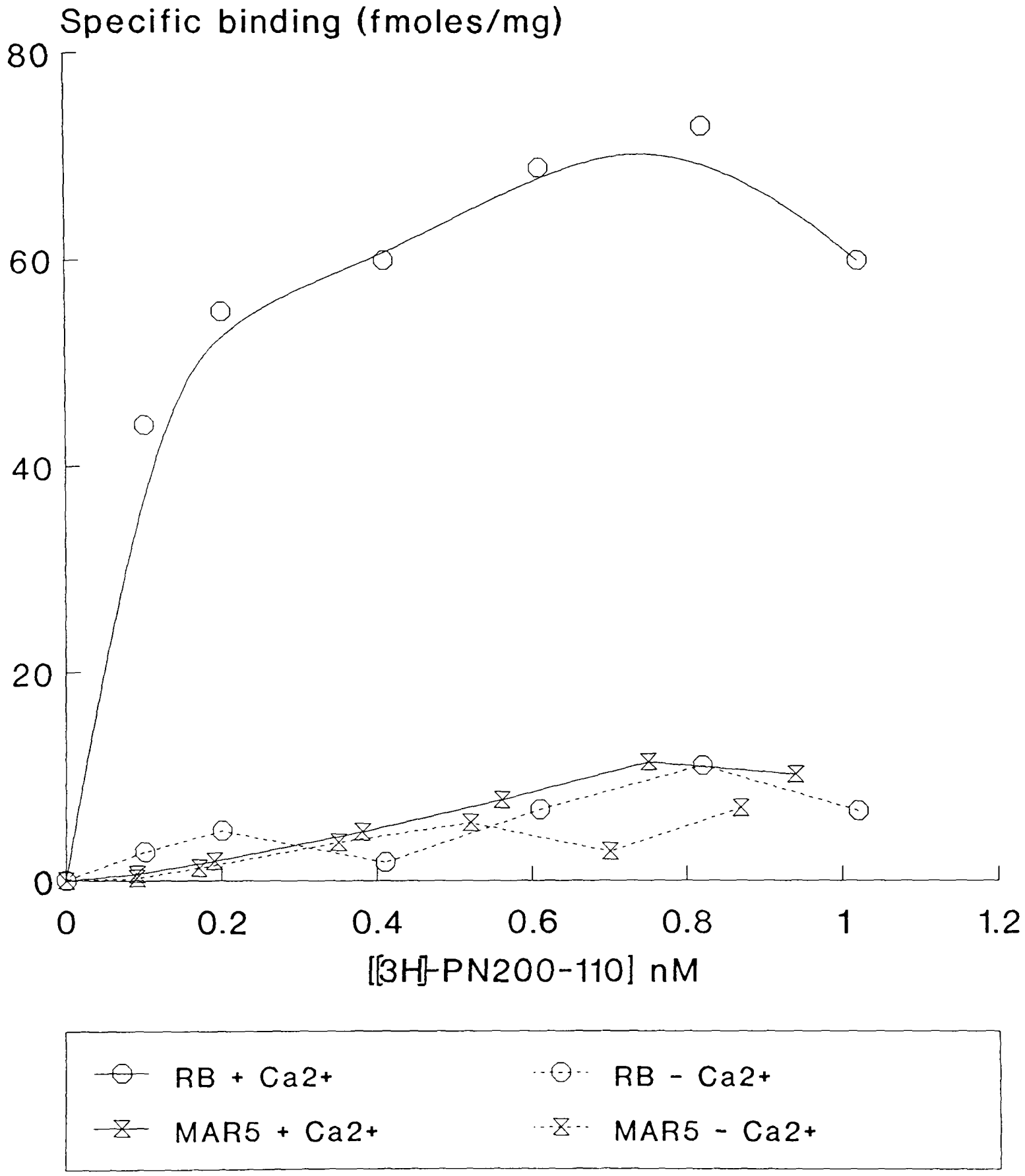
The dependency of specific [^{3}H]-PN200-110 binding on the presence of calcium was demonstrated in rat brain membranes. When $CaCl_2$ was omitted from the incubation buffer, specific binding at saturable concentrations of ligand was reduced by 84±3% (n=4). By contrast, specific binding in MAR5 membranes was reduced by only 27±6% (n=4), and in NG108 membranes by 52% (n=1). Binding curves for rat brain and MAR5 membranes in the presence and absence of calcium are shown in Figure 4.9.

4.3.5. The effect of dibutyryl cAMP on [^{3}H]-PN200-110 binding

NG108 cells were grown for 4 days in the presence of 1mM cAMP. During this time the cells developed a neuronal appearance and growth was halted. [^{3}H]-PN200-110 binding to membranes prepared from treated cells was compared with binding to untreated cells grown in parallel. There was no difference in binding site density or apparent ligand affinity between the two membrane preparations (Figure 4.10).

Figure 4.9: Calcium dependency of [^{3}H]-PN200-110 binding

Binding assays were performed with rat brain (RB) membranes (O) and MAR5 membranes (X) using the standard incubation buffer containing 1.5mM $CaCl_2$ (solid lines) or incubation buffer without $CaCl_2$ (dotted lines).


Specific binding (fmoles/mg)
80
60
40
20
0
0
0.2
0.4
0.6
0.8
1
1.2
[[3H]-PN200-110] nM
RB + Ca2+
RB - Ca2+
MAR5 + Ca2+
MAR5 - Ca2+

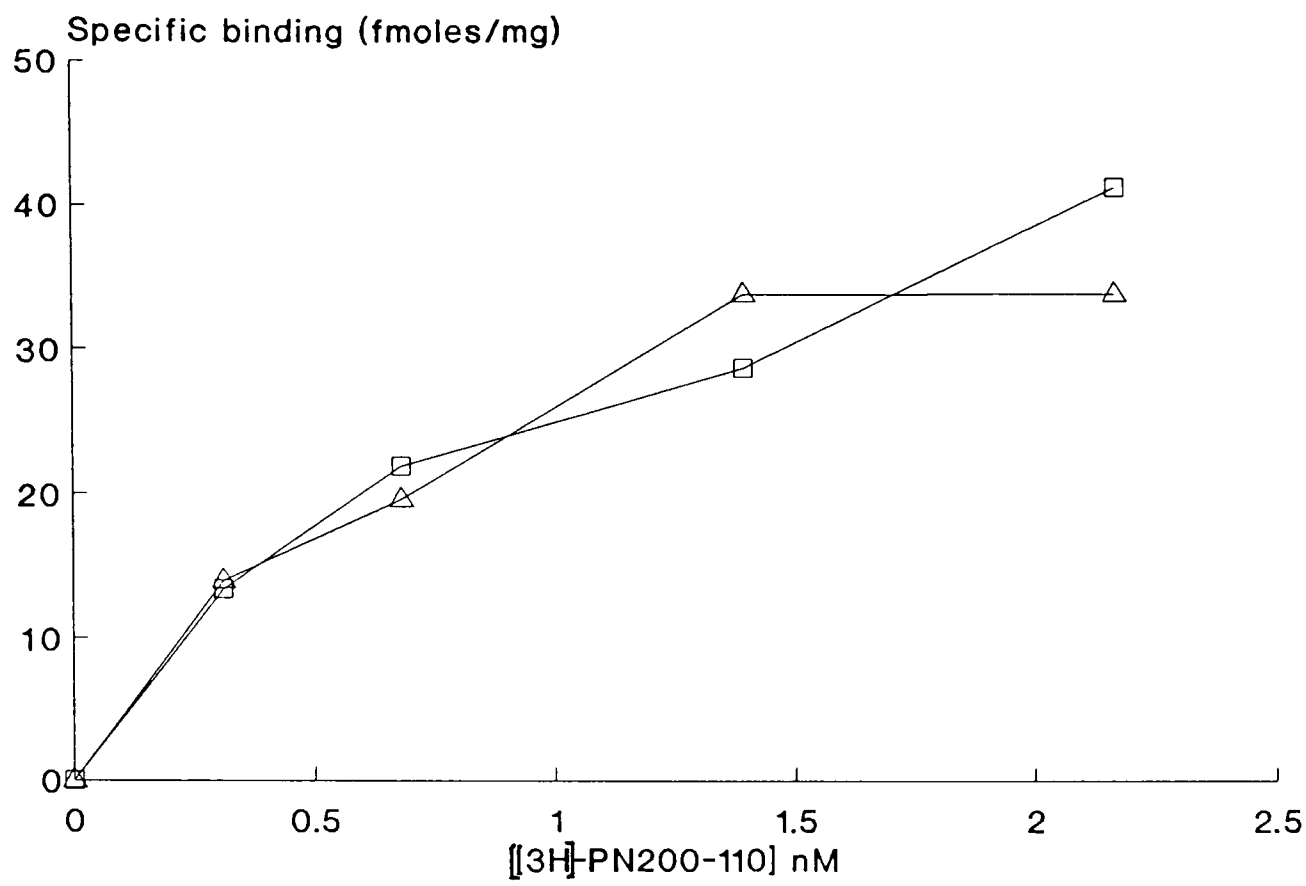


Figure 4.10: The effect of dibutyryl cAMP on [^{3}H]-PN200-110 binding

NG108 cells were grown in culture medium containing 1mM dibutyryl cAMP (△) for 4 days. Specific [^{3}H]-PN200-110 binding was determined in membranes prepared from these cells and from untreated cells grown in parallel (□).

4.3.6. Time course of ^{125}I-ω-conotoxin binding

The time course of specific ^{125}I-ωCgTx binding in SKNSH cell membranes is illustrated in Figure 4.11. Maximum binding was reached at approximately 60 minutes at room temperature. One hour incubations were therefore used in all further assays to reflect equilibrium binding.

To demonstrate the stability of the ^{125}I-ωCgTx-receptor complex, an excess concentration of unlabelled ωCgTx (0.1μM) was added to the membranes after maximum binding was reached. There was no significant dissociation of ligand for up to 90 minutes at room temperature after addition of unlabelled ωCgTx (Figure 4.11).

4.3.7. ^{125}I-ωCgTx binding to rat brain

A saturable population of specific ^{125}I-ωCgTx binding sites was detected in rat brain membranes (B_{max} = 238±63 fmoles/mg protein, n=5). The binding was of extremely high affinity (K_D = 6.6±2.3 pM, n=5). Total, non-specific and specific binding curves for a typical experiment using rat brain membranes are shown in Figure 4.12.

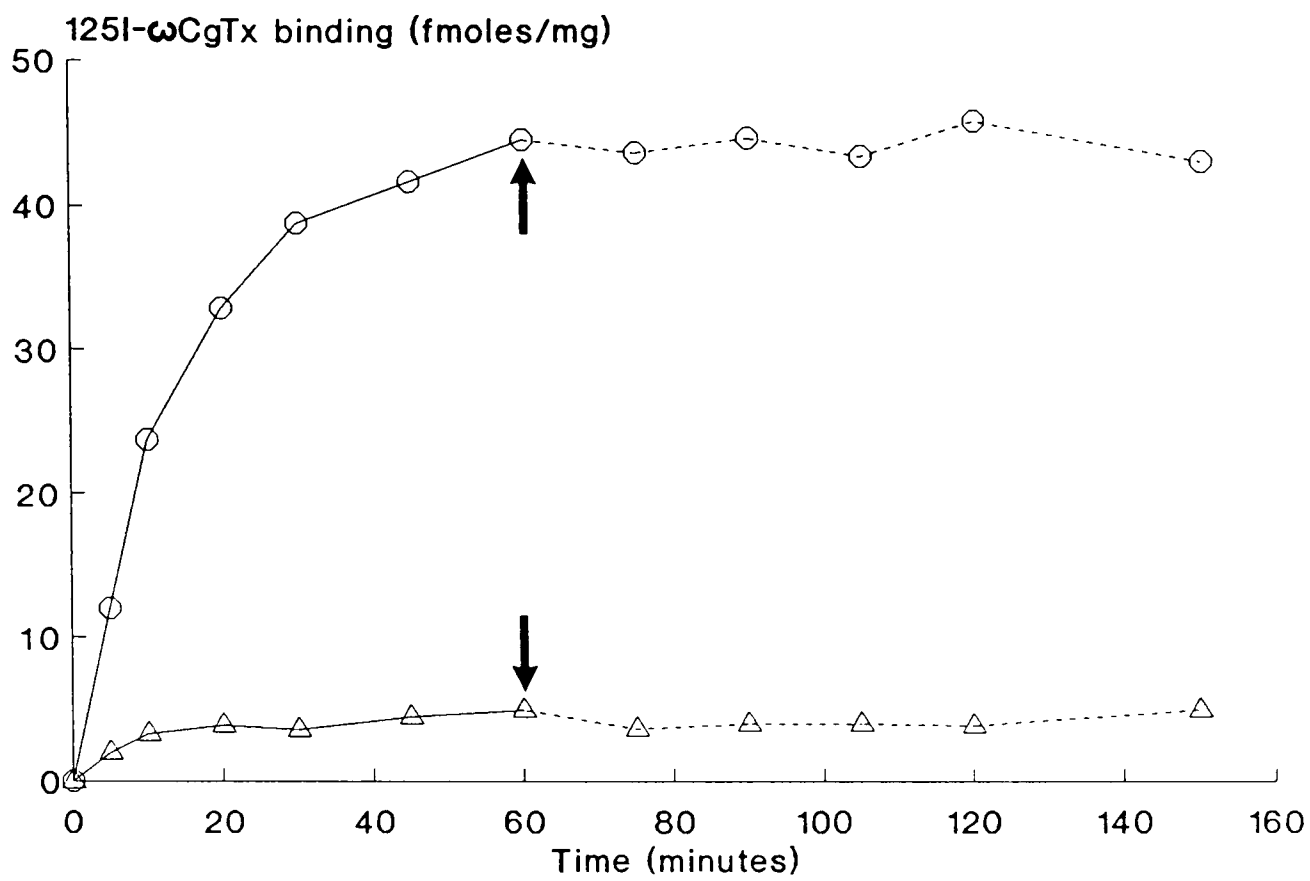


Figure 4.11: Time course of ^{125}I-ωCgTx binding to SKNSH membranes

Membranes were incubated with a saturating concentration of ^{125}I-ωCgTx (150pM) at room temperature. Specific binding (total - non-specific) (O) was determined from 5-60 minutes. At this point (arrow) membranes were diluted with buffer containing 0.1μM unlabelled ωCgTx and specific binding was determined for a further 90 minutes.

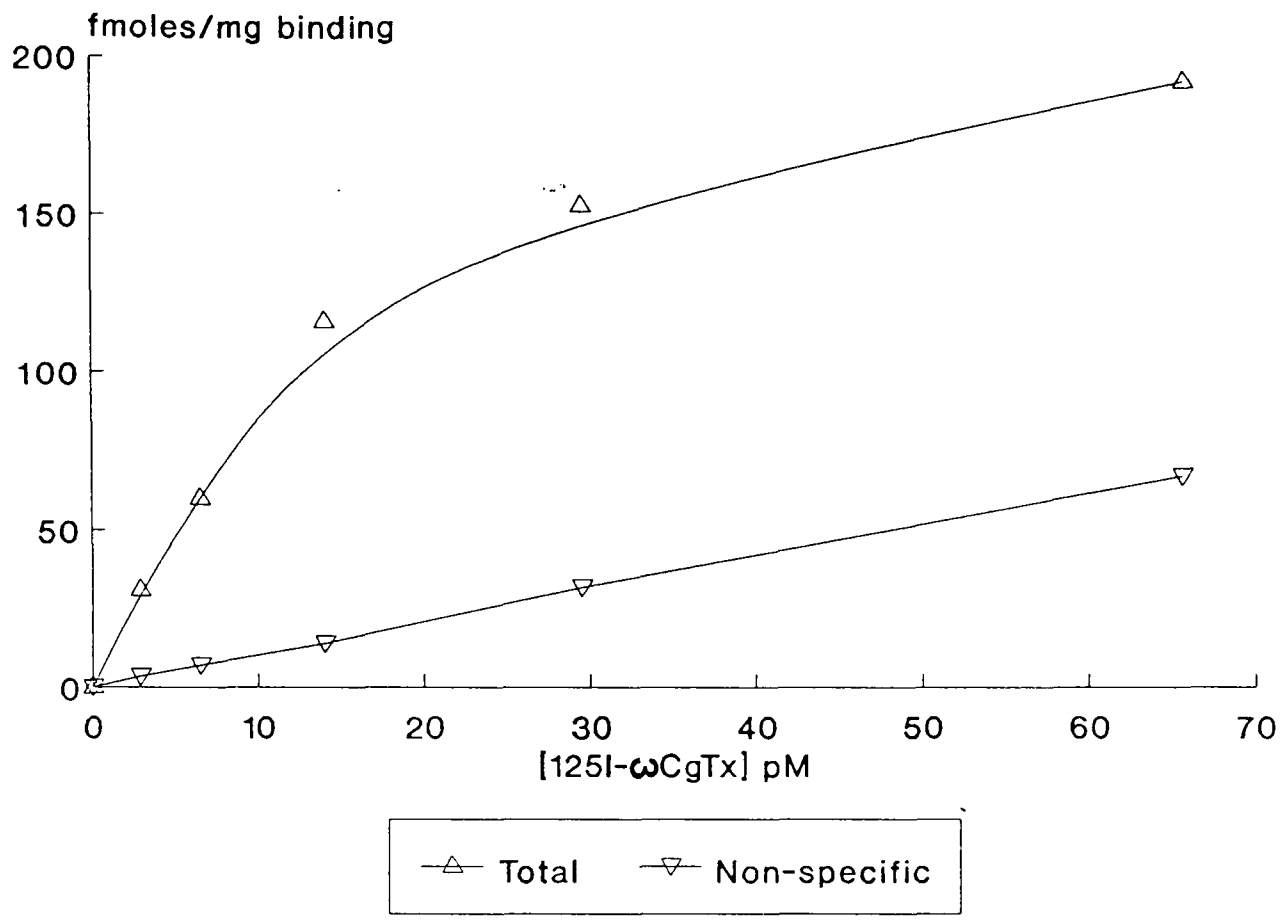
Non-specific binding (Δ) was determined by preincubating membranes with 0.5μM unlabelled ωCgTx for 5 minutes before the start of the time course.

Figure 4.12: ^{125}I-ωCgTx binding to rat brain membranes

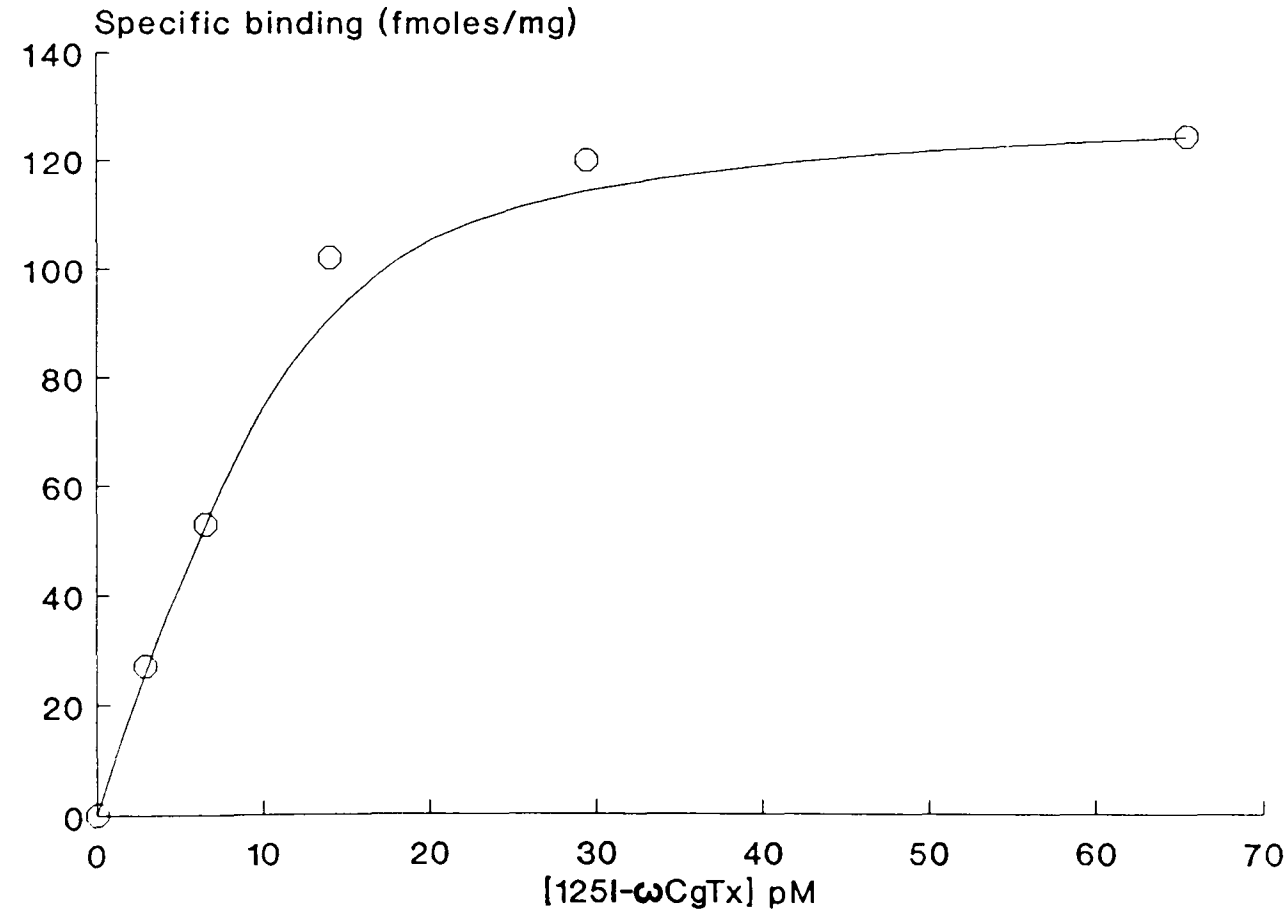
(a) Total binding was determined by incubating membranes with increasing amounts of ^{125}I-ωCgTx for one hour at room temperature. Non-specific binding was determined by preincubating membranes with 0.5μM unlabelled ωCgTx for 5 minutes before the addition of ligand.

(b) Specific (total - non-specific) binding of ^{125}I-ωCgTx to rat brain. B_{max} and K_D values (238±63 fmoles/mg protein and 6.6±2.3 pM respectively, n=5) were calculated by non-linear regression analysis.

(a)


fmoles/mg binding
200
150
100
50
0
0
10
20
30
40
50
60
70
[125I-ωCgTx] pM
Total
Non-specific

(b)


Specific binding (fmoles/mg)
140
120
100
80
60
40
20
0
0
10
20
30
40
50
60
70
[125I-ωCgTx] pM

4.3.8. ^{125}I-ωCgTx binding to neuronal cell membranes

Saturable, high-affinity ^{125}I-ωCgTx binding was found in SKNSH, Kelly, IMR32, MAR5 and NG108 membranes (see Table 4.2). Binding site density was relatively low, but the affinity of binding was of the same order of magnitude as that determined in rat brain. In general there was a higher level of non-specific binding in neuronal cell membranes than in brain membranes.

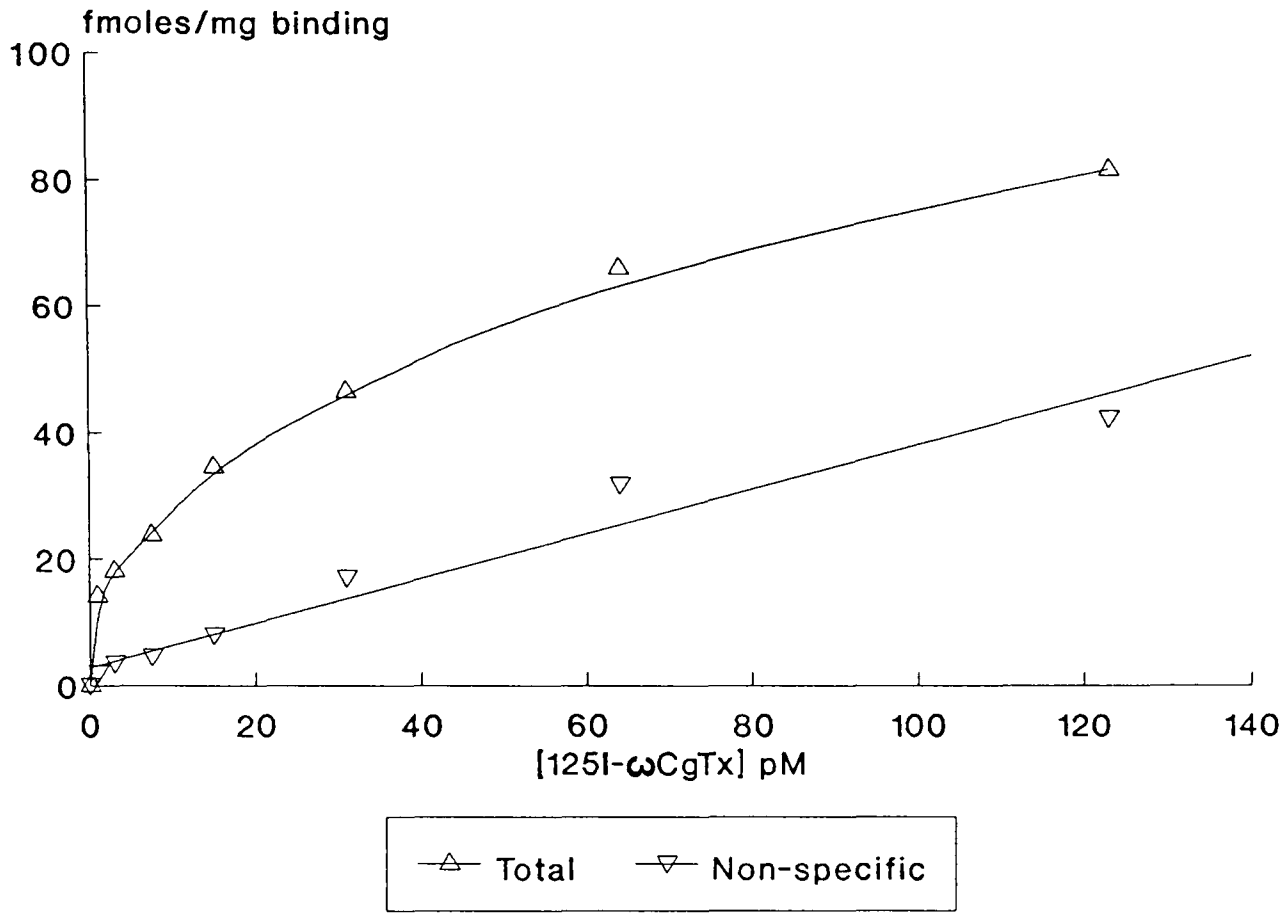
SKNSH cells had the highest density of ^{125}I-ωCgTx binding sites, therefore these were studied in greatest detail. Figure 4.13 shows typical binding curves for the SKNSH cell line. Specific binding was inhibited by unlabelled ωCgTx (K_i = 5.7 pM, n=2, Figure 4.14), but was unaffected by high concentrations (10μM) of the other calcium antagonists nitrendipine, nifedipine, methoxyverapamil or diltiazem (data not shown). Specific binding was also inhibited by the divalent cations Ca^{2+}, Mg^{2+}, Ba^{2+}, Co^{2+} and Mn^{2+} with K_is of 0.79 mM (n=3), 0.81 mM (n=2), 0.97 mM (n=2), 0.48 mM (n=1) and 0.73 mM (n=2) respectively. Typical cation inhibition curves are shown in Figure 4.15.

^{125}I-ωCgTx binding to MAR5 cell membranes is illustrated in Figure 4.16, showing the low density of binding sites and the high level of non-specific binding in this preparation. Specific binding was inhibited by low concentrations of unlabelled ωCgTx (K_i = 4.0 pM, n=2, Figure 4.17). Specific ^{125}I-ωCgTx binding curves for the remaining cell lines are shown in Figure 4.18. Specific binding was not detectable in PC12 membranes, but the presence of binding sites at a density below the level of sensitivity of the assay cannot be ruled out.

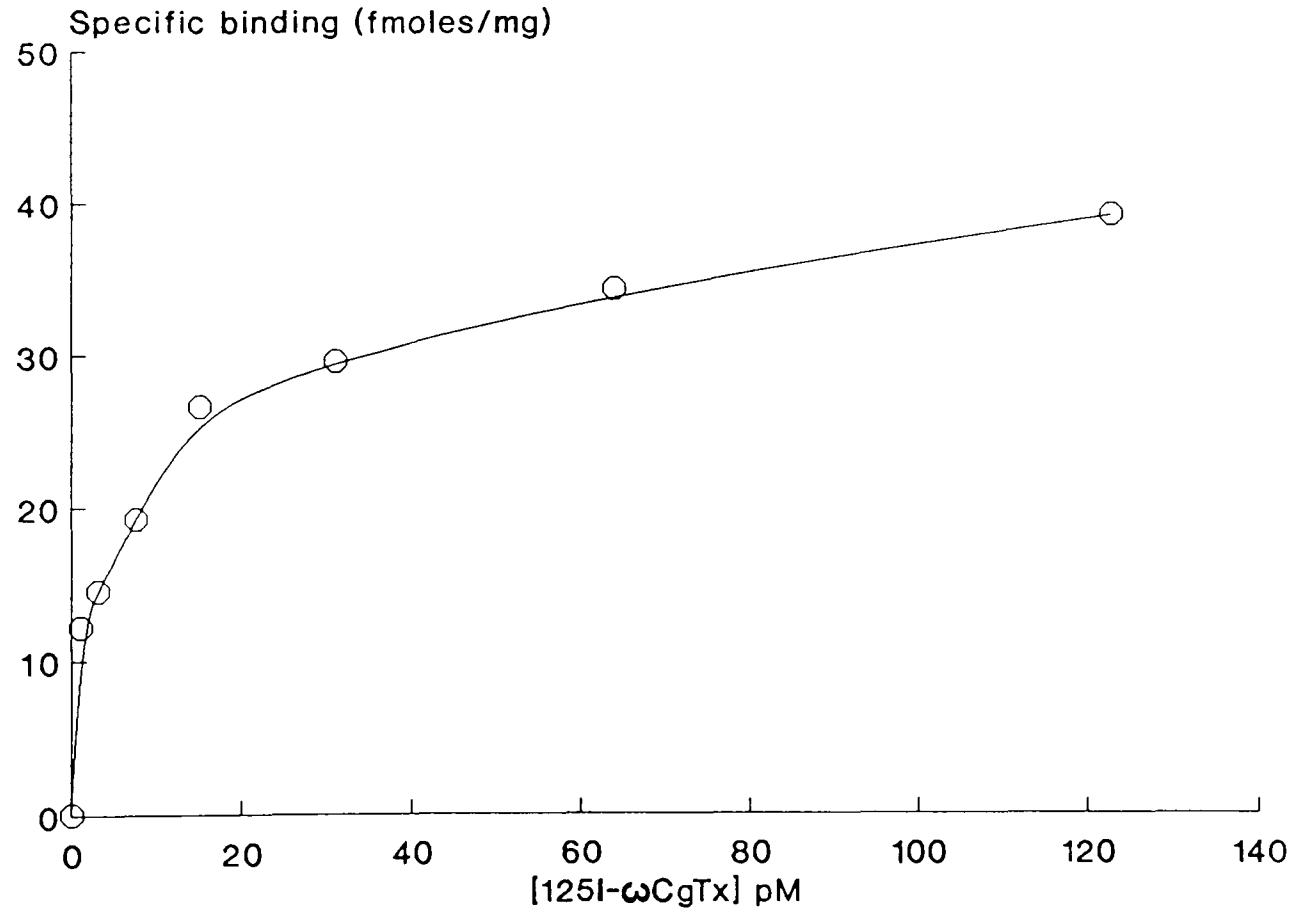
Figure 4.13: ^{125}I-ωCgTx binding to SKNSH membranes

(a) Total, non-specific and (b) specific ^{125}I-ωCgTx binding to membranes prepared from the human neuroblastoma cell line, SKNSH. Non-specific binding was defined by the presence of 0.5μM unlabelled ωCgTx. (B_{max} = 63±9 fmoles/mg protein, K_D = 13.7±3.6 pM, n=3.)

(a)


fmoles/mg binding
100
80
60
40
20
0
0
20
40
60
80
100
120
140
[125I-ωCgTx] pM
Total
Non-specific

(b)


Specific binding (fmoles/mg)
50
40
30
20
10
0
0
20
40
60
80
100
120
140
[125I-ωCgTx] pM

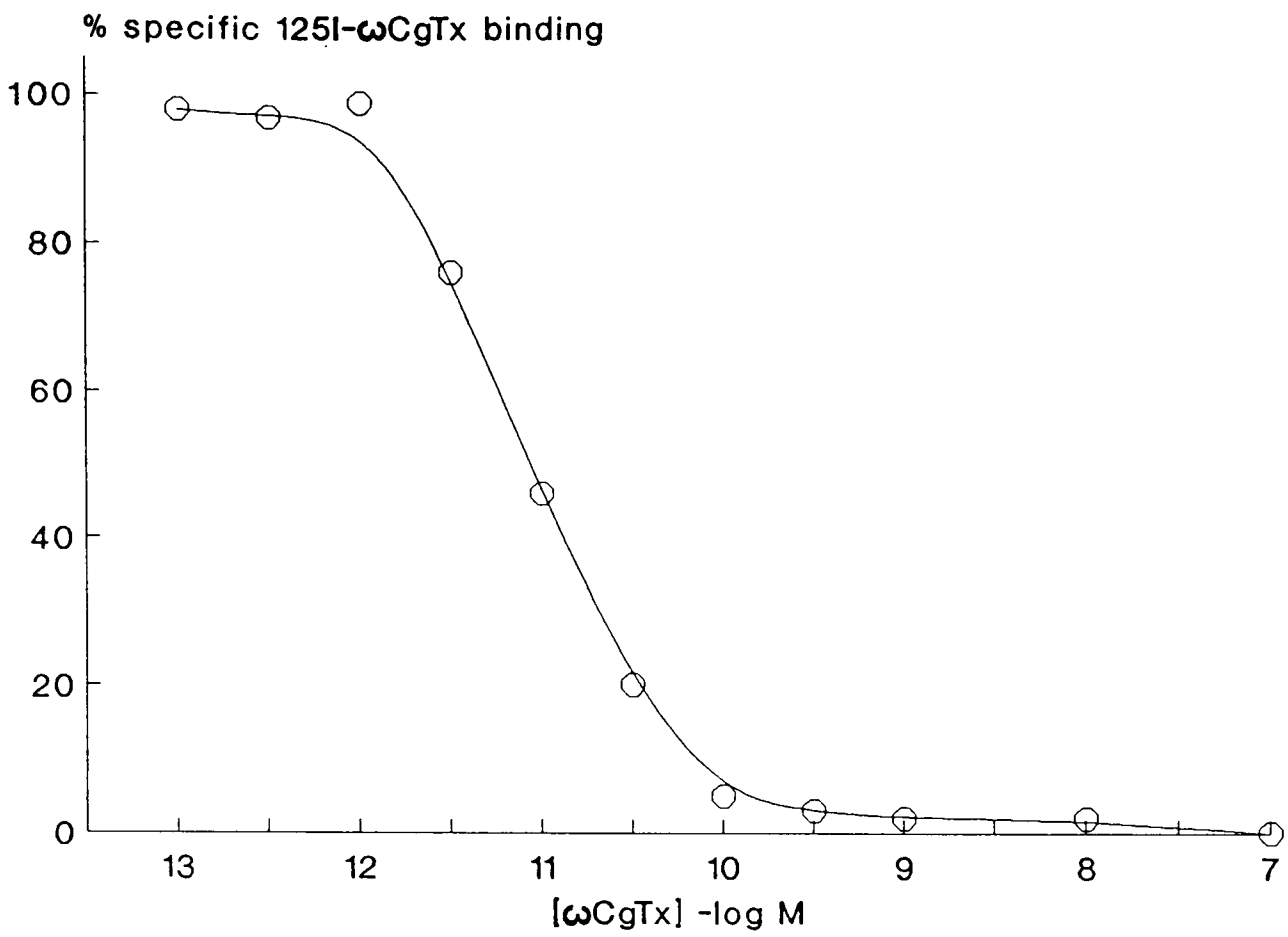


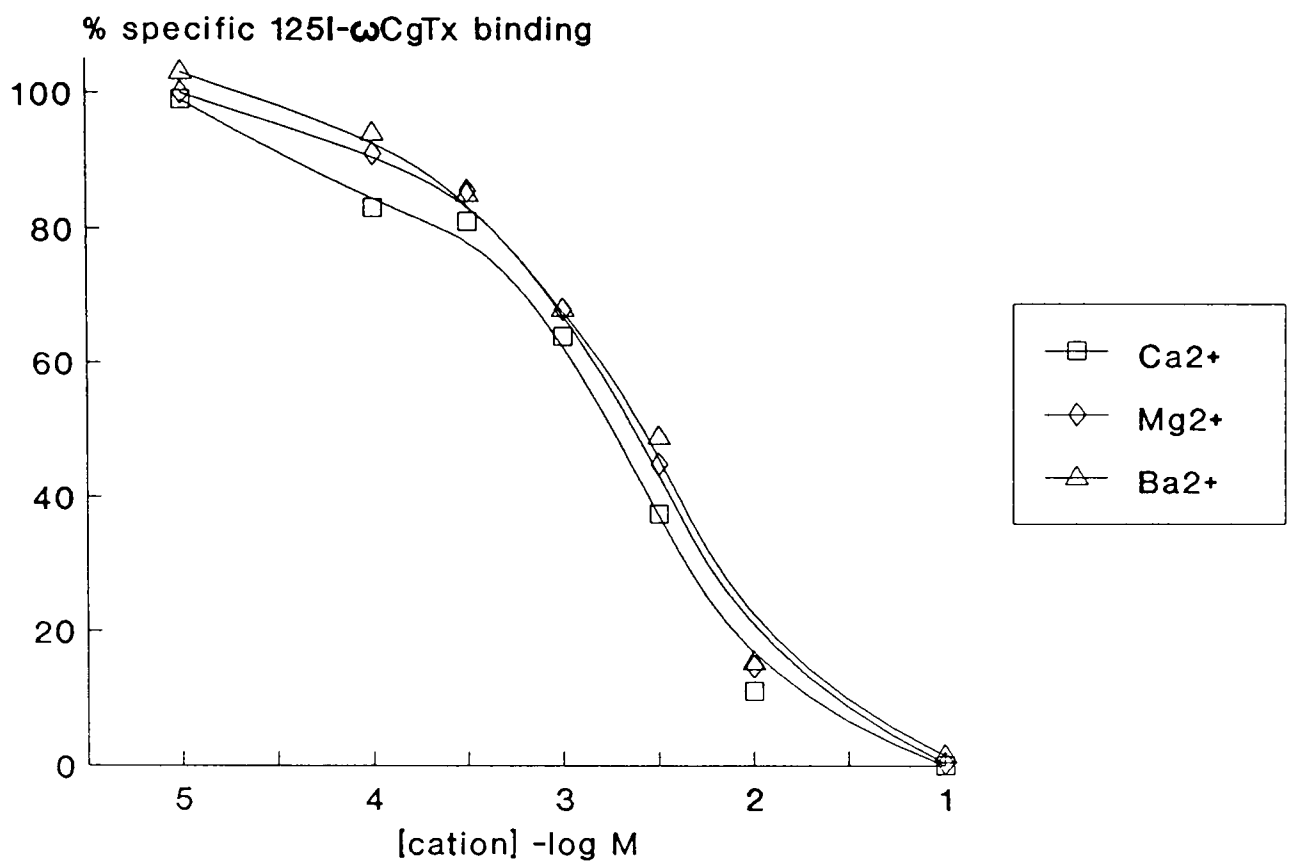
Figure 4.14: Inhibition of ^{125}I-ωCgTx binding to SKNSH membranes by unlabelled ωCgTx.

Membranes were preincubated with increasing concentrations of unlabelled ωCgTx before the addition of ligand at an approximate K_D concentration (15pM). Binding is expressed as the percentage of specific binding (ie. amount bound in the absence of antagonist - amount bound in the presence of 0.5μM unlabelled ωCgTx). IC_{50} values were calculated by non-linear regression.

(K_i = 5.7pM, n=2)

Figure 4.15: Inhibition of ^{125}I-ωCgTx binding to SKNSH membranes by divalent cations

Membranes were preincubated with increasing concentrations of the cations indicated before the addition of 10-20pM ligand. Binding is expressed as the percentage of specific binding measured in the absence of antagonist. K_i values are as follows: Ca^{2+} 0.79mM (n=3), Mg^{2+} 0.81mM (n=2), Ba^{2+} 0.97mM (n=2), Co^{2+} 0.48mM (n=1), Mn^{2+} 0.73mM (n=2).


% specific 125I-ωCgTx binding
100
80
60
40
20
0
5
4
3
2
1
[cation] -log M
Ca2+
Mg2+
Ba2+

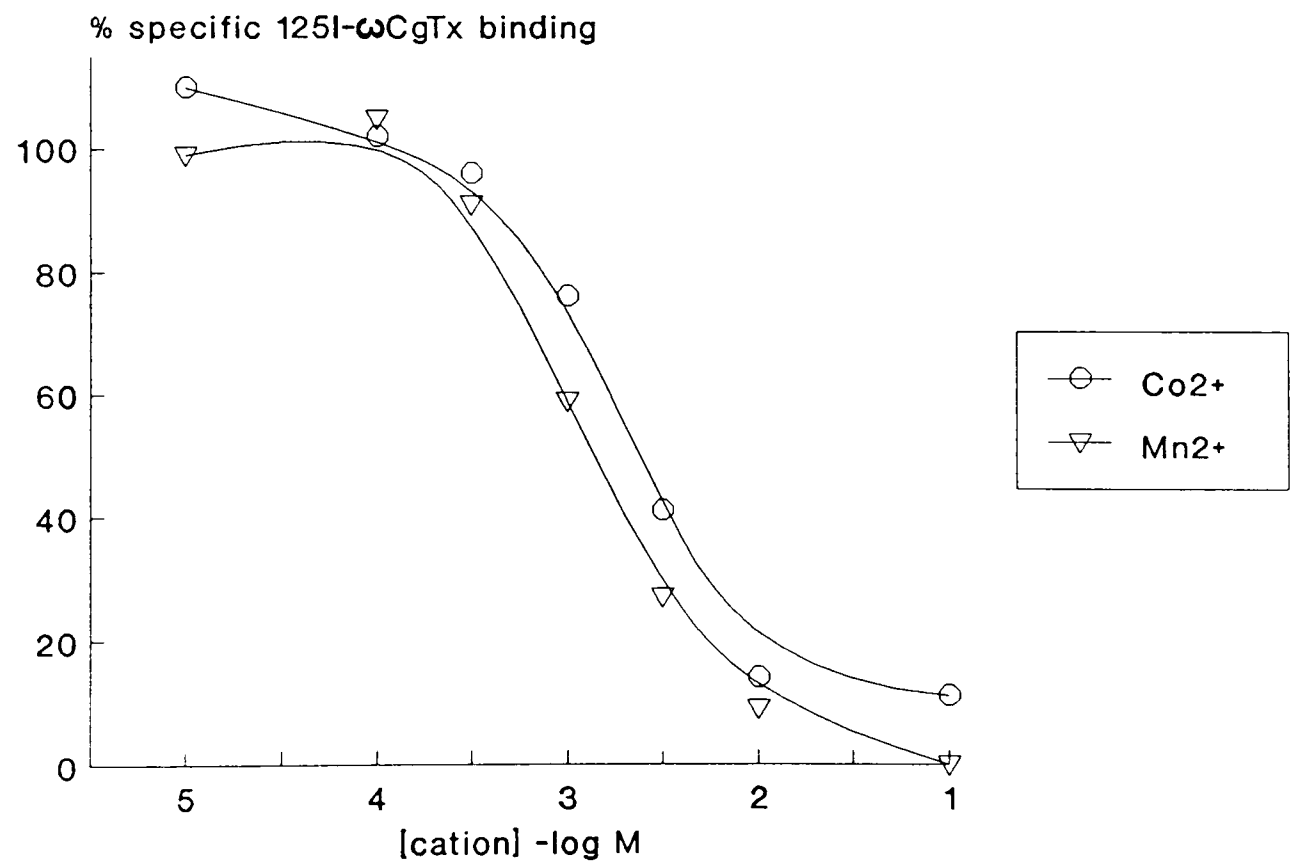
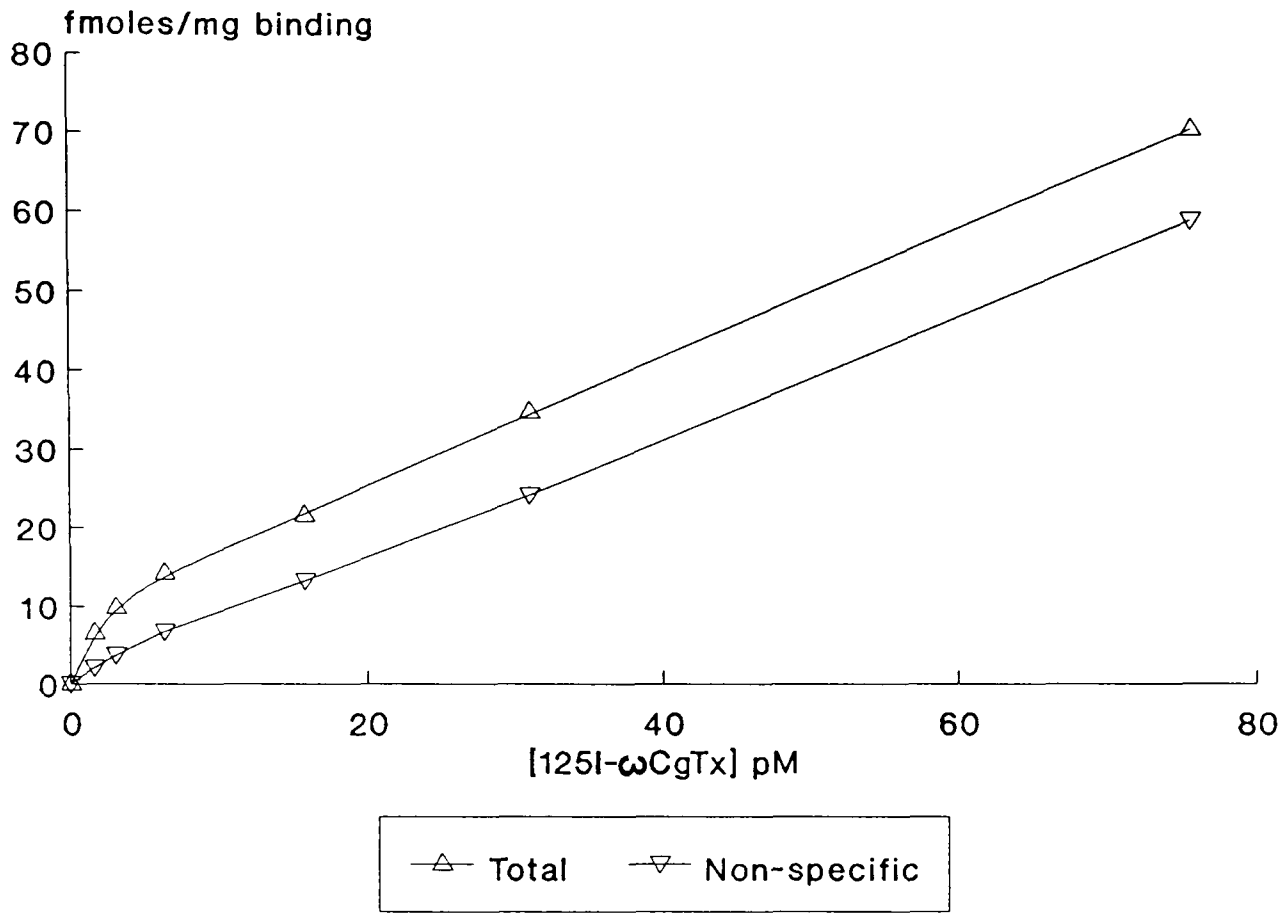

% specific 125I-ωCgTx binding
100
80
60
40
20
0
5
4
3
2
1
[cation] -log M
Co2+
Mn2+

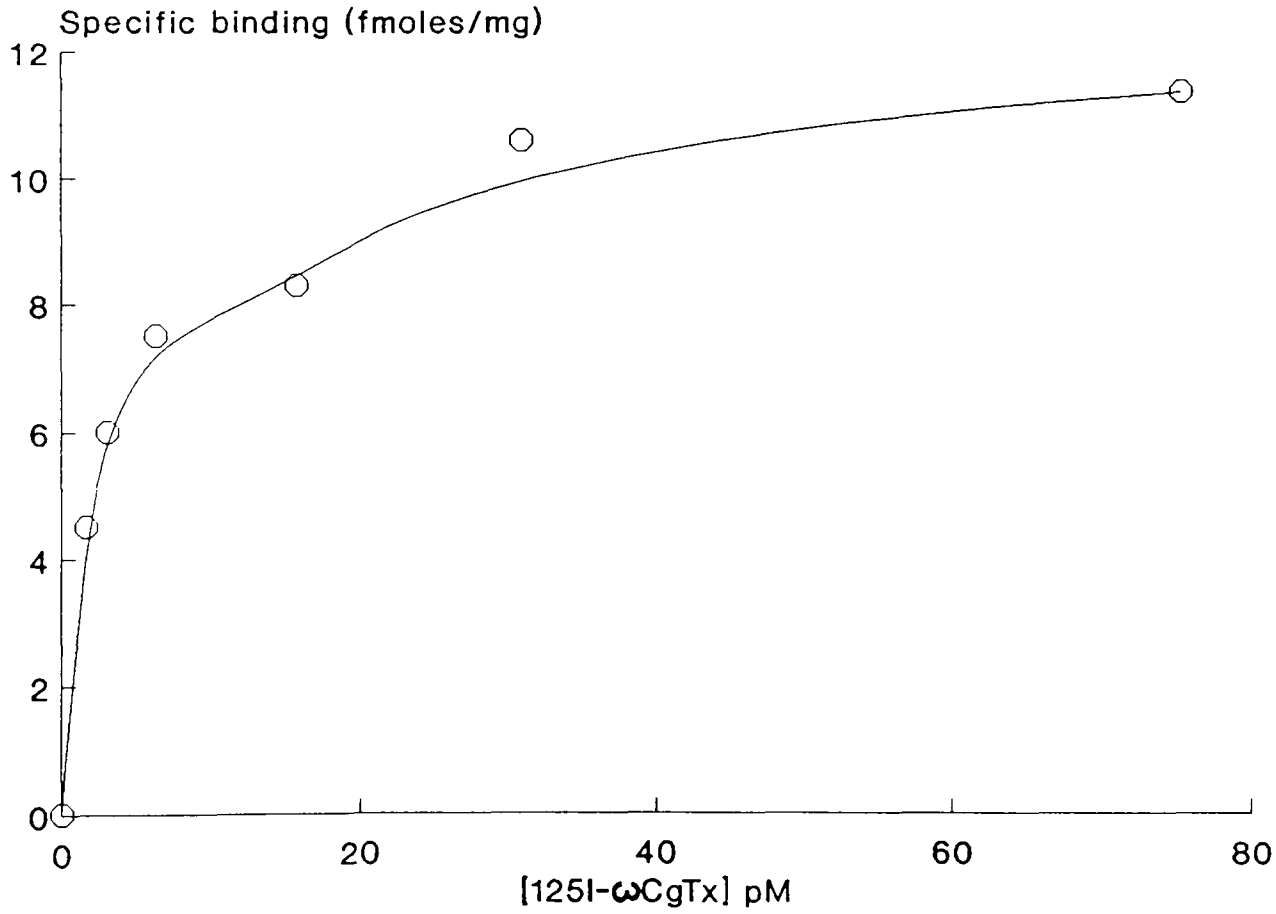
Figure 4.16: ^{125}I-ωCgTx binding to MAR5 membranes

(a) Total, non-specific and (b) specific binding to membranes prepared from the human small cell lung carcinoma line, MAR5. Non-specific binding was defined as the amount measured in the presence of 0.5μM unlabelled ωCgTx. (B_{max} = 13±1 fmoles/mg protein, K_D = 7.2±1.3 pM, n=3.

(a)


fmoles/mg binding
80
70
60
50
40
30
20
10
0
0
20
40
60
80
[125I-ωCgTx] pM
Total
Non-specific

(b)


Specific binding (fmoles/mg)
12
10
8
6
4
2
0
0
20
40
60
80
[125I-ωCgTx] pM

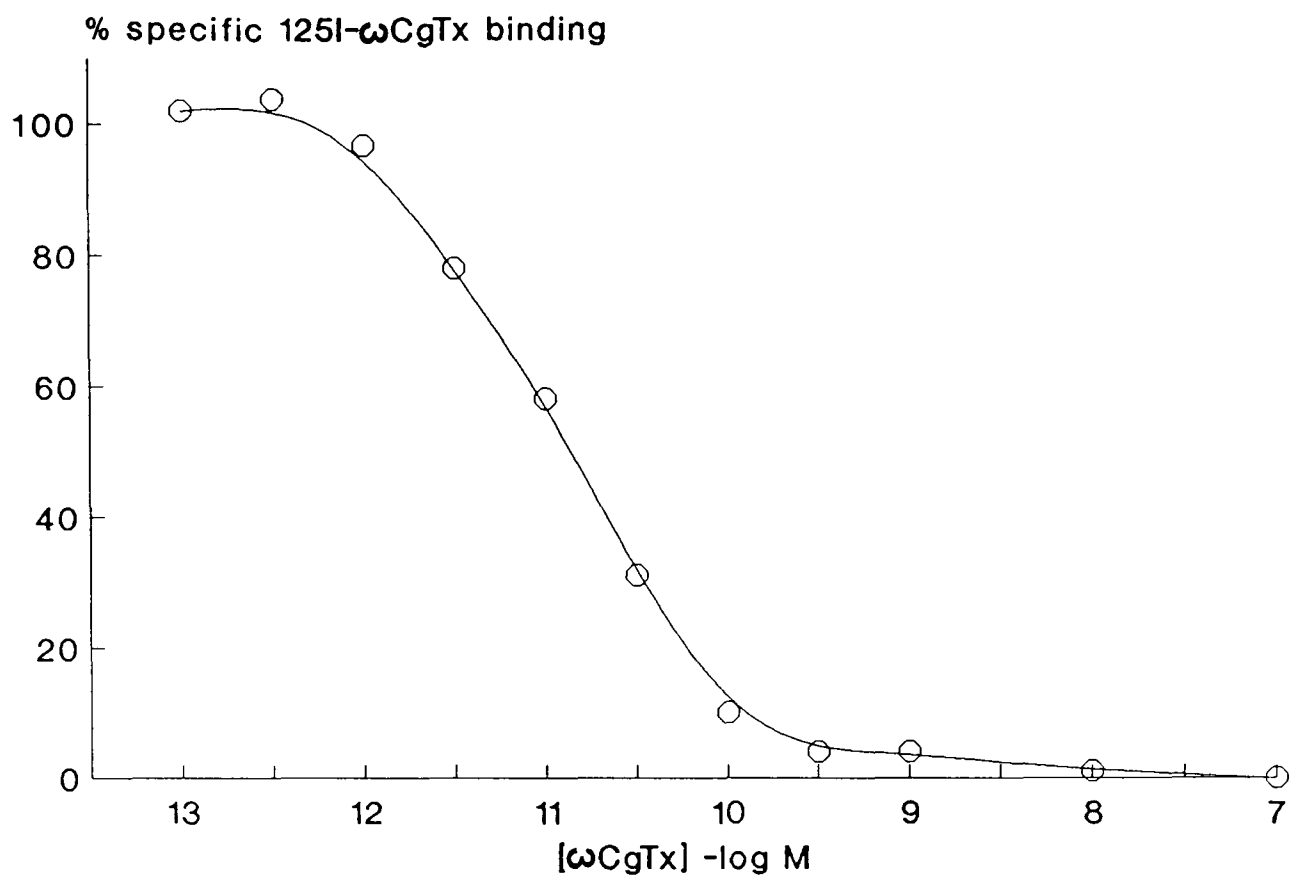


Figure 4.17: Inhibition of ^{125}I-ωCgTx binding to MAR5 membranes by unlabelled ωCgTx.

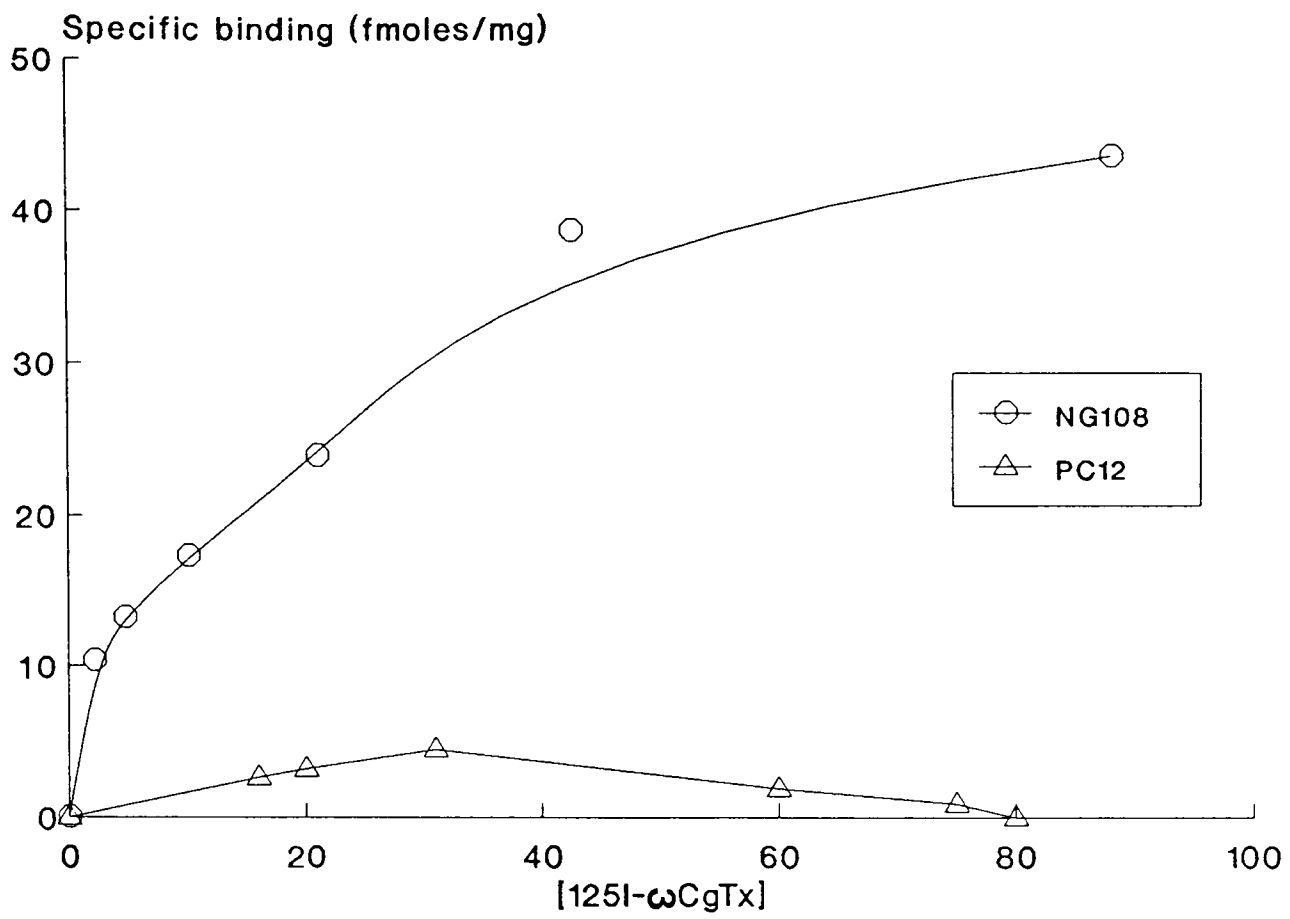
Membranes were preincubated with increasing concentrations of unlabelled ωCgTx before the addition of 15-20pM ligand. Results are expressed as the percentage of specific binding (ie. amount bound in the absence of antagonist - amount bound in the presence of 0.5μM unlabelled ωCgTx). (K_i = 4.0pM, n=2)

Figure 4.18: ^{125}I-ωCgTx binding to NG108, PC12, IMR32 and Kelly membranes.

Specific ^{125}I-ωCgTx binding was determined in membranes prepared from the cell lines indicated. Non-specific binding was defined as that measured in the presence of 0.5μM unlabelled ωCgTx. B_{max} and K_D values respectively are as follows: **NG108** 45 fmoles/mg protein, 26pM, n=2; **IMR32** 30 fmoles/mg protein, 2.3pM, n=1; **Kelly** 17 fmoles/mg protein, 29pM, n=2; **PC12** no binding detected.

Levels of non-specific binding at K_D concentrations = 49% of the total binding (NG108), 23% (IMR32) and 60% (Kelly).

(a)


Specific binding (fmoles/mg)
50
40
30
20
10
0
0
20
40
60
80
100
[125I-ωCgTx]
NG108
PC12

(b)

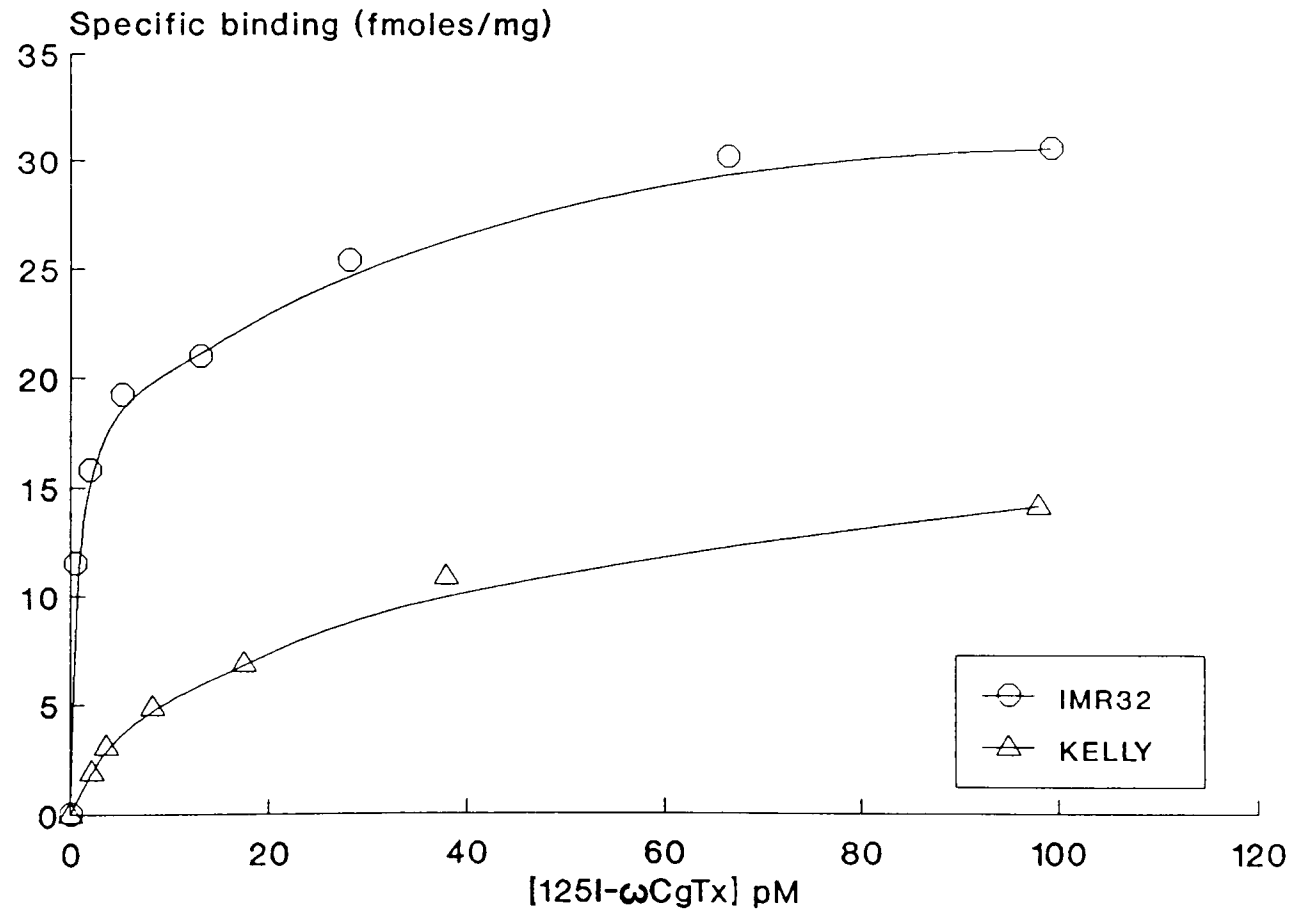

Specific binding (fmoles/mg)
35
30
25
20
15
10
5
0
0
20
40
60
80
100
120
[125I-ωCgTx] pM
IMR32
KELLY

Table 4.2

Properties of ^{125}I-ωCgTx binding to neuronal membranes

Tissue/Cell line	B_{max} (fmol/mg protein)	K_D (pM)	Number of determinations
Rat brain	238±63	6.6±2.3	5
SKNSH	63±9	13.7±3.6	3
Kelly	17	28.7	2
IMR32	30	2.3	1
MAR5	13±1	7.2±1.3	3
NG108	45	26.1	2
PC12	ND		3

ND = not detected

4.3.9. The effect of LEMS IgG on ^{125}I-ωCgTx binding

SKNSH and MAR5 cells were grown for two days in the presence of either pooled or individual preparations of IgG. The LEMS and OND pools were the same as those used for the calcium flux experiments described in the previous chapter. The amount of specific ^{125}I-ωCgTx binding to membranes prepared from cells exposed to IgG was determined using a saturable concentration of ligand (150pM). Results were expressed as a percentage of the specific binding measured in membranes from untreated cells (Figure 4.19). Binding site density in SKNSH cells exposed to pooled LEMS IgG was reduced to 43±7% ($p < 0.02$, n=3) of the density in control cells, whereas the number of binding sites in cells exposed to OND or HC IgG pools was not significantly changed (120±25% and 115±17% respectively, n=3). Similarly, MAR5 cells grown in pooled LEMS IgG contained 57±11% ($p < 0.02$, n=5) of control levels of binding sites, whereas cells exposed to OND pools were unaffected (93±25%, n=4).

IgG from individual LEMS patients did not have the same effect on the number of ^{125}I-ωCgTx binding sites as pooled IgG. The mean amount of binding in SKNSH cells exposed to LEMS or OND IgG was not significantly different from control levels (112±6%, n=12 and 110±4%, n=5 respectively). MAR5 cells exposed to LEMS IgG appeared to have a slightly reduced binding site density (78±8%, n=9). However, this value was similar to that found in cells exposed to OND IgG (86±11%, n=5).

In the above experiments, membranes prepared from treated cells were washed several times and IgG was not present in the incubation buffer of the binding assay. However it is possible

that the reduction of specific binding by pooled LEMS IgG was due to direct competition for the binding site by residual IgG. This was investigated by measuring ^{125}I-ωCgTx binding in SKNSH cell membranes in the presence of 2mg/ml IgG. Specific binding was reduced to 82±24% (n=4) of control levels by pooled LEMS IgG. This inhibition was not significant owing to the large variation of results and is not large enough to account for the reduction in binding site density reported above. The presence of pooled OND IgG did not affect ^{125}I-ωCgTx binding in SKNSH membranes (104±15%, n=7).

Figure 4.19: The effect of IgG on ^{125}I-ωCgTx binding.

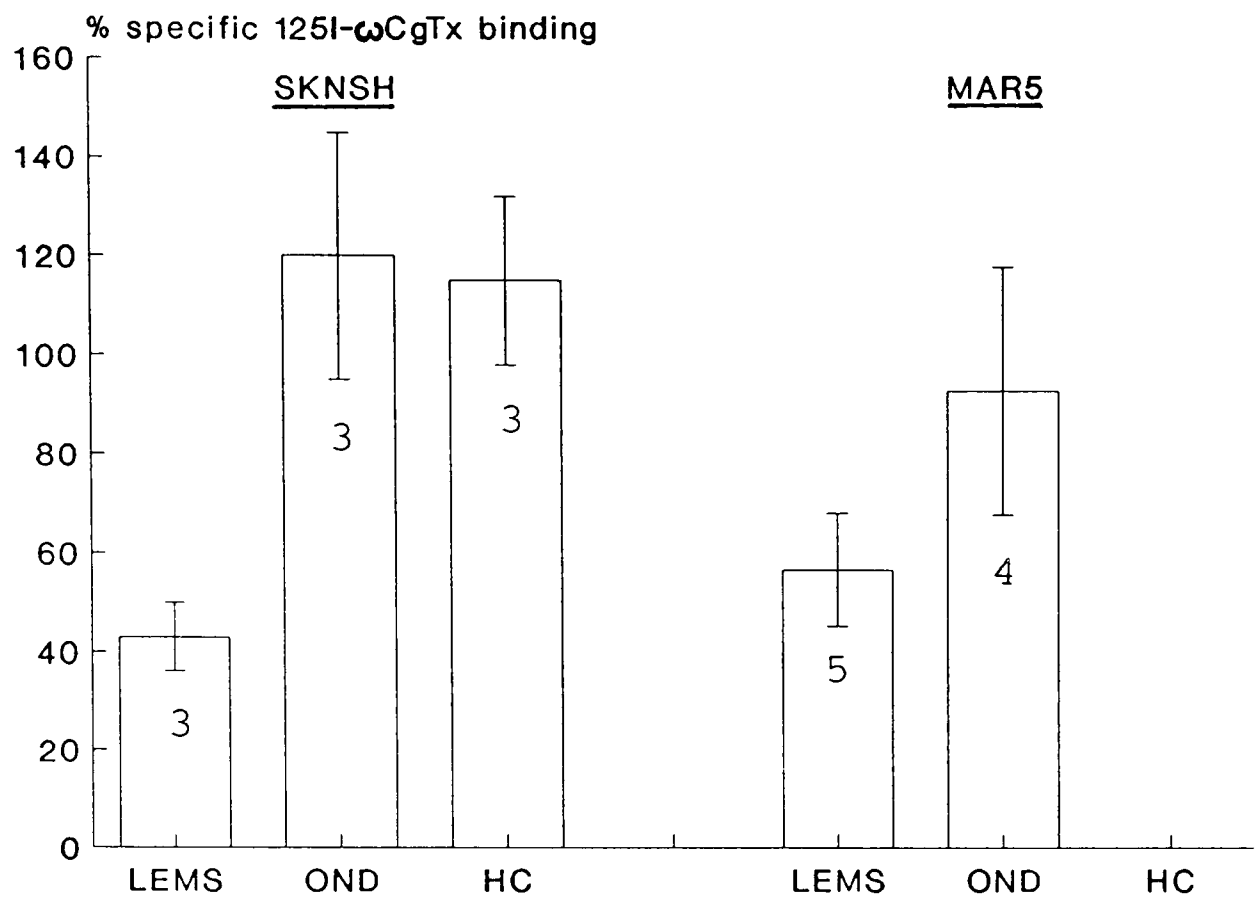
(a) SKNSH and MAR5 cells were grown for two days in culture medium containing pooled IgG, composed of six individual preparations, at a final concentration of 2mg/ml.

(b) SKNSH and MAR5 cells were grown in culture medium containing 2mg/ml IgG from single patients with either LEMS or OND.

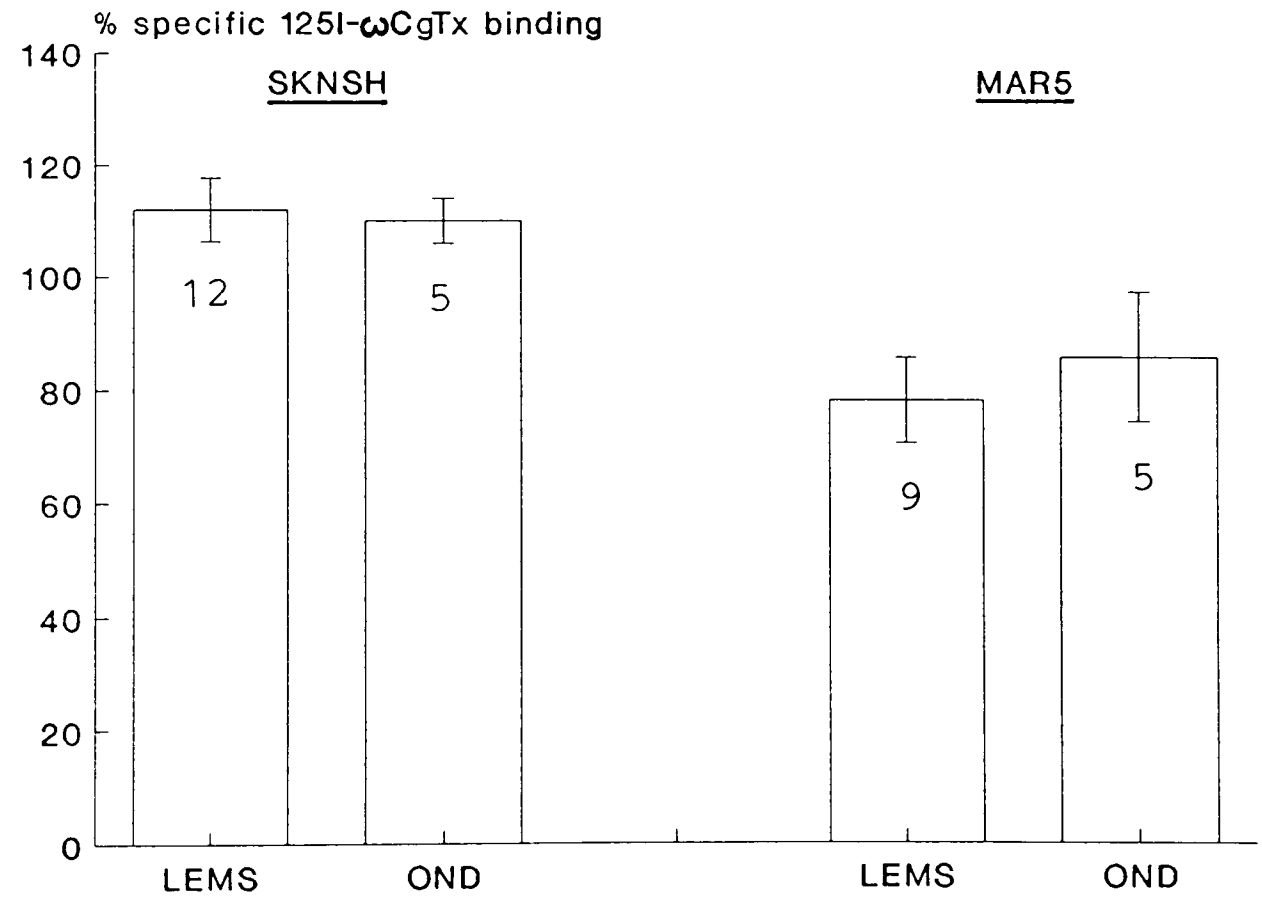
Specific binding of a saturating concentration of ^{125}I-ωCgTx (150pM) was determined in membranes prepared from IgG-treated cells and expressed as the percentage of specific binding measured in untreated cells grown in parallel. LEMS = Lambert-Eaton myasthenic syndrome, OND = other neurological disorder, HC = healthy control.

Results are the mean ± SEM of the number of determinations indicated.

(a)


% specific 125I-ωCgTx binding
160
140
120
100
80
60
40
20
0
SKNSH
MAR5
3
3
3
5
4
LEMS
OND
HC
LEMS
OND
HC

(b)


% specific 125I-ωCgTx binding
140
120
100
80
60
40
20
0
SKNSH
MAR5
12
5
9
5
LEMS
OND
LEMS
OND

4.4. Discussion

In this chapter, the nitrendipine derivative [^{3}H]-PN200-110 was used to detect the presence of DHP binding sites in neuronal preparations. The time course of [^{3}H]-PN200-110 binding to PC12 membranes agreed with a previous detailed kinetic analysis in rat brain in which maximum ligand association was found at approximately 60 minutes, regardless of ligand concentration (Weiland and Oswald 1985).

Saturable, high affinity [^{3}H]-PN200-110 binding representing one class of binding sites was found in crude homogenates of whole rat brain. However, the affinity of specific binding was not as great as that reported by other groups. This may reflect the purity of the membrane preparation. Studies using cerebral cortex only (Lee et al 1984) or pure brain synaptosomes (Weiland and Oswald 1985) have found a slightly higher binding site density and a greater ligand affinity (see also Table 1.2).

A saturable population of binding sites was also detected in membranes prepared from the rat phaeochromocytoma cell line, PC12. DHP binding sites at comparable levels have previously been detected in PC12 cells using [^{3}H]-nitrendipine (eg. 27.5 fmoles/mg protein, Toll 1982, 6.5 fmoles/mg protein, Takahashi and Ogura 1983). However, there was a 10-fold difference between the affinities of [^{3}H]-nitrendipine reported in these two studies (1.1nM and 0.15nM respectively) suggesting that the properties of the DHP receptor may vary between preparations, even of the same cell line. The affinity of [^{3}H]-PN200-110 cannot be directly compared with these studies, but is generally reported to be greater than that of [^{3}H]-nitrendipine. The affinity found here (0.59nM) is closer to

that reported for skeletal muscle than for neurones (eg. 1nM in guinea pig skeletal muscle, Goll et al 1983).

The specificity of [^{3}H]-PN200-110 binding to both rat brain and PC12 membranes was demonstrated by antagonist inhibition studies. Other DHPs (nitrendipine and nifedipine) abolished specific binding with inhibition constants in the nanomolar range. Phenylalkylamines, such as verapamil or methoxyverapamil, only slightly reduced specific binding at high concentrations (>100nM). Binding studies have shown that the three major classes of calcium antagonists, DHPs, phenylalkylamines and benzothiazepines, bind to separate sites on VGCCs, but that they interact in a complex manner due to allosteric linkage of the binding sites (Ferry et al 1985, Reynolds et al 1986, Triggle 1987). Thus, verapamil affects the affinity of [^{3}H]-PN200-110 binding in rat brain without changing the binding density (Lee et al 1984). The partial inhibition of specific binding by high concentrations of phenylalkylamines is therefore explained by this shift in ligand affinity. The localisation of the ω-conotoxin binding site on the VGCC is unknown, but it has been shown that there is no interaction between DHP and ωCgTx binding to adrenal medullary membranes (Jan et al 1990). Consistent with this is the lack of effect of ωCgTx on [^{3}H]-PN200-110 binding to rat brain seen here.

Low levels of specific [^{3}H]-PN200-110 binding were detected in other cell lines (MAR5, NG108, SKNSH and Kelly) but saturability could not be demonstrated within the concentration range studied. Accurate estimations of specific binding at higher ligand concentrations could not be achieved due to the large proportion of non-specific binding. It was shown in the previous chapter that

nitrendipine partially inhibited K^+-dependent calcium fluxes in NG108, SKNSH and Kelly cells. The sensitivity of K^+-stimulated flux to nitrendipine in MAR cells has previously been reported (Roberts et al 1985). Other groups have demonstrated the sensitivity of cultured neuroblastoma cells to DHPs using patch clamp techniques (Peers et al 1990, Carbone et al 1990). Furthermore, high affinity [^{3}H]-DHP binding has been characterised in NG108 cells (Miller 1987). There seems little doubt that calcium currents measured in the neuronal cell lines studied here are at least partially carried by DHP-sensitive VGCCs. There are several reasons for the lack of detection of the DHP binding sites associated with these channels:

1. The binding site density is too low to be detected with a ligand of low specific activity. It is difficult to predict the number of binding sites in a membrane preparation from physiological studies using intact cells. A very low number of functional VGCCs could be responsible for the calcium flux measured in the previous chapter.

2. The affinity of binding is low. It has been postulated that DHP binding sites in membrane fragments that maintain no membrane potential represent inactivated VGCCs that have a lower affinity for ligand binding than those in depolarised intact tissue (Miller 1987). Alternatively, cells maintained in culture may have an altered VGCC structure with a lower affinity for DHPs.

3. The presence of low affinity binding sites in large numbers prevents accurate definition of the high affinity binding. Analysis of the binding data by Scatchard transformation supports the presence of two binding sites, although more data is needed to confirm this hypothesis. The low affinity binding sites may not be

connected with DHP actions at VGCCs, but may represent other receptors or ion channels, transport proteins or other entities (Miller 1987). These sites did not appear to be present in the rat brain, PC12 or IMR32 membrane preparations.

The presence of the high-affinity DHP binding site on NG108 membranes was apparent by the inhibition of [^{3}H]-PN200-110 binding by other DHPs but not by methoxyverapamil.

The dependency of [^{3}H]-PN200-110 binding on the presence of calcium has been demonstrated in brain, cardiac and smooth muscle, but not in skeletal muscle, in which the removal of calcium by EDTA actually enhances DHP binding (Miller and Freedman 1984, Ferry et al 1985). The removal of calcium from the incubation buffer in the present study resulted in a large decrease in specific [^{3}H]-PN200-110 binding in rat brain, and to a lesser extent in MAR5 and NG108 membranes. The residual binding in MAR5 and NG108 membranes possibly represents the proportion of DHP binding to entities lacking the characteristics of the DHP receptor. Unfortunately, this experiment was not performed in PC12 membranes. It would be interesting to determine whether the DHP receptor of PC12 cells resembles that of brain or skeletal muscle in this respect.

NG108 cells were differentiated by treatment with the cyclic nucleotide, dibutyryl cAMP. It has been reported that, treated in this way, NG108 cells show a substantial increase in high affinity [^{3}H]-DHP binding (Miller 1987). However, in this study no difference in levels of [^{3}H]-PN200-110 binding between cAMP-treated and untreated cells was detected, consistent with the lack of change in DHP-sensitive calcium uptake reported in the previous chapter.

Specific ^{125}I-ωCgTx binding of very high affinity was detected in

all of the preparations tested, with the exception of the PC12 cells. The time course of association and stability of the toxin-receptor complex was consistent with previous reports (Cruz and Olivera 1986, Sher et al 1988). Binding site density in rat brain was higher than the density of DHP binding sites, suggesting the existence of two VGCC subtypes. Both the affinity and number of ^{125}I-ωCgTx binding sites in rat brain were comparable with published data (Barhanin et al 1988, Marqueze et al 1988). The properties of ^{125}I-ωCgTx (high specific activity, high affinity and low levels of non-specific binding) made it possible to detect relatively low binding site densities in the neuronal cell lines. Specific ^{125}I-ωCgTx binding was inhibited by unlabelled ωCgTx but not by DHPs, methoxyverapamil or diltiazem. This is consistent with several studies showing the lack of interaction between the binding of ωCgTx and that of other calcium antagonists (Cruz and Olivera 1986, Sher et al 1988, Ballesta et al 1989, Jan et al 1990). The inhibition of specific binding by divalent cations is also in agreement with previous reports (Marqueze et al 1988, Ballesta et al 1989). Thus the properties of ^{125}I-ωCgTx binding to neuronal membranes described in this chapter seem to agree with the published data of ^{125}I-ωCgTx binding to brain and other neuronal preparations.

The levels of specific binding found here may be partly accounted for by the binding of ^{125}I-ωCgTx to DHP-sensitive VGCCs. This would agree with electrophysiological studies in DRG neurones showing the sensitivity of both L and N channels to ωCgTx (McCleskey et al 1987). However, high affinity ^{125}I-ωCgTx binding sites were not detected in PC12 cells, despite the presence of

specific [^{3}H]-PN200-110 binding described above. This confirms the presence of a pure population of non-ωCgTx-sensitive, DHP-sensitive VGCCs in this cell line. On the basis of binding studies in chick tissues, L channels have been subdivided into those that are ωCgTx-insensitive such as those found in muscle (L_m) and those that are ωCgTx-sensitive, located on neurones (L_n) (Cruz et al 1987). Undifferentiated PC12 cells are thought to resemble adrenal chromaffin cells rather than sympathetic neurones (Miller 1987) and therefore may express VGCCs with non-neuronal properties. However, ^{125}I-ωCgTx binding sites and ωCgTx-sensitive calcium currents have been described in both PC12 (Sher et al 1988) and adrenal chromaffin cells (Ballesta et al 1989, Jan et al 1990). The affinity of ^{125}I-ωCgTx binding varied widely between these studies, suggesting that the properties of the ωCgTx-sensitive channel may vary even in the same tissue. It appears that the PC12 cells used in the present study do not express ωCgTx-sensitive VGCCs: this may reflect different growth conditions used in our laboratory. The authors of the above studies agree that ωCgTx and DHPs act on different populations of VGCCs in PC12 and adrenal chromaffin cells. Also, there is growing evidence that in certain neurones, including neuroblastoma cells, DHPs and ωCgTx act on distinct VGCC subtypes (Carbone et al 1990). Thus it seems that the L_n channel postulated by Cruz et al (1987) may only be expressed by certain neurones, such as chick DRG cells.

The effect of LEMS IgG on the number of ^{125}I-ωCgTx binding sites was investigated in the neuroblastoma line, SKNSH, and the small cell lung carcinoma line, MAR5. Membranes were prepared from cells

grown for two days in the presence of either pooled or single IgG preparations. Specific binding was reduced in both cell lines by pooled LEMS IgG, but not by IgG from healthy controls or from patients with other neurological disorders. The addition of IgG to membranes had no direct effect on specific ^{125}I-ωCgTx binding, indicating that the reduction of binding sites was due to specific down-regulation of VGCCs. This finding agrees with the proposed mechanism of action of LEMS antibodies; ie. reduction of VGCC density by cross-linkage and accelerated internalisation (Fukuoka et al 1987, Nagel et al 1988). Electrophysiological studies have demonstrated an inhibitory effect of LEMS IgG on VGCC function with no immediate pharmacological blockade (Prior et al 1985). The down-regulation of ^{125}I-ωCgTx binding sites by pooled LEMS IgG has been reported previously in the human neuroblastoma line, IMR32 (Sher et al 1989).

LEMS IgG has been shown to block L channels in NG108 cells (Peers et al 1990) and in adrenal chromaffin cells (Kim and Neher 1988). However, the presence of N channels was not demonstrated in these preparations. The reduction of ^{125}I-ωCgTx binding sites shown here provides evidence for the action of LEMS IgG at N channels. The reduction of calcium flux by LEMS IgG shown in the previous chapter was due to equivalent effects on both L and N channels. The lack of discrimination by LEMS IgG between these two VGCC subtypes can be explained by (1) structural similarities and, therefore, shared epitopes between L and N channels or (2) a heterogeneous population of LEMS antibodies acting on different epitopes.

Reduction of ^{125}I-ωCgTx binding to SKNSH and MAR5 membranes was

not demonstrated by IgG from individual LEMS patients. This is consistent with the results of the calcium flux studies, and suggests that antibody binding to several epitopes is required for successful cross-linkage and down-regulation of calcium channels. The pathogenic significance of the antibodies detected in these experiments is, therefore, unclear.

4.5. Summary

A saturable population of specific [^{3}H]-PN200-110 binding sites was found in membranes prepared from rat brain and cultured PC12 cells (98 and 23 fmoles/mg protein respectively). The binding was of high affinity and was displaced by DHPs but not by other calcium antagonists. In rat brain, specific binding was shown to be dependent on the presence of Ca^{2+}. Saturable binding was not demonstrable in NG108, human small cell lung carcinoma (MAR5) or human neuroblastoma cells within the concentration range studied. Differentiation with cAMP did not increase DHP binding site density in NG108 cells.

By contrast, saturable, high affinity ^{125}I-ωCgTx binding was demonstrated in rat brain (238 fmoles/mg), NG108 (45 fmoles/mg), MAR5 (13 fmoles/mg), SKNSH (63 fmoles/mg), Kelly (17 fmoles/mg) and IMR32 cells (30 fmoles/mg). Specific binding was inhibited by unlabelled ωCgTx and divalent cations but was not affected by DHPs and other calcium antagonists. ^{125}I-ωCgTx binding was not detected in PC12 cell membranes.

The results indicate the presence of both DHP-sensitive (L type) and ωCgTx-sensitive (N type) VGCCs in rat brain, although ^{125}I-ωCgTx may bind to both channel subtypes in this tissue. The presence of L channels in PC12 cells is demonstrated by the specific binding of [^{3}H]-PN200-110; however these channels do not contain the binding site for ^{125}I-ωCgTx. The remaining cell lines appear to express primarily N type VGCCs, although the presence of low levels of L channels cannot be excluded.

The density of ^{125}I-ωCgTx binding sites was reduced in SKNSH and MAR5 cells after exposure to pooled LEMS IgG. This effect was not found in cells treated with IgG from individual patients.

CHAPTER 5

IMMUNOPRECIPITATION STUDIES

5.1. Introduction

There is considerable evidence to suggest that an autoimmune aetiology underlies LEMS (reviewed by Vincent et al 1989). Electrophysiological and morphological studies have implicated the voltage-gated calcium channel (VGCC) as the likely target for the LEMS antibody (Lang et al 1987, Nagel et al 1988). The reduction of voltage-dependent calcium flux by LEMS IgG has been demonstrated in several cultured cell lines (Roberts et al 1985, De Aizpurua et al 1988) and the amount of inhibition has been correlated with disease severity (Lang et al 1989b). However, there are several practical limitations to the use of the calcium flux assay for the routine detection of LEMS antibodies. Cells are cultured for several days in the presence of LEMS IgG before a reduction of K^+-stimulated calcium flux is induced, making it a lengthy procedure. Also large volumes of serum are required for the preparation of IgG. Thus the diagnosis of LEMS relies on clinical findings and electromyographic recordings.

The peptide toxin, ωCgTx, has recently become available as a probe for the study of neuronal VGCCs. The presence of high affinity and irreversible ^{125}I-ωCgTx binding to neuronal cell membranes as described in the previous chapter led to the development of a radioimmunoassay for the detection of anti-VGCC antibodies in serum. SKNSH neuroblastoma cells were chosen as the source of antigen owing to the relatively high number of ^{125}I-ωCgTx

binding sites (see Table 4.2). The partial inhibition of K^+-stimulated calcium flux by ωCgTx in SKNSH cells suggests that these binding sites are associated with functional VGCCs.

The sera of 78 LEMS patients and 88 controls, including patients with other neurological and immunological disorders, were tested for the presence of anti-VGCC antibodies by the immunoprecipitation of ^{125}I-ωCgTx-labelled VGCCs extracted from SKNSH cells. Antibody titres were compared with those obtained using VGCCs extracted from the human SCLC line, MAR5. Preliminary results using smaller groups of patients have been published (Leys et al 1989 and 1991). Similar radioimmunoassays using antigen extracted from SCLC lines and the neuroblastoma line, IMR32 have also been described (Lennon and Lambert 1989, Sher et al 1989 and 1990).

5.2.Methods

Aliquots of cell membranes were incubated with approximately 200pM ^{125}I-ωCgTx in buffer (25mM Tris-HCl, 5mM Hepes, 0.32M sucrose, 1μM pepstatin, 2μM leupeptin, 0.1mM PMSF, 20μg/ml soybean trypsin inhibitor, 0.5% BSA, pH 7.4). After 1 hour at 4°C, the unbound toxin was removed by centrifugation (15,000rpm, 10 minutes). The pellet was washed once in 2ml buffer, resuspended in buffer containing 1% Triton X-100 and left for 2 hours on ice. Unsolubilised material was spun down (13,000rpm, 30 minutes) and the supernatant used as 'extract' in the assay. A volume of extract containing 5 fmoles ^{125}I-ωCgTx binding sites (calculated by counting a sample of supernatant) was added to test or control serum in a total volume of 100μl. Increasing amounts of each serum sample between 0.25 and 5μl were tested but each tube was made up to a total of 5μl with carrier serum, composed of a pool of two healthy controls. After 2 hours at 4°C, 50μl goat anti-human IgG was added to each tube. 1ml PTX (20mM phosphate buffer, 0.002% sodium azide, 0.02mM PMSF, 0.1% Triton X-100, pH 7.4) was added after the formation of a visible precipitate (20-30 minutes) and left for a further 30 minutes. The tubes were then centrifuged at 13,000rpm for 3 minutes and the pellets washed twice with PTX before counting. Results were expressed as pmoles ^{125}I-ωCgTx binding sites precipitated per litre of serum (pM) and were calculated by regression analysis from the linear part of the titration curve. Each sample was assayed on at least two separate occasions.

5.3. Results

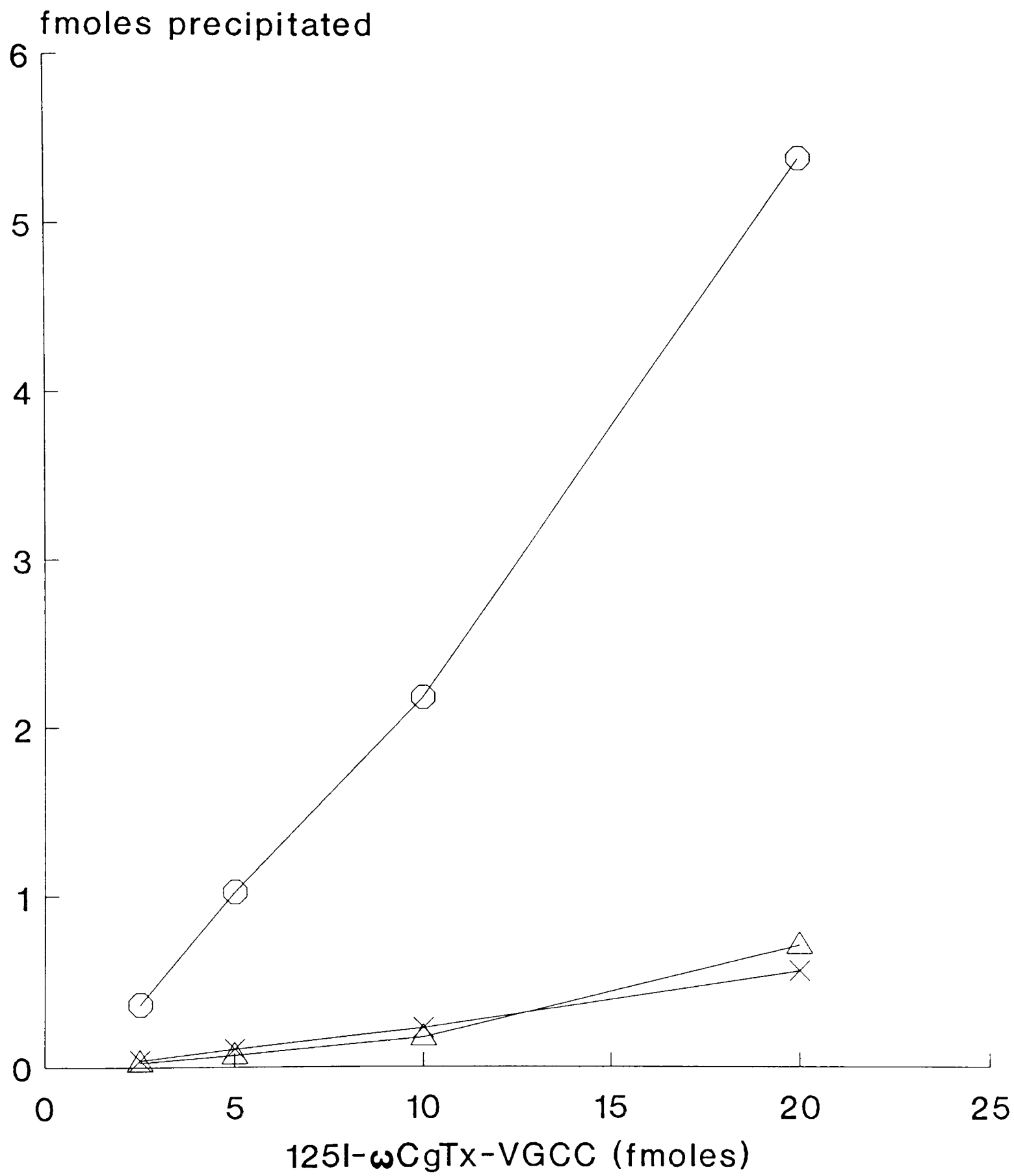
5.3.1. Assay conditions

Preliminary experiments determined the optimum conditions which were used for all subsequent assays. It was found that immunoprecipitation was reduced when serum was incubated with antigen for more than two hours. As the binding of ^{125}I-ωCgTx is essentially irreversible (see Figure 4.11), this reduction may be due to degradation of the ^{125}I-ωCgTx-VGCC complex. Short incubation and washing times were therefore used to maximise antibody titres.

Figure 5.1 shows the dependence of antibody titre on concentration of antigen. There was a linear increase in the amount of antigen precipitated by 1µl serum over the range studied (2.5-20 fmoles in 100µl, ie. 25-200pM). It was impossible to achieve higher concentrations of antigen due to the low density of ^{125}I-ωCgTx binding sites on neuronal cell membranes, therefore true antibody titres could not be calculated. The titres described below were calculated from the precipitation of a constant amount of antigen (5 fmoles).

Figure 5.1: The dependence of anti-VGCC antibody titre on antigen concentration.

A constant amount of serum (1µl) from LEMS patients 38 (○) and 24 (×) and a SCLC non-LEMS control (△) was incubated with increasing amounts of ^{125}I-ωCgTx binding sites extracted from SKNSH human neuroblastoma cells.


fmoles precipitated
6
5
4
3
2
1
0
0
5
10
15
20
25
125I-ωCgTx-VGCC (fmoles)

5.3.2. Precipitation of ^{125}I-ωCgTx-VGCCs from SKNSH cells

Serum from 78 patients with LEMS and 88 control subjects were tested for the presence of anti-VGCC antibodies, using SKNSH cells as the source of antigen. The clinical details and antibody titres obtained for the LEMS patients are listed in Table 5.1.

Titration curves from 0.25 to 5µl serum were performed for all samples tested. The precipitation of antigen by the sera of three LEMS patients is illustrated in Figure 5.2. The serum of patient 37 (see Table 5.1) reached maximum precipitation at about 2µl serum, characteristic of those sera giving titres greater than 200pM. In these cases the gradient of the linear part of the curve only was used to calculate antibody titre. Precipitation by the sera of patients 24 and 71 increased linearly over the range studied, typical for both LEMS and control sera with low levels of anti-VGCC antibody (<100pM). In these cases the gradient of the entire line was used to calculate antibody titre. The dotted lines show the lack of immunoprecipitation of antigen when prepared in the presence of an excess concentration of unlabelled ωCgTx (0.5µM).

Figure 5.3 shows the precipitation of VGCCs by two control sera with low antibody titres (one from a patient with RA and one from a SCLC non-LEMS patient) and the lack of precipitation by the serum of a healthy subject.

The anti-VGCC antibody titres for the sera of 18 healthy subjects ranged from 0 to 31 pM, with a mean and SEM of 0±4 pM. A positive titre was defined as greater than 2 SDs above the mean for the healthy controls (>30 pM).

The antibody titres for the 78 LEMS patients ranged from 0 to

1466 pM, with a mean and SEM of 126 ± 37 pM. 33 of these samples (42%) were positive for the presence of anti-VGCC antibodies (Figure 5.4). The patients with LEMS were divided into three groups (see Table 5.1): (1) those with biopsy-proven SCLC (SCLC-LEMS, n=29); (2) those with no detectable cancer and a case history of at least five years (NCD-LEMS, n=26); and (3) those whose cancer status was unclear (SU-LEMS, n=23). The last group included patients with lung cancer but not proven SCLC, patients with other malignancies and patients followed for less than five years. In a review of 50 LEMS patients it was found that neurological symptoms preceded the diagnosis of a tumour by up to 3.8 years (O'Neill et al 1988) and, therefore, the presence of SCLC in the last group of patients cannot be excluded. The mean titres and SEMs for the NCD-LEMS and the SU-LEMS groups were 150 ± 76 and 156 ± 68 pM respectively, with 46% and 52% positive for antibody (Table 5.2). The mean titre and incidence of positive sera was lower in the SCLC group (80 ± 49 pM, 31% positive for antibody), although these values were not significantly different from those of the other two LEMS groups (Wilcoxon rank sum test for unpaired data and chi-square test). The incidence of antibody-positive sera compared with the incidence in the healthy controls was significant in the NCD-LEMS and the SU-LEMS groups ($p < 0.02$ and $p < 0.01$ respectively) and in the LEMS group as a whole ($p < 0.01$), but not in the SCLC-LEMS group (Table 5.2).

The titres for the control sera (from healthy subjects and patients with other diseases) ranged from 0 to 82 pM, with a mean and SEM of 19 ± 3 pM. 21 of these sera were antibody positive as defined using the above criteria. The antibody-positive sera were

predominantly from patients with SCLC but without LEMS, or from those with either RA or SLE. The incidence was significant in both of these control groups when compared to healthy subjects ($p < 0.02$ and $p < 0.01$ respectively). The incidence in the OND, MG (Ab +ve) or MG (Ab -ve) groups and the control group as a whole was not significant.

In chapters 3 and 4 the effect of pooled IgG on VGCC function and number of ^{125}I-ωCgTx binding sites in SKNSH cells was described. The anti-VGCC antibody titres of the same LEMS and control pools were 628pM and 45pM respectively (mean of two determinations). The predicted titres, taking a mean of the results for the individual sera comprising each pool, were 229pM and 13pM respectively.

Table 5.1

Clinical details of the patients with Lambert-Eaton Myasthenic Syndrome

Patient Number	Age at onset	Sex	LEMS duration[a] (years)	Initial (mV)	Increment[b] (%)	Titre (pM)
SCLC-LEMS						
1	53	M	0.9	5.2	35	0
2	44	F	0.4	1.2	1233	41
3	53	M	0.3	1.5	327	0
4	64	M	0.8	0.55	2445	46
5	60	M	0.3	1.0	200	7
6	62	M	1.3	0.1	3900	40
7	53	M	0.3	5.3	43	12
8	69	M	0.1	1.3	438	16
9	58	F	1.0	2.1	335	23
10	58	F	0.8	3.2	431	15
11	61	M	0.2	5.0	160	0
12	65	F	0.4	0.2	800	0
13	34	M	1.0	0.7	1757	14
14	na	F	na	na	na	1404
15	55	M	1.3	7.6	137	7
16	63	F	1.1	8.4	112	0
17	na	M	na	na	na	355
18	71	F	0.2	6.4	191	0
19	56	F	0.5	1.8	333	12
20	66	M	0.1	0.6	1150	24
21	58	M	0.8	4.4	161	3
22	58	M	0.8	3.6	289	0
23	59	M	1.7	1.3	1169	40
24	66	F	0.4	10.5	65	54
25	38	F	3.6	0.4	3275	218
26	53	F	0.2	4.1	146	36
27	64	F	0.9	6.6	188	4
28	62	M	1.2	4.0	180	0
29	66	M	0.7	1.8	205	2
NCD-LEMS						
30	15	F	4.0	3.6	428	733
31	50	M	11.3	1.5	933	11
32	64	F	2.7	0.8	112	4
33	60	M	2.8	8.8	16	33
34	42	M	10.0	1.0	250	47
35	60	F	4.8	na	na	34
36	28	M	8.0	1.5	500	28
37	29	F	0.5	0.3	1800	1466
38	61	F	4.2	0.75	1967	1275
39	17	F	2.5	3.0	433	21
40	61	M	4.3	1.0	1860	0
41	43	M	3.3	0.4	3400	7
42	22	M	4.0	3.5	285	30

Patient Number	Age at onset	Sex	LEMS duration[a] (years)	Initial (mV)	Increment[b] (%)	Titre (pM)
NCD-LEMS						
43	79	M	0.7	7.5	140	0
44	69	M	2.8	1.6	650	38
45	56	F	4.0	5.4	126	0
46	51	F	15.0	na	na	20
47	48	M	2.8	2.0	166	36
48	60	M	1.5	4.2	376	8
49	47	M	1.6	6.1	146	37
50	54	M	1.2	3.9	448	31
51	30	M	7.0	6.6	120	0
52	70	F	2.1	0.9	788	22
53	74	M	5.9	0.8	1275	41
54	52	F	4.0	2.6	260	4
55	58	M	3.0	2.0	960	22
SU-LEMS						
56	47	M	1.0	1.2	650	329
57	42	M	0.7	1.5	927	20
58	55	M	0.3	7.5	147	14
59	53	F	0.2	2.6	92	49
60	66	M	3.1	3.4	518	58
61	40	F	13.0	0.4	3275	1447
62	59	M	8.0	4.4	125	45
63	na	M	na	na	na	602
64	42	F	0.8	6.3	233	7
65	60	F	1.8	4.6	222	22
66	28	F	0.3	2.8	400	2
67	49	M	0.2	2.0	240	65
68	25	F	3.7	7.2	111	1
69	52	M	1.2	1.05	1040	0
70	23	F	0.2	8.5	88	21
71	31	F	0.5	3.9	35	100
72	70	M	0.6	1.6	369	33
73	51	M	0.6	4.0	150	489
74	na	M	na	na	na	208
75	15	M	0.7	1.5	933	1
76	63	M	1.3	0.5	2380	58
77	64	F	1.1	1.6	481	11
78	78	M	1.6	3.2	259	20

a At time of first sample
b % increase in CMAP amplitude after 15 seconds maximum voluntary contraction.

CMAP = compound muscle action potential, SCLC = small cell lung carcinoma, NCD - no cancer detected, SU = status uncertain, na = not available.

Patients 58, 59, 63 and 69 had carcinoma of the lung for which histology was not available. Patient 67 had squamous cell carcinoma of the lung, patient 60 had a lymphoma and patient 61 had breast cancer. The presence of anti-AChR antibodies indicated the possible co-existence of myasthenia gravis in patients 62 and 71. The remainder of the patients in the SU group had a case history of less than 5 years, therefore the presence of SCLC cannot be excluded.

Figure 5.2: Precipitation of ^{125}I-ωCgTx-VGCCs from SKNSH cells by LEMS sera.

Increasing amounts of serum from LEMS patients 37 (○), 71 (□) and 24 (△) were incubated with ^{125}I-ωCgTx binding sites (5 fmoles) extracted from SKNSH cells. The antibody titres for these patients were 1466, 100 and 54 pM (pmoles ^{125}I-ωCgTx binding sites precipitated/litre serum) respectively. The dotted lines show the amount of precipitation obtained with the same sera when ^{125}I-ωCgTx was bound to SKNSH membranes in the presence of 0.5μM unlabelled ωCgTx. The specific activity of ^{125}I-ωCgTx was 1200 Ci/mmole.

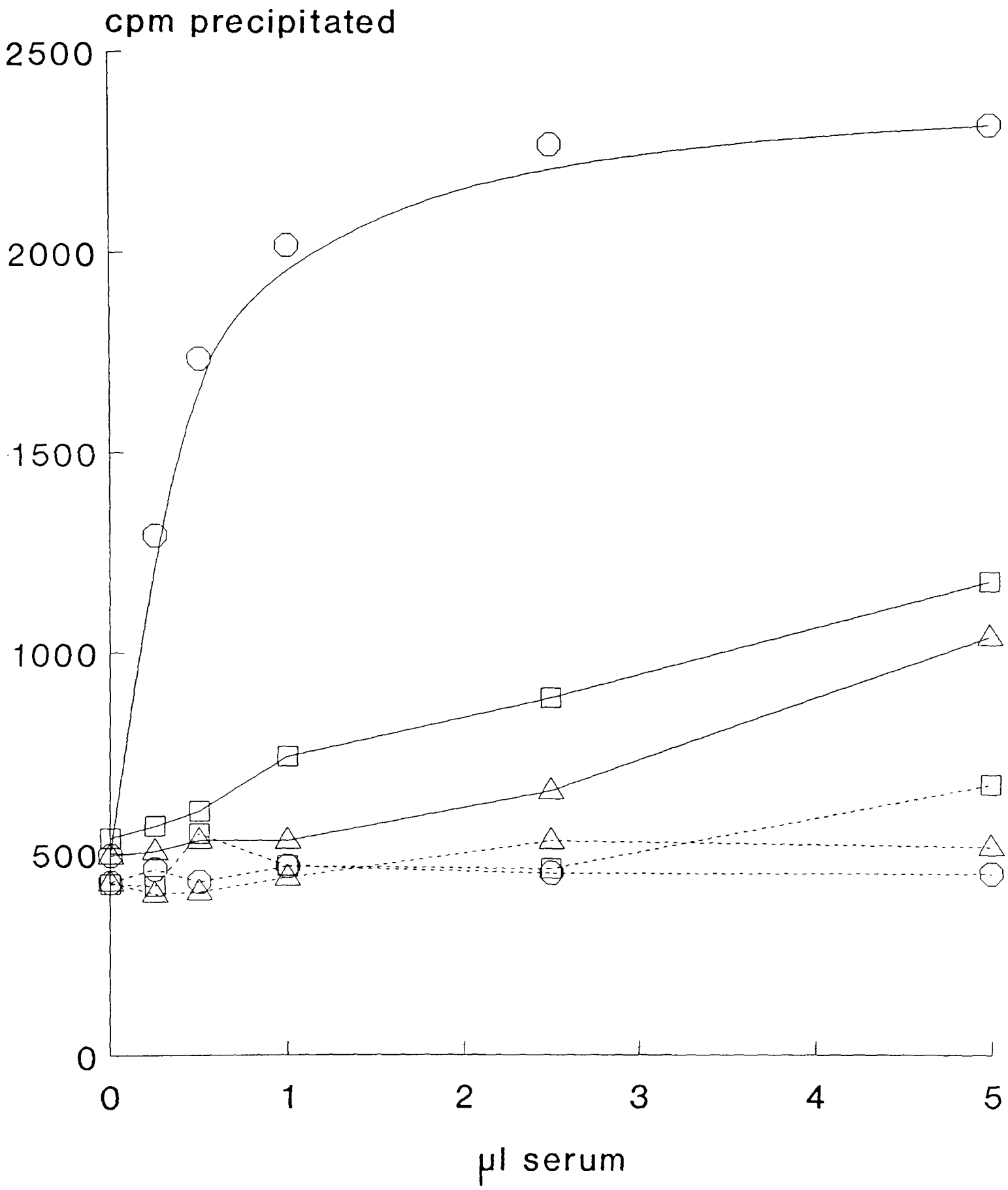

cpm precipitated
2500
2000
1500
1000
500
0
0
1
2
3
4
5
µl serum

Figure 5.3: Precipitation of ^{125}I-ωCgTx-VGCCs from SKNSH cells by control sera.

Sera from a patient with RA (○), a SCLC non-LEMS patient (△) and a healthy control (◇) were incubated with ^{125}I-ωCgTx binding sites (5 fmoles) extracted from SKNSH cells. The antibody titres for these sera were 62, 38 and 0 pM respectively. The dotted lines show the precipitation of antigen prepared in the presence of 0.5μM unlabelled ωCgTx by the same sera. The specific activity of ^{125}I-ωCgTx was 1200 Ci/mmole.

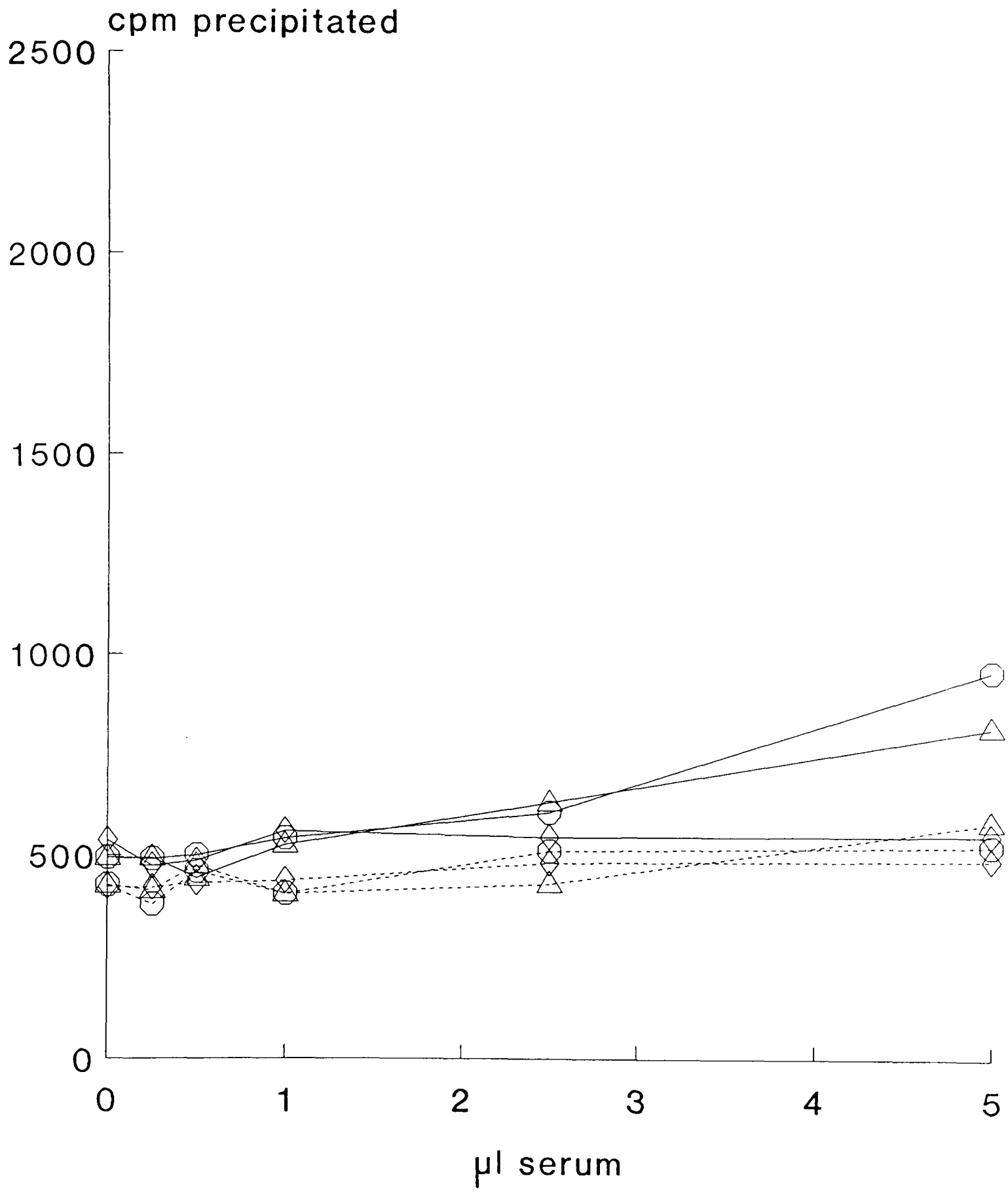

cpm precipitated
2500
2000
1500
1000
500
0
0
1
2
3
4
5
µl serum

Figure 5.4: Anti-VGCC antibody titres of 78 LEMS and 88 control sera using SKNSH antigen.

Serum antibodies were measured by the immunoprecipitation of ^{125}I-ωCgTx-labelled VGCCs extracted from SKNSH cells. Antibody titres were defined as positive if greater than 30 pM (2SDs above the mean for the healthy controls (HC), indicated by the dotted line). SCLC = small cell lung carcinoma, NCD = no cancer detected, SU = status uncertain, OND = other neurological disorder, MG +ve = myasthenia gravis positive for anti-AChR antibodies, MG -ve = myasthenia gravis negative for anti-AChR antibodies, RA = rheumatoid arthritis, SLE = systemic lupus erythematosus.

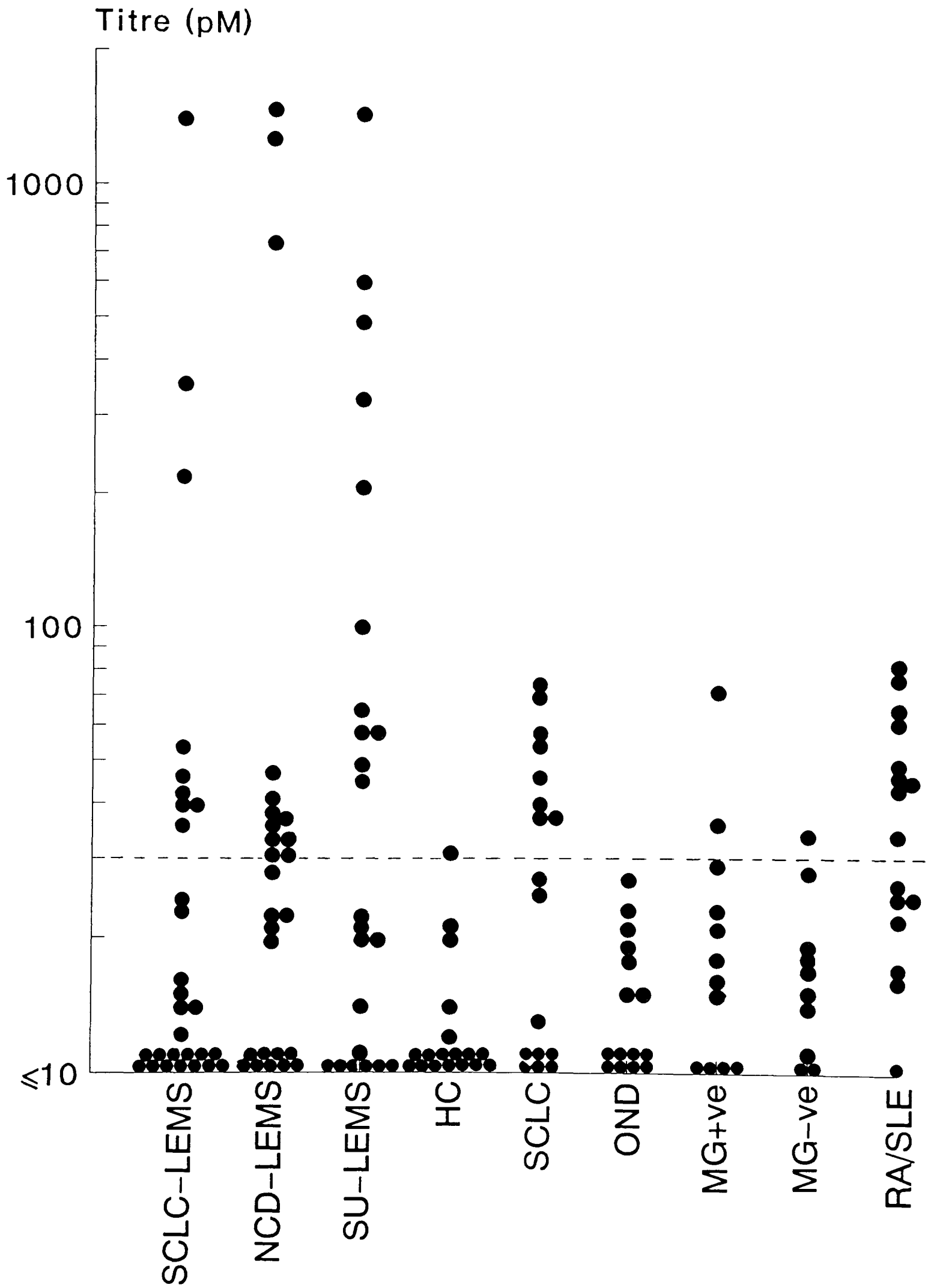

Titre (pM)
1000
100
⩽10
SCLC–LEMS
NCD–LEMS
SU–LEMS
HC
SCLC
OND
MG+ve
MG–ve
RA/SLE

Table 5.2

Anti-VGCC antibodies in LEMS and control sera using SKNSH neuroblastoma antigen

Group	n	Antibody titre (pM) (mean±SE)	Positive for antibody (>30pM)
LEMS	78	126±37	33 (42%) **
SCLC-LEMS	29	80±49	9 (31%)
NCD-LEMS	26	150±76	12 (46%) *
SU-LEMS	23	156±68	12 (52%) **
CONTROLS	88	19+3	21 (24%)
HC	18	0±4	1 (6%)
SCLC	17	30±6	8 (47%) *
OND	15	8±4	0
MG (Ab+ve)	12	18±6	2 (17%)
MG (Ab-ve)	10	17±3	1 (10%)
RA/SLE	16	40±6	9 (56%) **

* = $p<0.02$, ** = $p<0.01$ (chi-square test versus the healthy controls with Yates correction).

5.3.3. Precipitation of ^{125}I-ωCgTx-VGCCs from MAR5 cells

The sera of 28 LEMS patients and 40 controls were tested for anti-VGCC antibodies using antigen extracted from MAR5 cells. Figure 5.5 shows the precipitation curves obtained with two LEMS and two control sera when tested with this antigen. A positive titre was defined as greater than 21pM (2SDs above the mean titre for the healthy controls, n=8). 20 of the LEMS sera tested had previously been found to be antibody-positive using antigen extracted from SKNSH cells. 16 of these were also found to be antibody-positive using the MAR5 antigen, with titres ranging from 21-1260pM (Figure 5.6). The four samples that were not positive for antibody all had very low titres when tested with the SKNSH antigen (30-40pM). There was a high correlation between the titres obtained for the 28 LEMS sera when tested with the two sources of antigen (Spearman rank correlation coefficient (RS) = 0.89, $p < 0.001$) (Figure 5.7).

Of the control sera tested, none were positive in the healthy control group, while 9 were found to be slightly positive from the SCLC, OND and MG groups (21-59pM). Only three of these were previously found to be positive when tested with SKNSH antigen. The incidence of antibody-positive sera in patients with RA or SLE was confirmed (5 out 8 samples tested; 6 were positive in the SKNSH assay). However, there was no clear correlation between the titres obtained for this group of patients in the two assays (RS = 0.55, n = 8).

Figure 5.5: Precipitation of ^{125}I-ωCgTx-VGCCs from MAR5 cells by LEMS and control sera.

Sera from LEMS patients 37 (○) and 56 (△), a patient with SLE (□) and a healthy control (▽) were incubated with ^{125}I-ωCgTx binding sites (5 fmoles) extracted from a human SCLC line, MAR5. The antibody titres using this antigen were 934, 77, 50 and 0 pM respectively. The specific activity of ^{125}I-ωCgTx was 1800 Ci/mmole.

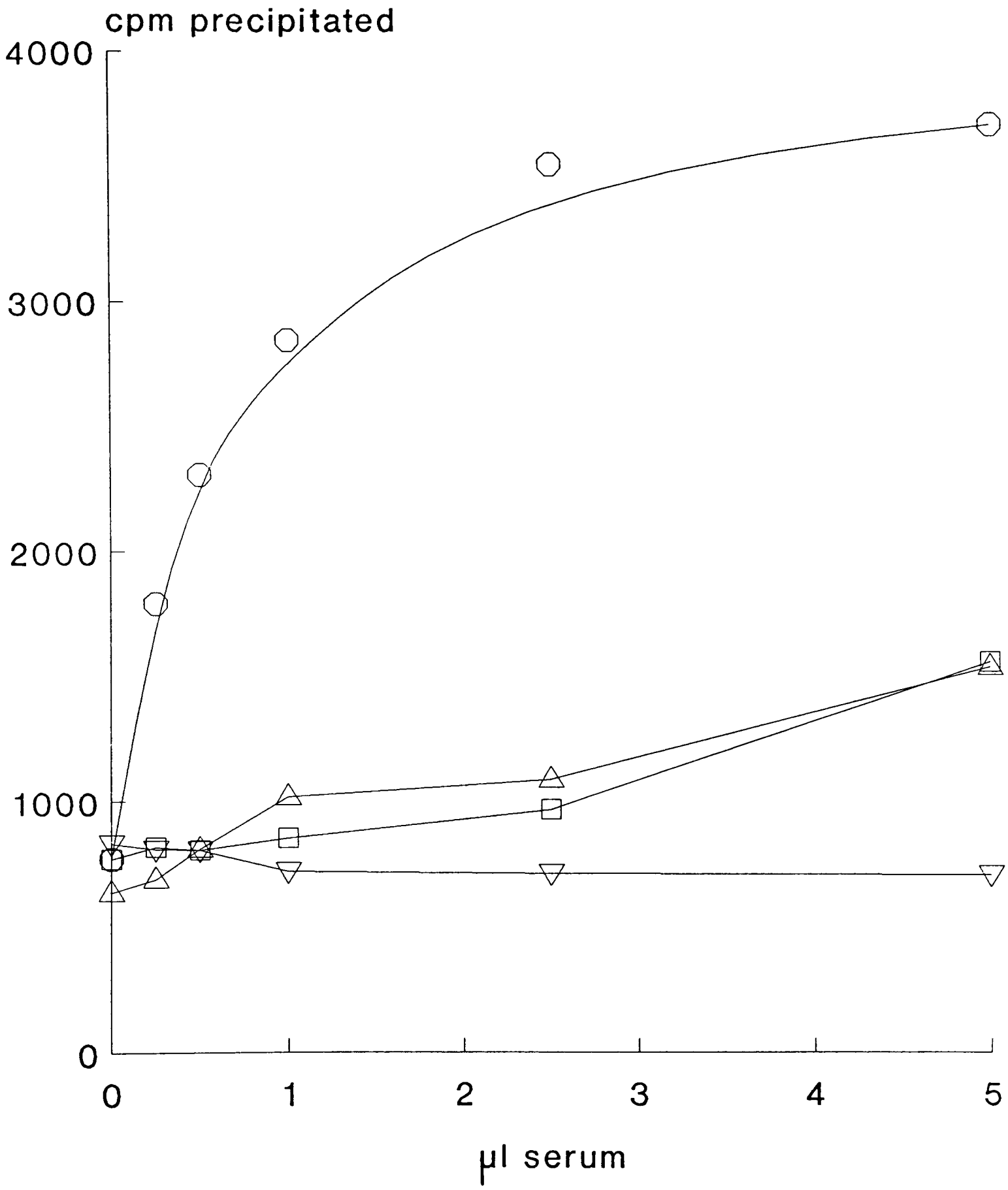

cpm precipitated
4000
3000
2000
1000
0
0
1
2
3
4
5
µl serum

Figure 5.6: Anti-VGCC antibody titres of 28 LEMS and 40 control sera using MAR5 antigen.

Serum antibodies were measured by the immunoprecipitation of ^{125}I-ωCgTx-labelled VGCCs extracted from MAR5 cells. Antibody titres were defined as positive if greater than 21 pM (2SDs above the mean for the healthy controls, indicated by the dotted line). The non-SCLC LEMS group includes patients from both the NCD-LEMS and the SU-LEMS groups.

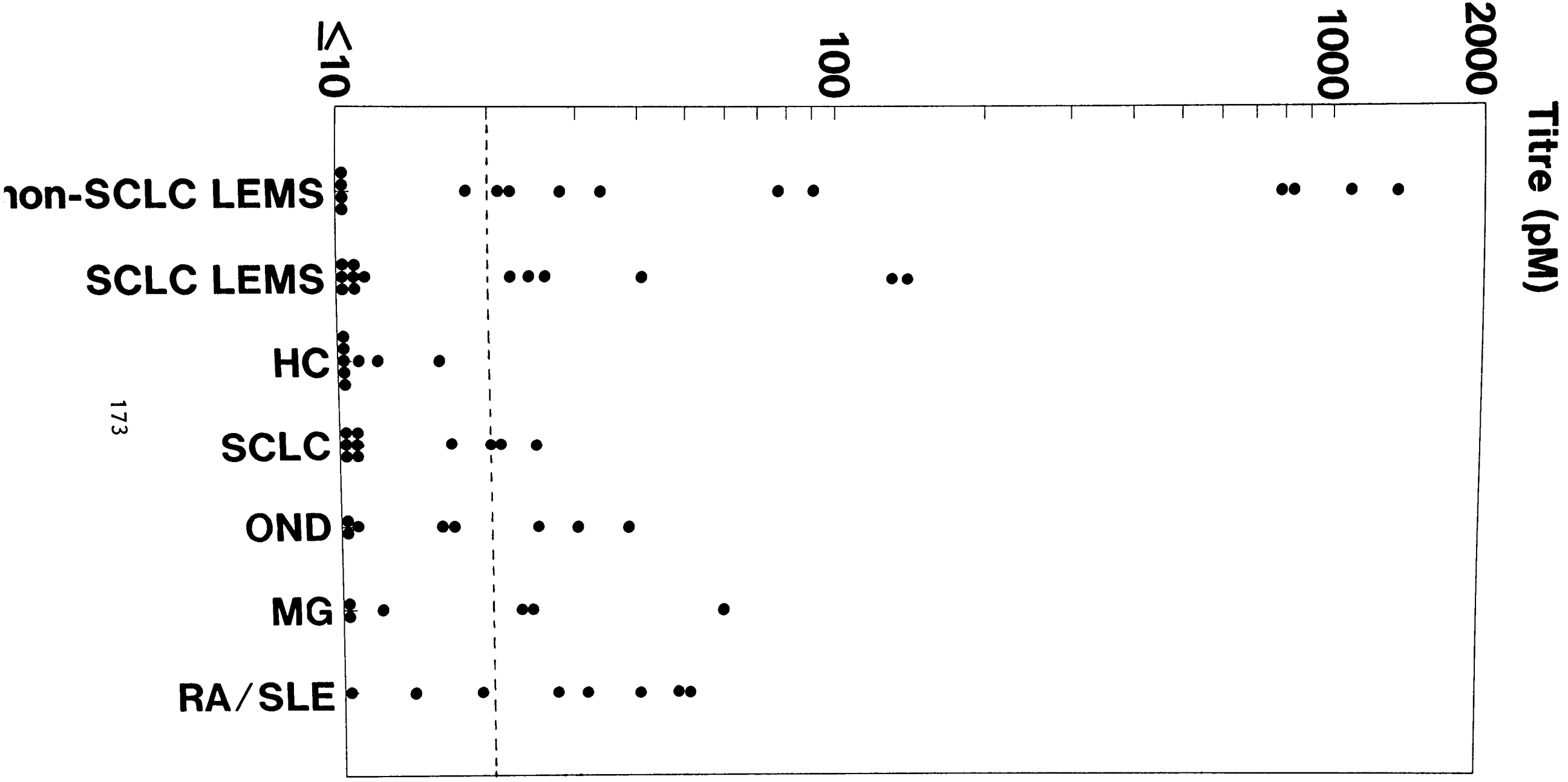
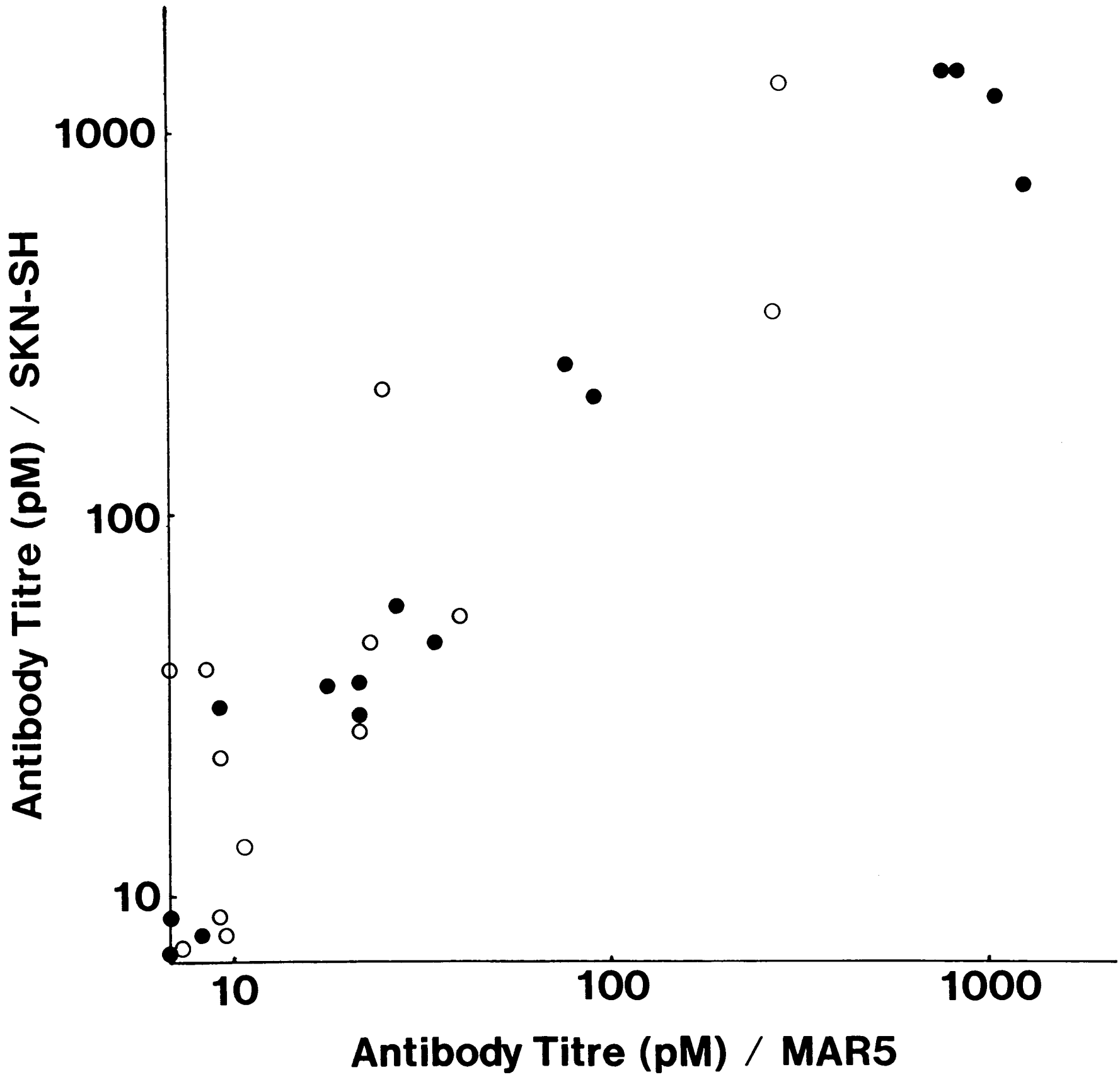

Titre (pM)
≤10
100
1000
2000
non-SCLC LEMS
SCLC LEMS
HC
SCLC
OND
MG
RA/SLE

Figure 5.7: Correlation of anti-VGCC antibody titres using antigen extracted from SKNSH and MAR5 cells.

There was a high correlation between the antibody titres obtained by immunoprecipitation of ^{125}I-ωCgTx-labelled VGCCs from the two human cell lines, SKNSH and MAR5 (RS = 0.89, $p < 0.001$, $n = 28$). (O) = SCLC-LEMS, (●) = non-SCLC LEMS.


1000
100
10
10
100
1000
Antibody Titre (pM) / SKN-SH
Antibody Titre (pM) / MAR5

5.3.4. Precipitation of ^{125}I-ωCgTx-VGCCs from rat brain

A few samples were tested for anti-VGCC antibodies using antigen extracted from rat brain membranes. The titres obtained are compared with those measured using the SKNSH and MAR5 antigens in Table 5.3.

Table 5.3

Comparison of anti-VGCC antibody titres using three sources of antigen

		Antibody Titre (pM)		
		SKNSH	MAR5	Rat brain
Patient No.	Status			
24	SCLC	54	41	54
38	NCD	1275	1083	453
55	NCD	22	ND	0
56	SU	254	77	244
61	SU	1447	823	328
Control				
HC		9	11	5
SCLC		25	ND	38
OND		19	5	36
OND		0	38	8
MG		0	10	0

ND = not determined

5.3.5. Correlation of anti-VGCC antibody titre with disease severity

Two indices of the severity of LEMS were measured: the CMAP amplitude and the percentage increment in amplitude after 15 seconds maximum voluntary contraction (see Table 5.1). These values were available for 72 of the 78 LEMS patients studied. Antibody titre using SKNSH antigen was compared with the corresponding indices of disease severity when the electromyographic measurements were taken within one month of the serum sample tested (Figure 5.8). No correlation between antibody titre and either the CMAP amplitude or the percentage increment for these patients was observed (RS = 0.1 and 0.13 respectively, n = 50).

5.3.6. Longitudinal studies of two LEMS patients

Serum samples had been collected over several years from two LEMS patients receiving immunosuppressive therapy. These were tested for anti-VGCC antibodies using the SKNSH antigen (Figure 5.9). Both patients had high initial antibody titres. Neither of the patients had detectable SCLC. Patient 38 (see Table 5.1), followed for 6 years, showed a pronounced clinical improvement during prednisolone therapy, indicated by an increase in CMAP amplitude towards the normal range (>8.5mV). There was a corresponding decrease in anti-VGCC antibody titre from 2525pM to 45pM (Figure 5.9a). In patient 37, followed for 11 years, antibody levels showed a similar inverse relation with CMAP amplitude (Figure 5.9b), although the antibody titre remained high (above 500pM) even when the CMAP amplitude was in the normal range.

The change in antibody titre in the serum of these two patients was reproduced using the MAR5 antigen (Figure 5.10), thus confirming the above findings.

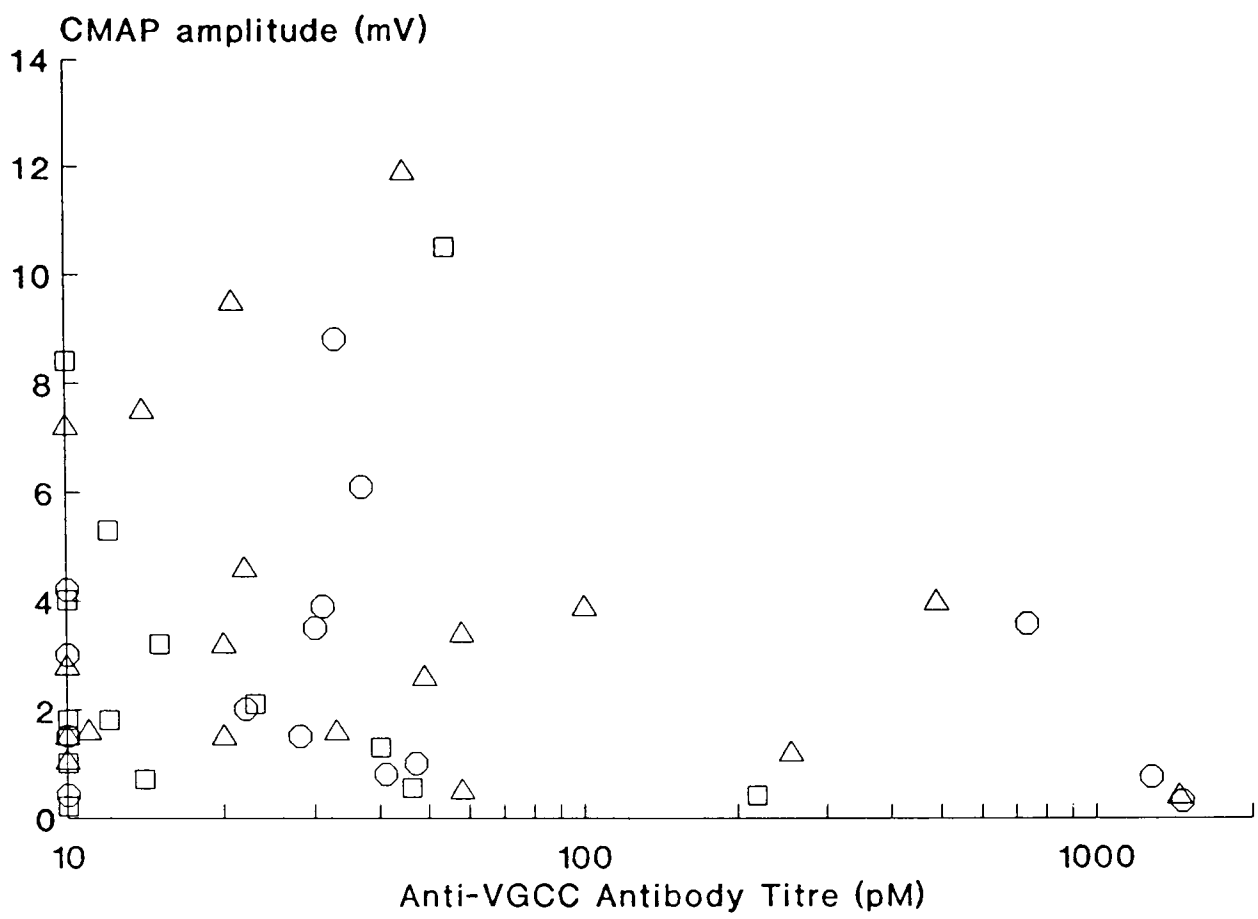
5.3.7. The co-existence of LEMS and MG in two patients

An initial diagnosis of LEMS was made in patients 62 and 71 (Table 5.1) based on clinical and electromyographic criteria. Anti-VGCC antibody titres were raised in both cases (45 and 100pM respectively, using the SKNSH antigen). Patient 62 had already responded to immunosuppressive therapy when his serum was tested and an earlier sample when LEMS was clinically more severe was not available. Although there was little clinical evidence for the existence of MG in these two patients, the anti-AChR antibody titres were high in both cases (124 x 10^{-10} M and 317 x 10^{-10} M respectively, upper limit of normal = 5 x 10^{-10} M). This antibody is specific for MG and is present in about 90% of patients. It seems likely therefore that the anti-AChR antibodies contributed to the myasthenic weakness in these two patients (Newsom-Davis et al, in press).

Figure 5.8: Comparison of anti-VGCC antibody titre with indices of disease severity.

Serum antibody levels are shown against (a) the corresponding compound muscle action potential (CMAP) amplitudes and (b) the percentage increment in CMAP amplitude after 15 seconds maximum voluntary contraction. The electromyographic measurements were made within one month of the date of the serum sample tested for antibody. There was no correlation between antibody titre and either of these indices of disease severity (RS = 0.1 and 0.13 respectively, n = 50). Source of antigen = SKNSH cells. (□) = SCLC-LEMS, (O) = NCD-LEMS, (△) = SU-LEMS.

(a)


CMAP amplitude (mV)
14
12
10
8
6
4
2
0
10
100
1000
Anti-VGCC Antibody Titre (pM)

(b)

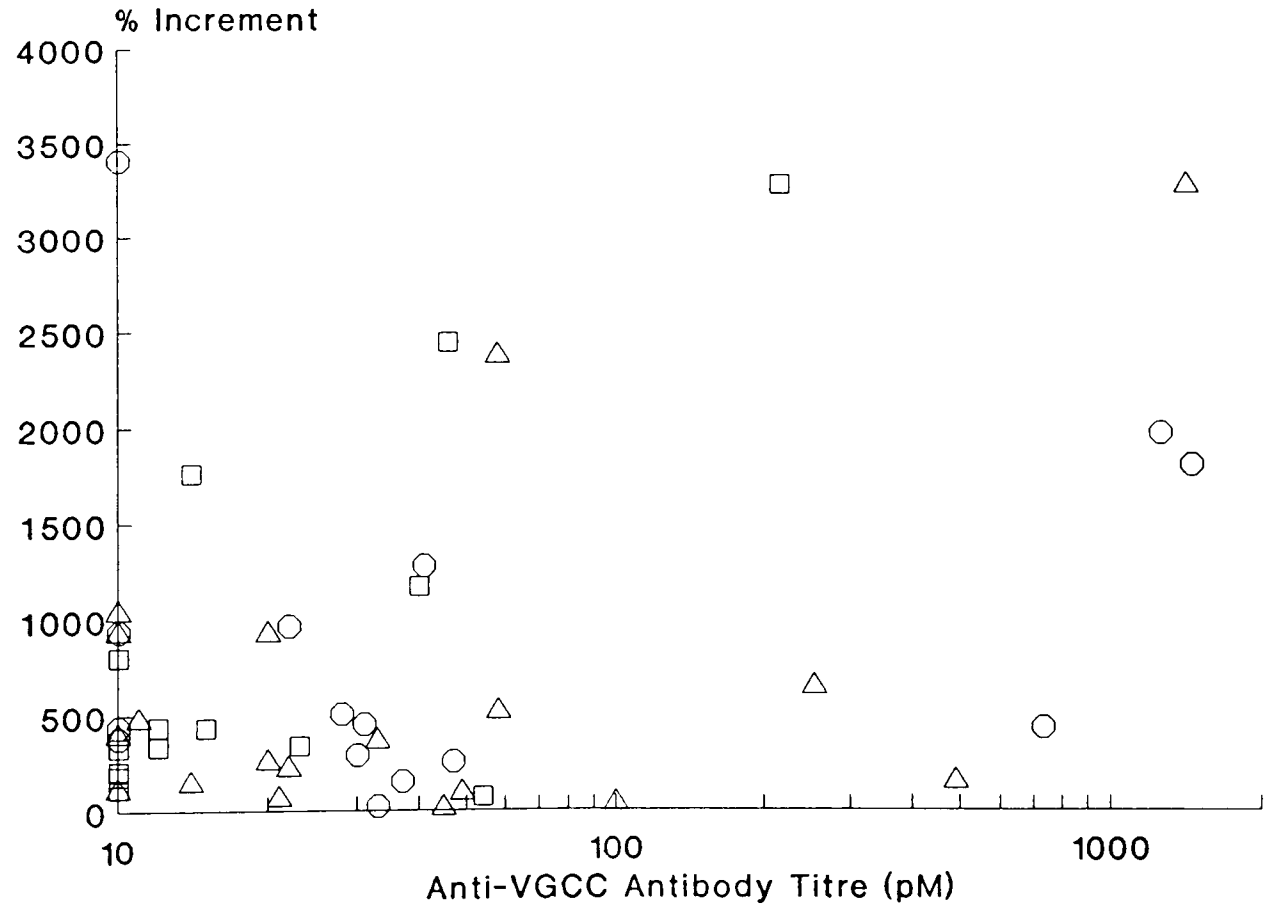
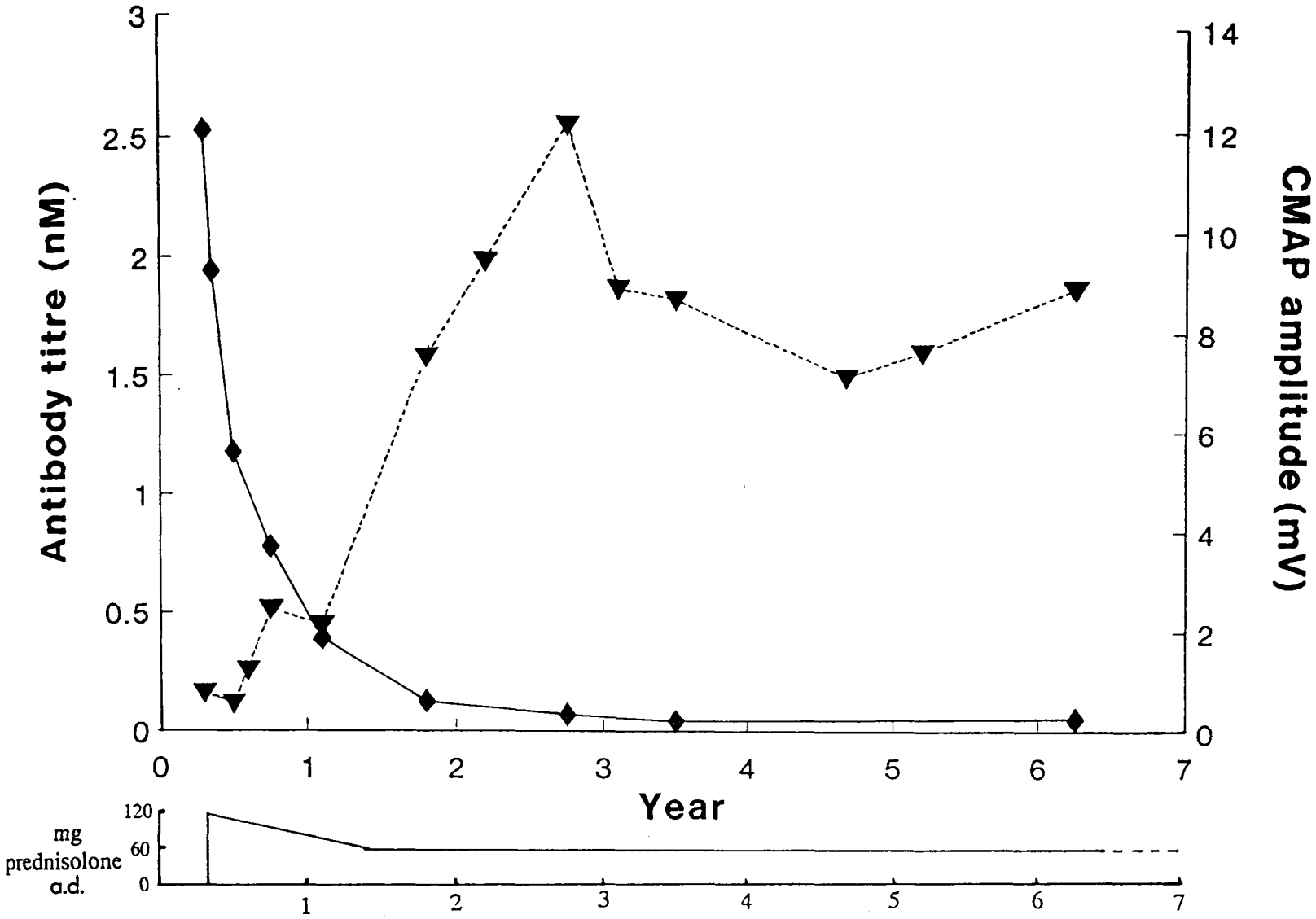

% Increment
4000
3500
3000
2500
2000
1500
1000
500
0
10
100
1000
Anti-VGCC Antibody Titre (pM)

Figure 5.9: Longitudinal studies of anti-VGCC antibody titre in two LEMS patients using SKNSH antigen.

The change in serum antibody levels (◆, solid line) and the corresponding CMAP amplitudes (▼, dotted line) were measured in retrospective studies of 2 LEMS patients: (a) patient number 38 (see Table 5.1), followed for 6 years, and (b) patient number 37, followed for 11 years. The serum samples for each patient were assayed for antibody on the same occasion. The alternate day (a.d.) dose of prednisolone administered is illustrated diagrammatically beneath each graph. In addition, patient 38 was treated with 120mg 3,4-diaminopyridine daily and patient 37 with 100mg azathioprine daily, throughout the period of study.

(a)


Antibody titre (nM)
CMAP amplitude (mV)
Year
mg prednisolone a.d.
120
60
0

(b)

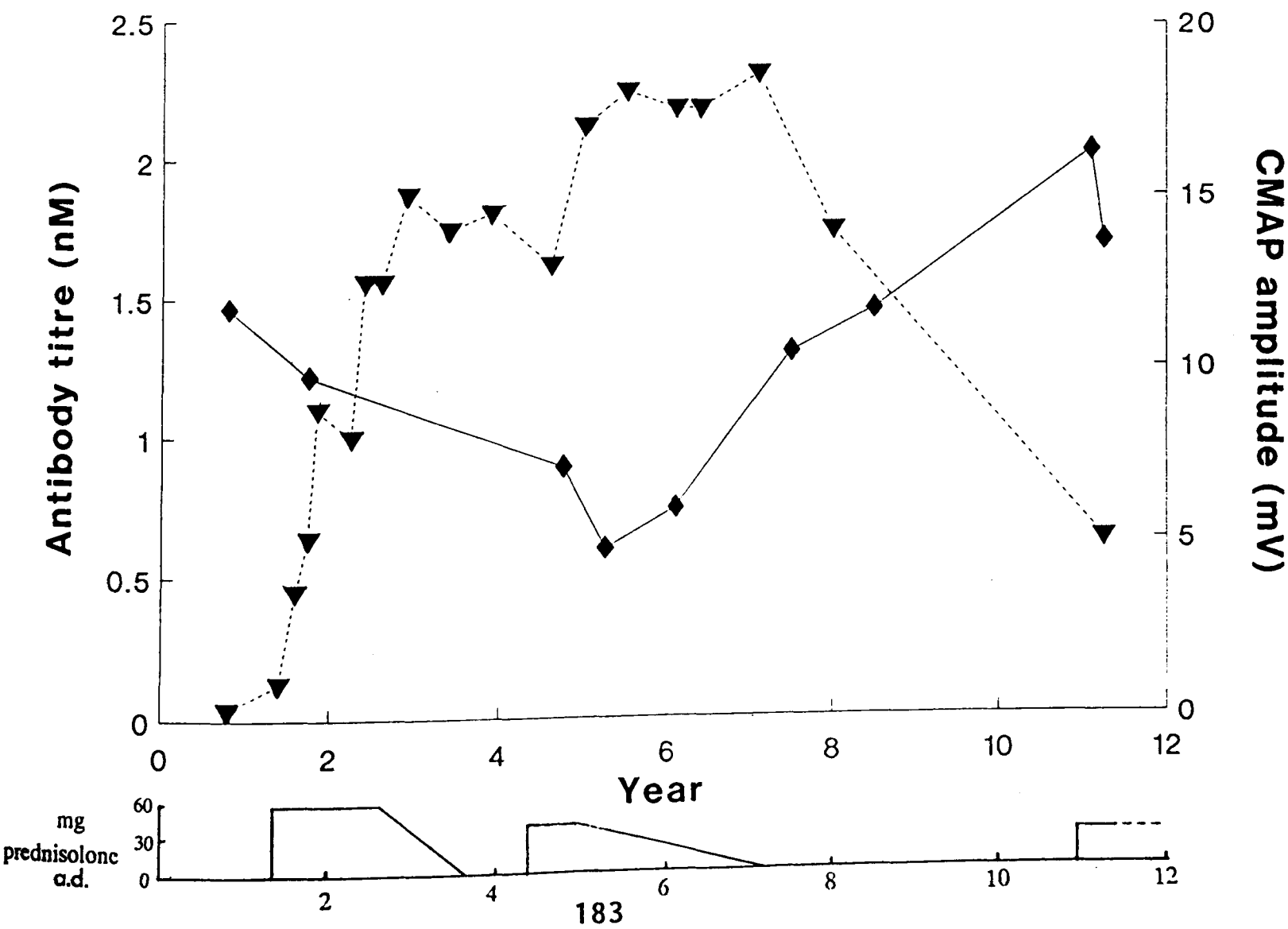
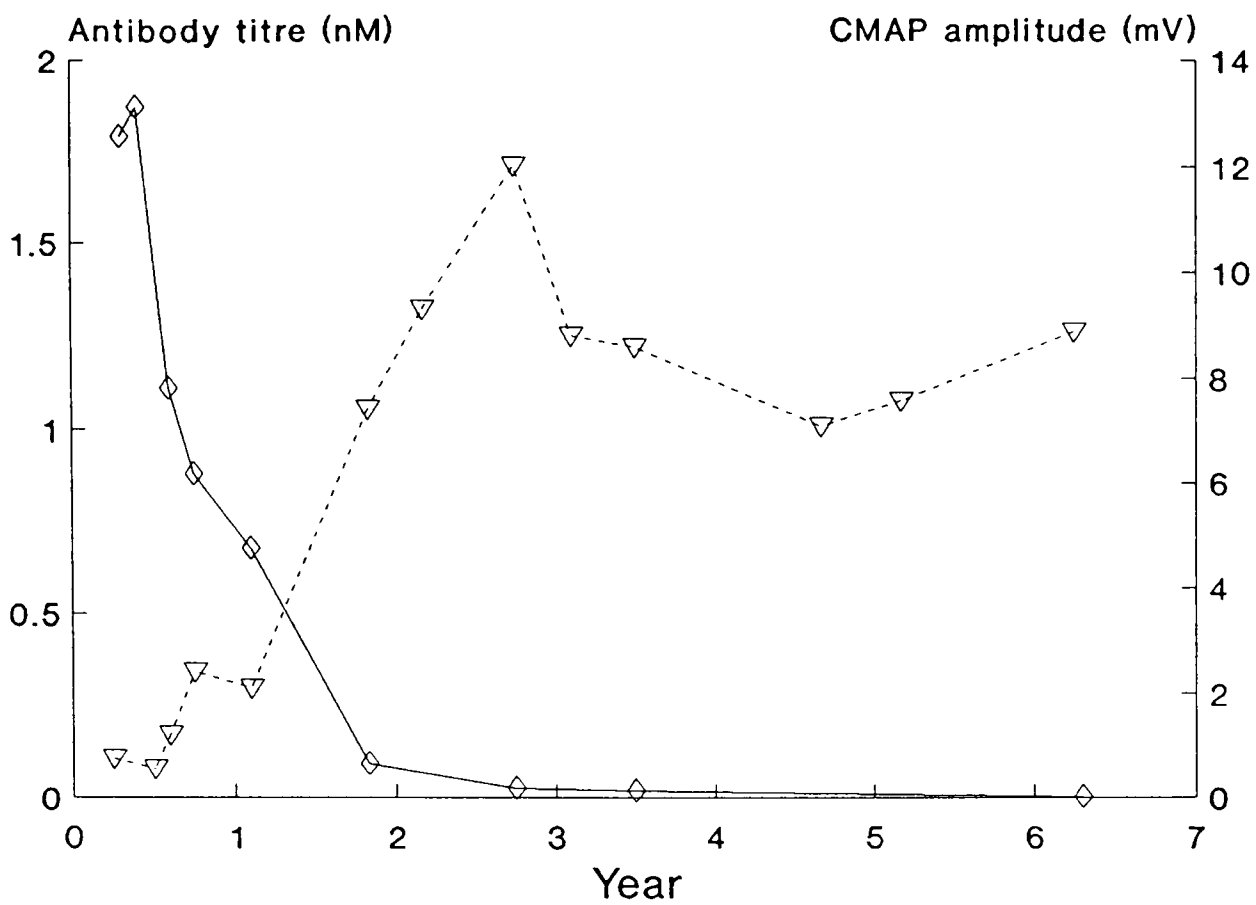

Antibody titre (nM)
CMAP amplitude (mV)
Year
mg prednisolone a.d.
60
30
0
183

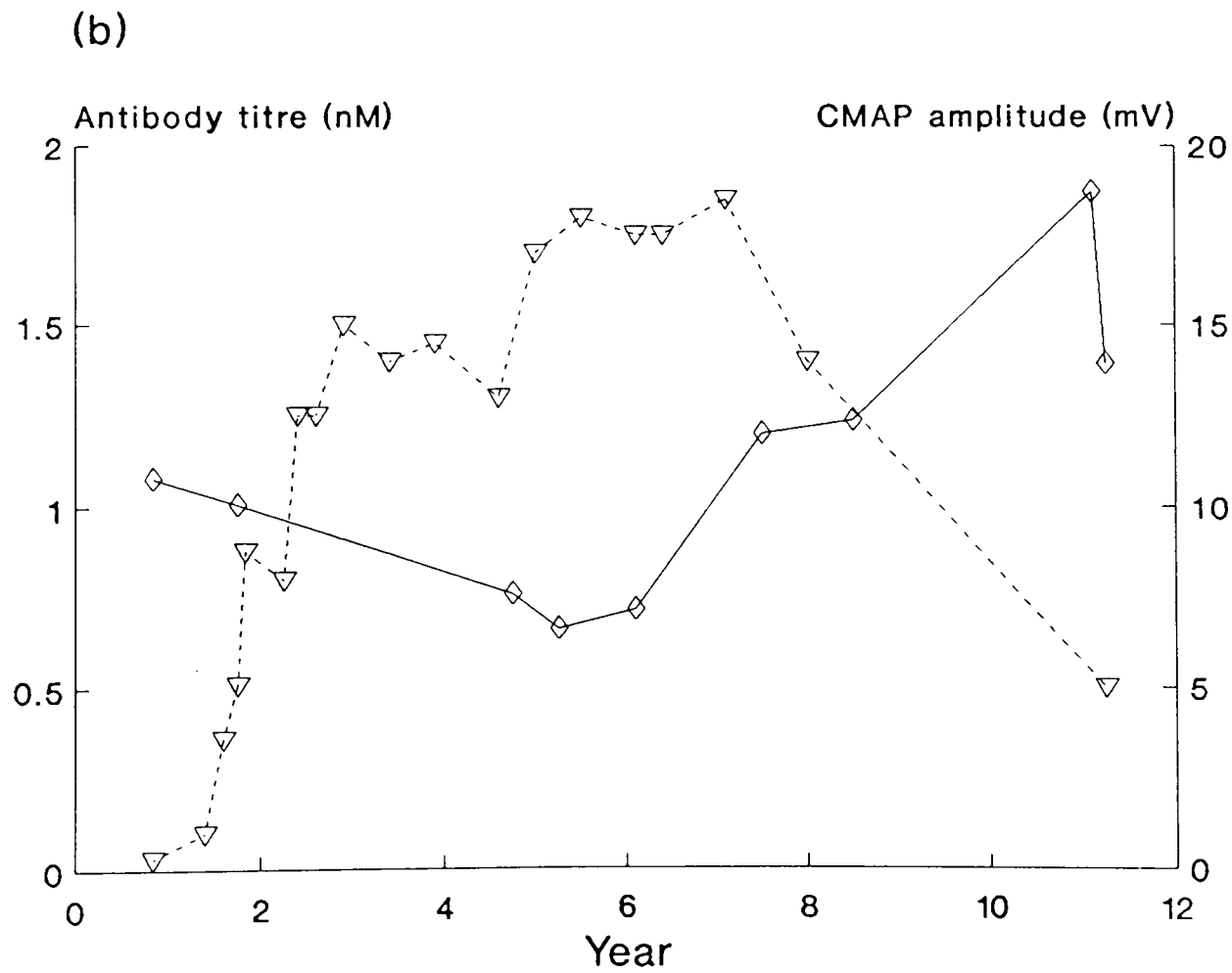
Figure 5.10: Longitudinal studies of anti-VGCC antibody titre in two LEMS patients using MAR5 antigen.

Serum antibody levels (◇, solid line) and CMAP amplitudes (▽, dotted line) were measured for the same two patients as described in Figure 5.9., using MAR5 cells as the source of ^{125}I-ωCgTx-labelled VGCCs.

(a)


Antibody titre (nM)
CMAP amplitude (mV)
2
1.5
1
0.5
0
14
12
10
8
6
4
2
0
0
1
2
3
4
5
6
7
Year

(b)


Antibody titre (nM)
CMAP amplitude (mV)
2
1.5
1
0.5
0
20
15
10
5
0
0
2
4
6
8
10
12
Year

5.4. Discussion

A radioimmunoassay has been described for the detection of anti-VGCC antibodies in the serum of patients with LEMS. Antibody levels were measured by the immunoprecipitation of ^{125}I-ωCgTx-labelled VGCCs extracted from the human neuroblastoma line, SKNSH. Although this cell line had the highest density of ^{125}I-ωCgTx binding sites of those tested, the binding site density was low (63 fmoles/mg protein). It was thus impossible to extract antigen at concentrations greater than 200 pM. Apparent antibody titres of both LEMS and control sera increased linearly with antigen concentration over the range studied and true titres could not be achieved. This may explain why the antibody titres obtained appear low compared to, for example, anti-AChR antibody titres in the serum of patients with MG. These are measured by the immunoprecipitation of ^{125}I-α-bungarotoxin-labelled AChRs from human skeletal muscle and serum is incubated with a concentration of antigen sufficient to saturate most anti-AChR antibodies (500pM) (Vincent and Newsom-Davis 1985).

It was decided to compare the serum antibody titres of the LEMS patients and the patients with other neurological or immunological disorders with the titres obtained for a group of healthy subjects. 33 of the 78 LEMS sera (42%) had titres greater than 30pM (2SDs above the mean for the healthy controls). This compares with 27 out of 52 patients (52%) positive for antibody reported by Lennon and Lambert (1989) using similar criteria (>31pM; 2.5SDs above the mean for a group of healthy subjects). Sher et al (1989) reported that 20 out of 22 LEMS sera (91%) contained detectable antibody (>24pM), although the significance of this value compared

to control titres is not defined.

Using a smaller group of patients, we have previously reported a higher incidence of positive sera among LEMS patients without detectable cancer than among those with SCLC (Leys et al 1991). Conversely, Lennon and Lambert (1989) found a higher percentage of positive sera in the group of LEMS patients with associated SCLC. In the present study, using a larger group of patients than in any previous study, there was no significant difference in the incidence of positive sera among LEMS patients with SCLC, those with no detectable cancer or those whose cancer status is uncertain. This agrees with the finding that the sera of LEMS patients with or without SCLC exert similar inhibitory effects on voltage-dependent calcium flux (Roberts et al 1985, De Aizpurua et al 1988, Lang et al 1989b).

Low levels of anti-VGCC antibodies were found in three patients in whom a clinical diagnosis of MG only had been made, two being positive for anti-AChR antibodies. It is possible that anti-VGCC antibodies partially contributed to the myasthenic weakness in these patients. **Furthermore**, it was found that two patients with clinically diagnosed LEMS also had high levels of anti-AChR antibodies, while clinical symptoms of MG were not apparent (Newsom-Davis et al, in press). The occurrence of both LEMS and MG in a single patient has been described (Taphoorn et al 1988), although this is difficult to establish based on clinical and electromyographic criteria alone. The co-existence of LEMS and MG might be expected since both disorders have similar HLA associations (Compston et al 1980, Willcox et al 1985). The availability of radioimmunoassays for the detection of both

anti-AChR and anti-VGCC antibodies may provide immunological confirmation of the presence of both LEMS and MG in some patients.

About 10% of patients with MG do not have detectable anti-AChR antibodies. There is evidence that serum antibodies in these patients affect neuromuscular transmission by binding to non-AChR determinants at the neuromuscular junction (Mossman et al 1986). The presence of LEMS in antibody-negative MG patients is unlikely, due to the normal CMAP amplitude, the absence of post-tetanic potentiation and the lack of associated SCLC. In confirmation, 10 patients in this category were tested for the presence of anti-VGCC antibodies and the incidence of positive sera was not significant.

Eight out of 17 patients (47%) with SCLC but no neurological symptoms had low levels of anti-VGCC antibodies (38-74 pM). The presence of anti-VGCC antibodies in SCLC patients has been reported by other groups (Lennon and Lambert 1989, Sher et al 1989). It has been suggested that in LEMS associated with SCLC, the autoimmune response is triggered by tumour determinants (Chalk et al 1990). Antibodies generated against tumour VGCCs would, therefore, affect neuromuscular transmission by cross-reacting with VGCCs at the NMJ. If this is the case, it may be expected that some patients with SCLC have anti-VGCC antibodies at levels too low for neurological symptoms to be manifested. Alternatively, some antibodies may be generated that do not cause a loss of functional VGCCs and, therefore, do not produce such symptoms. The trigger for the autoimmune response in LEMS not associated with cancer is unknown.

Low antibody titres (34-82 pM) were also found in 9 out of 16

patients (56%) with either RA or SLE. Patients with non-organ specific autoimmune disorders have not previously been tested for anti-VGCC antibodies, although Lennon and Lambert (1989) found anti-VGCC antibodies in the serum of a single patient with RA. Non-organ specific autoimmune disorders such as RA and SLE are associated with autoantibodies directed against a diverse array of cellular components, primarily located in the nucleus or cytoplasm. A characteristic of these autoantigens is that they are not tissue-specific, but are found in all cell types. It is possible that serum containing such a complex array of autoantibodies may cross-react with VGCC determinants. It is not known if the antibodies in these sera modulate VGCCs in intact cells, as do anti-VGCC antibodies in the serum of LEMS patients. They may be 'false positives' caused by the precipitation of membrane proteins unrelated to calcium channel function that remain associated with VGCCs during the extraction procedure. Cytotoxic antibodies to components of SKNSH membranes have been described in SLE sera (Bluestein 1978), although the precise target was not identified. It was suggested that these antibodies may play a part in the neuropsychiatric symptoms seen in some SLE patients.

The above findings indicate that the presence of antibodies against determinants on VGCCs may be widespread, but that high antibody titres (>100pM) are specific to patients with LEMS. 12 of the 78 LEMS sera (15%) had antibodies higher than this level. Low levels of anti-AChR antibodies have been reported in the serum of a few subjects without clinical evidence of MG. These include a small proportion of relatives of MG patients, a very few patients

with a predisposition to autoimmune disorders and some non-myasthenic thymoma patients (Vincent and Newsom-Davis 1985).

Interestingly, no patient in the OND group had serum antibodies which precipitated VGCCs from SKNSH cells. This group included six patients with Guillain-Barré Syndrome (GBS) and two with chronic inflammatory demyelinating neuropathy (CIDP). Both of these disorders are thought to be mediated by autoimmune damage to peripheral nerve myelin (van Doorn et al 1987, Quarles 1989). Antibodies directed towards gangliosides and other myelin glycolipids have been detected in the serum of patients with GBS (Ilyas et al 1988, Quarles 1989). Using an immunofluorescence assay, antibodies against a neuroblastoma cell line were detected in serum from GBS and CIDP patients, but not from patients with other disorders (van Doorn et al 1988).

The results described above were compared with those obtained using ^{125}I-ωCgTx-labelled VGCCs extracted from the human SCLC line, MAR5. The inhibition of VGCC function in SCLC lines by ωCgTx has been reported (De Aizpurua et al 1988). The presence of high affinity ^{125}I-ωCgTx binding sites in MAR5 membranes is described in Chapter 4. Radioimmunoassays using the MAR5 antigen gave results similar to those obtained with the SKNSH antigen. There was a high correlation between the titres obtained for the LEMS sera in the two assays. Similar correlations have been reported between two SCLC lines and between a SCLC line and the neuroblastoma line, IMR32 (Lennon and Lambert 1989). Also, the variation of antibody

titre in longitudinal studies of two LEMS patients using the SKNSH antigen was exactly mirrored using the MAR5 antigen. These results indicate an antigenic similarity between neuroblastoma and SCLC VGCCs. Similar titres were also obtained with a few sera tested with VGCCs extracted from rat brain. A further study of 25 LEMS sera has shown a high correlation between the titres obtained using SKNSH cells and rat brain ($RS = 0.89$, $p<0.001$) (A. Williams, unpublished data). These results suggest the presence of shared determinants between human and rodent neuronal VGCCs.

The high incidence of positive sera from patients with RA or SLE was confirmed with the MAR5 antigen, although no correlation was demonstrable between the titres obtained and those obtained using SKNSH VGCCs. The sera with raised titres among the other controls were mostly from patients different from those positive in the SKNSH assay. This lack of correlation suggests that the use of two sources of VGCC may help to eliminate false positives.

The results of the radioimmunoassays indicate that anti-VGCC antibodies in a proportion of LEMS patients are not being detected. This suggests that the population of antibodies in LEMS sera is **heterogeneous** and only some sera contain antibodies that cross-react with neuroblastoma VGCCs. The pathological significance of the antibodies detected was investigated by comparing antibody titre with the corresponding CMAP amplitude and percentage increment in amplitude. There was a poor correlation across individuals between antibody titre and these indices of disease severity. This contrasts with the close correlation of disease severity with the functional effects of IgG on voltage-dependent calcium flux (Lang et al 1989b). The results are

reminiscent of the finding in patients with MG in whom anti-AChR antibody titres correlate poorly with muscle weakness (Vincent and Newsom-Davis 1980). There is a much stronger correlation in longitudinal studies of individual patients with MG during plasma exchange and immunosuppressive therapy (Newsom-Davis et al 1978). Longitudinal studies of anti-VGCC antibody titres in two high-titre LEMS patients receiving immunosuppressive therapy indicated that there may be a similar inverse relationship between antibody levels and disease severity in individual LEMS patients.

There is a further reason for questioning the role of the antibodies detected in the radioimmunoassay described above. Sensitivity to ωCgTx has not been demonstrated at the mammalian neuromuscular junction (Yoshikami et al 1989). Thus the ωCgTx-labelled VGCCs extracted from neuronal cell lines may differ antigenically from those affected at the nerve terminal by LEMS antibodies. The radioimmunoassay may therefore detect some anti-VGCC antibodies that do not contribute to the pathophysiological changes seen in LEMS at the neuromuscular junction.

5.5. Summary

An immunoprecipitation assay for the detection of serum antibodies to VGCCs was developed using ^{125}I-ωCgTx-labelled VGCCs extracted from the human neuroblastoma cell line, SKNSH. 42% of LEMS patients had significant levels of antibody (30-1466 pM) compared with healthy control individuals (<31 pM). The incidence of positive sera among patients with other neurological disorders or with myasthenia gravis was not significant. However, 47% of patients with SCLC and 56% of patients with RA or SLE had raised titres (30-82 pM). Antibody titres for the LEMS sera correlated strongly with those obtained using VGCCs extracted from the human small cell lung carcinoma line, MAR5.

Anti-VGCC antibody titres did not correlate with the severity of LEMS across individuals, but longitudinal studies in two patients receiving immunosuppressive therapy showed an inverse relation between antibody titre and an electromyographic index of disease severity, the CMAP amplitude. The radioimmunoassay detects antibodies that cross-react with neuroblastoma and SCLC VGCCs. Some of these may contribute to the defect in neuromuscular transmission seen in LEMS.

CHAPTER 6

GENERAL DISCUSSION AND FUTURE PERSPECTIVES

In these studies the presence of functional voltage-gated calcium channels was demonstrated in cultured cell lines of neuronal origin by the technique of K^+-induced $^{45}Ca^{2+}$ influx. The results suggested that two mutually exclusive subtypes of VGCC were expressed in the cell lines studied, one being sensitive to dihydropyridines and the other to ω-conotoxin. The exception was the PC12 line, in which the calcium current was carried by DHP-sensitive VGCCs only. The existence of two classes of calcium channel was further investigated using radioligand binding studies to cell membranes. The lack of competition between DHPs and ωCgTx implied separate binding sites for these two antagonists, although not necessarily on different molecules. However, the lack of stoichiometry between the numbers of DHP and ωCgTx binding sites suggested the presence of at least two classes of VGCC. HVA currents in neuronal cells have been divided into L and N channels based on their different electrophysiological and pharmacological properties. L-type (DHP-sensitive) VGCCs have been further subdivided into neuronal and non-neuronal types, based on the tissue specificity of ωCgTx (Cruz et al 1986). This subdivision was proposed, however, using electrophysiological data from chick DRG neurones, in which ωCgTx inhibits both L and N channels (McCleskey et al 1987). Other neuronal cells appear to express L channels that are not affected by ωCgTx (Carbone et al 1990), similar to those expressed by the cells studied here.

The number of ^{125}I-ωCgTx binding sites in a particular cell line broadly correlated with the inhibition by ωCgTx of K^+-dependent calcium flux. For example, SKNSH cells had the highest number of ωCgTx binding sites (63 fmoles/mg protein) and also the highest percentage inhibition of calcium flux by ωCgTx (53%) (see Tables 3.2 and 4.2). The effects of DHPs were more difficult to compare, as saturable DHP binding was not detected in four cell lines (see Table 4.1). However, the two cell lines with detectable DHP binding (PC12s and IMR32s) also had the highest percentage of calcium flux blocked by nitrendipine (95 and 87% respectively).

The effect of LEMS antibodies on K^+-stimulated calcium flux was investigated in two neuroblastoma lines, SKNSH and Kelly. LEMS IgG from individual patients has previously been shown to reduce calcium flux in other cell lines such as human SCLC (Roberts et al 1985, De Aizpurua et al 1988). These findings were not reproduced in the cells studied here. However, a pool of antibodies from six LEMS patients did result in a reduction of K^+-stimulated calcium flux in the SKNSH cell line. This suggests that the presence of several antibodies with different specificities results in successful cross-linking and down-regulation of VGCCs in this cell line. It was shown that the LEMS IgG pool did not discriminate between the two classes of VGCC present on SKNSH cells. L and N channels in neurones may be similar in terms of electrophysiological properties, but have different drug sensitivities (Swandulla et al 1991). This suggests that the basic structure of L and N channels is similar, with variations in the regions of antagonist binding. Therefore, there may be extensive antigenic similarity between the two VGCC subtypes. This has been

compared to the antigenic similarity of three pharmacologically distinct nicotinic ACh receptors found in adult and foetal skeletal muscle and neuronal tissues (De Aizpurua et al 1988).

The down-regulation of both classes of VGCC on SKNSH cells could in theory result in a complete inhibition of K^+-dependent calcium flux. However, a maximum of 40% of K^+-stimulated flux was inhibited by the pooled LEMS IgG. There are several possible explanations for the incomplete inhibition of calcium flux by the LEMS pool, and also the lack of inhibition by individual samples. The cells may not have been exposed for long enough to the antibodies, particularly if the affinity of antibody for the SKNSH calcium channels was low. Also the low density of VGCCs on the cell membrane may inhibit successful cross-linking by antibody. This may explain why no effect of IgG was found in the Kelly cell line, which had an even lower density of ^{125}I-ωCgTx binding sites. Alternatively, internalisation of cross-linked calcium channels may be followed by an increased rate of VGCC synthesis and reinsertion into the cell membrane in an attempt to stabilise the number of functional calcium channels. Such a compensatory mechanism has been described for the ACh receptor in muscle endplates after treatment with IgG from MG patients (Wilson et al 1983).

In agreement with the calcium flux studies, the density of ^{125}I-ωCgTx binding sites on SKNSH membranes was reduced by a pool of LEMS antibodies, but not by IgG from individual patients. The binding site density was reduced by 57%, providing further evidence that a proportion of calcium channels was resistant to the effects of LEMS IgG. It is not known, however, if all of the

^{125}I-ωCgTx binding sites measured were associated with functional VGCCs, therefore the reduction of binding site density cannot be directly compared with the inhibition of K^+-stimulated calcium flux, although the IgG pool was the same in both series of experiments.

The presence of antibodies to calcium channels in LEMS serum was further investigated by the immunoprecipitation of ^{125}I-ωCgTx binding sites extracted from cell membranes. Using this technique, anti-VGCC antibodies were detected in the sera of 42% of LEMS patients, at levels significantly higher than those in healthy control sera. However, raised antibody titres were also found in the sera of some patients with other diseases, particularly those with SCLC or non-organ specific autoimmune disorders (RA and SLE). Although the control SCLC group did not have clinically diagnosed LEMS, it is possible that some of the patients had some neurological symptoms. A group of 61 patients with SCLC is currently being investigated for anti-VGCC antibodies using the radioimmunoassay described here (I.Johnston, unpublished results). The patients are divided into those with known LEMS, those with diminished tendon reflexes, those with some form of weakness and those with no neurological symptoms. The results will show whether anti-VGCC antibody titre correlates with the presence of neurological symptoms among patients with SCLC.

Similarly, it would be interesting to study a larger group of patients with RA and SLE and to correlate the presence of raised antibody titres with any neurological symptoms in these patients. It is possible that the raised titres found in these sera were due to the precipitation of proteins not related to VGCC function.

This could be investigated by measuring the effect of IgG from patients with RA or SLE on K^+-dependent calcium flux. Alternatively, a purified form of the ^{125}I-ωCgTx binding site could be used in future assays in an attempt to eliminate these 'false positives'.

Titres higher than 100pM were detected in 15% of LEMS sera. No control sample had an antibody titre in this range. It is possible that this proportion of LEMS patients represents a subpopulation with antibodies that cross-react with high affinity to the VGCCs extracted from the cell lines used. The low-titre sera may contain antibodies that cross-react with low affinity to VGCC epitopes. These low-affinity antibodies could be present in the serum of patients with other diseases, particularly other autoimmune diseases, at concentrations too low to affect neuromuscular transmission.

Anti-VGCC antibodies in a proportion of LEMS sera were not detected using antigen extracted from SKNSH cells. Other sources of antigen were used in an attempt to detect antibodies in a higher percentage of LEMS patients. However, similar results were obtained using VGCCs extracted from cultured human SCLC and rat brain. It is possible that these 'negative' LEMS sera contain antibodies to ωCgTx-insensitive VGCCs and that these are not detected using ^{125}I-ωCgTx as a label. An attempt to perform a similar assay using [^3H]-PN200-110-labelled VGCCs was unsuccessful owing to the reversibility of binding and low specific activity of the ligand. The detection of antibodies against other types of VGCC is, therefore, impractical until more suitable radioligands become available.

Some of the negative LEMS sera had previously been shown to inhibit K^+-stimulated calcium flux in the SCLC line, MAR (Roberts et al 1985). This may be due to inhibition of a subtype of VGCC not detected in the radioimmunoassay. The inhibition of calcium flux by LEMS IgG is related to the severity of the neurological symptoms (Lang et al 1989) while the anti-VGCC antibody titre is not. This may be explained by the fact that the calcium flux assay detects antibodies to all classes of VGCC, while the radioimmunoassay detects only antibodies to ωCgTx-sensitive channels. Longitudinal studies in two LEMS patients suggested that the anti-VGCC antibody titre may, however, be a useful index of disease severity within an individual.

There are other reasons why anti-VGCC antibodies are not detected in some LEMS sera. For example, some antibodies may not be recognised by the anti-human IgG used for precipitation, although a polyspecific antiserum was used. It has recently been suggested that the defect in neuromuscular transmission in seronegative MG patients may be caused by low affinity IgM antibodies which cannot be detected by radioimmunoassay (Yamamoto et al, in press). Alternatively, antibodies might bind to other components of the presynaptic membrane and indirectly cause the loss of functional VGCCs. Previous attempts using Western blotting techniques to identify the proteins to which LEMS antibodies bind were unsuccessful (Chester et al 1988).

The use of ωCgTx-labelled VGCCs for the detection of antibodies in LEMS serum may be critisised as ωCgTx does not affect transmission at the mammalian neuromuscular junction (Olivera et al 1987, Yoshikami et al 1989). However, as mentioned above,

different types of calcium channel may have many antigenic sites in common. N-type VGCCs are thought to be involved in neurotransmitter release at nerve terminals. A slight change in these channels at the human NMJ could result in the loss of the ωCgTx binding site, but they may otherwise resemble the ωCgTx-sensitive VGCCs on the cell lines used in these studies. The radioimmunoassay may, therefore, be an effective way of detecting some of the antibodies involved in the pathogenesis of LEMS. Conversely, some antibodies may be detected that do not act on the calcium channels at the human nerve terminal and are therefore not responsible for a defect in neuromuscular transmission. They may, however, play a part in the autonomic symptoms associated with LEMS.

Summary

K^+-stimulated calcium influx in six neuronal cell lines was measured. Five of the cell lines expressed both DHP-sensitive and ωCgTx-sensitive VGCCs, which may correspond to the L and N subtypes of calcium channel described for neuronal tissues. The PC12 line expressed DHP-sensitive VGCCs only.

A proportion of K^+-stimulated calcium flux was inhibited by pooled LEMS IgG in the neuroblastoma line SKNSH. This did not appear to be due to the inhibition of a particular subtype of VGCC.

The specificities of the VGCCs expressed was confirmed by radioligand binding studies in cell membranes. Saturable ^{125}I-ωCgTx binding was found in all but the PC12 cell line. By contrast, saturable [^{3}H]-PN200-110 binding was demonstrated in PC12 and IMR32 membranes only. The number of ^{125}I-ωCgTx binding sites in SKNSH cells and the human SCLC line, MAR5, was reduced after exposure to pooled LEMS IgG.

^{125}I-ωCgTx-labelled VGCCs extracted from SKNSH and MAR5 membranes were used in radioimmunoassays for the detection of antibodies in LEMS serum. 42% of LEMS patients had anti-VGCC antibody titres significantly above those for the healthy controls. However, raised titres were also found among patients with SCLC but not LEMS, and those with either RA or SLE. 15% of the LEMS patients had anti-VGCC antibody titres above those which were found in any of the control groups.

The results of the radioimmunoassay suggest that LEMS antibodies are heterologous, and only a proportion of them are detected. Those that are not detected may bind to other classes of VGCC, to

epitopes that are not present on the cell lines used, or to proteins not associated with VGCCs. The lack of correlation between antibody titre and disease severity suggests that some non-pathogenic antibodies are detected. Serial antibody titres may, however, be a useful indication of the severity of the disease within an individual. Anti-VGCC antibody titres greater than 100pM appear to be specific for LEMS, and may therefore be used to confirm a diagnosis of LEMS in these patients. Antibody titres between 30 and 100pM may be useful as an additional diagnostic aid for LEMS, although they may also indicate the presence of SCLC or other autoimmune disorders.

REFERENCES

Abe T. and Saisu H. (1987) J. Biol. Chem. **262:** 9877-9882.

Allan P.M., Garson J.A., Harper E.I., Asser U., Coakham H.B., Brownell B. and Kemshead J.T. (1983) Int. J. Cancer **31:** 591-598.

Anderson H.J., Churchill-Davidson H.C. and Richardson A. Lancet 1953 i: 1291-1293.

Aosaki T. and Kasai H. (1989) Pflugers Arch. **414:** 150-156.

Ballesta J.J., Palmero M., Hidalgo M.J., Gutierrez L.M., Reig J.A., Viniegra S. and Garcia A.G. (1989) J. Neurochem. **53:** 1050-1056.

Barhanin J., Schmid A. and Lazdunski M. (1988) Biochem. Biophys. Res. Commun. **150:** 1051-1062.

Bean B.P. (1989a) Annu. Rev. Physiol. **51:** 367-384.

Bean B. (1989b) Trends Neurosci. **12:** 128-130.

Beaty G.N., Cota G., Nicola Siri L., Sanchez J.A. and Stefani E. (1987) in: Structure and Physiology of the Slow Inward Calcium Channel (Venter J.C. and Triggle D. eds., Alan R. Liss Inc., New York) pp 123-140.

Biedler J.L., Helson L. and Spengler B.A. (1973) Cancer Research **33:** 2643-2652.

Bluestein H. (1978) Proc. Natl. Acad. Sci. **75:** 3965-3969.

Borsotto M., Norman R.I., Fosset M. and Lazdunski M. (1984) Eur. J. Biochem. **142:** 449-455.

Borsotto M., Barhanin J., Fosset M. and Lazdunski M. (1985) J. Biol. Chem. **260:** 14255-14263.

Carbone E. and Lux H.D. (1984) Nature **310:** 501-502.

Carbone E., Sher E. and Clementi F. (1990) Pflugers Arch. **416:**

170-179.

Catterall W.A. (1988) Science **242:** 50-61.

Chalfie M. and Perlman R.L. (1976) J. Pharmacol. Exp. Ther. **197:** 615-622.

Chalk C.H., Murray N.M.F., Newsom-Davis J., O'Neill J.H. and Spiro S.G. (1990) Neurology **40:** 1552-1556.

Cheng Y.-C. and Prusoff W.H. (1973) Biochem. Pharmacol. **22:** 3099-3108.

Chester K.A., Lang B., Gill J., Vincent A. and Newsom-Davis J. (1988) J. Neuroimmunol. **18:** 97-104.

Compston D.A.S., Vincent A., Newsom-Davis J. and Batchelor J.R. (1980) Brain **103:** 579-601.

Cruz L.J. and Olivera B.M. (1986) J. Biol. Chem. **261:** 6230-6233.

Cruz L.J., Johnson D.S. and Olivera B.M. (1987) Biochemistry **26:** 820-824.

Curtis B.M. and Catterall W.A. (1984) Biochemistry **23:** 2113-2118.

De Aizpurua H.J., Lambert E.H., Griesmann G.E., Olivera B.M. and Lennon V.A. (1988) Cancer Res. **48:** 4719-4724.

Dickson J.G., Flanigan T.P. and Walsh F.S. (1983) The EMBO Journal **2:** 283-288.

Docherty R.J. (1988) J. Physiol. **398:** 33-48.

Ellis S.B., Williams M.E., Ways N.R., Brenner R., Sharp A.H., Leung A.T., Campbell K.P., McKenna E., Koch W.J., Hui A., Schwartz A. and Harpold M.M. (1988) Science **241:** 1661-1664.

Ellison M.L., Hillyard C.J., Bloomfield G.A., Rees L.H., Coombes R.C. and Neville A.M. (1976) Clin. Endocrinol. **5:** 397S-406S.

Elmqvist D. and Lambert E.H. (1968) Mayo Clin. Proc. **43:** 689-713.

Ferry D.R., Goll A., Rombusch M. and Glossman H. (1985) Br. J.

Clin. Pharmacol. **20:** 233S-246S.

Fox A.P., Nowycky M.C. and Tsien R.W. (1985) Soc. Neurosci. Abstr. **11:** 792.

Fox A.P., Nowycky M.C. and Tsien R.W. (1987) J. Physiol. **394:** 149-172.

Freedman S.B. and Miller R.J. (1984) Proc. Natl. Acad. Sci. **81:** 5580-5583.

Fukunaga H., Engel A.G., Osame M. and Lambert E.H. (1982) Muscle and Nerve **5:** 686-697.

Fukunaga H., Engel A.G., Lang B., Newsom-Davis J. and Vincent A. (1983) Proc. Natl. Acad. Sci. **80:** 7636-7640.

Fukuoka T., Engel A.G., Lang B., Newsom-Davis J., Prior C. and W.-Wray D. (1987) Ann. Neurol. **22:** 193-199.

Galizzi J.-P., Borsotto M., Barhanin J., Fosset M. and Lazdunski M. (1986) J. Biol. Chem. **261:** 1393-1397.

Glossman H., Ferry D.R., Goll A. and Rombusch M. (1984) J. Cardiovasc. Pharmacol. **6:** S608-S621.

Goll A., Ferry D.R. and Glossman H. (1983) FEBS Letters **157:** 63-69.

Greene L. and Tischler A. (1976) Proc. Natl. Acad. Sci. **73:** 2424-2426.

Guttmann L., Crosby T.W., Takamori M. and Martin J.D. (1972) Am. J. Med. **53:** 354-356.

Henderson C. (1990) Trends Neurosci. **13:** 39-41.

Henson R.A. (1953) Proc. R. Soc. Med. **46:** 859-861.

Henson R.A. and Urich H. (1982) Cancer and the Nervous System, Blackwell Scientific Publications, Oxford.

Hille B. (1984) Ionic Channels of Excitable Membranes, Sinauer,

Sunderland.

Hirning L.D., Fox A.P., McCleskey E.W., Olivera B.M., Thayer S.A., Miller R.J. and Tsien R.W. (1988) Science **239:** 57-60.

Horejsi J. and Smetana R. (1956) Acta. Med. Scand. **155:** 65-70.

Humphrey J.H. and White R.G. (1963) Immunology for Students of Medicine, Blackwell Scientific Publications, Oxford.

Ilyas A.A., Willison H.J., Quarles R.H., Jungalwala F.B., Cornblath D.R., Trapp B.D., Griffin D.E., Griffin J.W. and McKhann G.M. (1988) Ann. Neurol. **23:** 440-447.

Jan C.-R., Titeler M. and Schneider A.S. (1990) J. Neurochem. **54:** 355-358.

Kerr L.M. and Yoshikami D. (1984) Nature **308:** 282-284.

Kim Y.I. (1985) Muscle and Nerve **8:** 162-172.

Kim Y.I. (1986) Muscle and Nerve **9:** 523-530.

Kim Y.I. and Neher E. (1988) Science **239:** 405-408.

Kim Y.I., Sanders D.B., Johns T.R., Phillips L.H. and Smith R.E. (1988) J. Neurol. Sci. **87:** 1-13.

Kongsamut S. and Miller R.J. (1986) Proc. Natl. Acad. Sci. **83:** 2243-2247.

Lambert E.H., Eaton L.M. and Rooke E.D. (1956) Am. J. Physiol. **187:** 612-613.

Lambert E.H. and Elmqvist D. (1971) Ann. N. Y. Acad. Sci. **183:** 183-199.

Lambert E.H. and Lennon V.A. (1988) Muscle and Nerve **11:** 1133-1145.

Lang B., Newsom-Davis J., Wray D. and Vincent A. Lancet 1981 ii: 224-226.

Lang B., Newsom-Davis J., Prior C. and Wray D. (1983) J. Physiol.

344: 335-345.

Lang B., Newsom-Davis J., Peers C., Prior C. and W.-Wray D. (1987) J. Physiol. **390:** 257-270.

Lang B., Leys K., Vincent A. and Newsom-Davis J. (1989a)Ann. N.Y. Acad. Sci. **560:** 294-296.

Lang B., Vincent A., Murray N.M.F. and Newsom-Davis J. (1989b)Ann. Neurol. **25:** 265-271.

Lee H.R., Roeske W.R. and Yamamura H.I. (1984) Life Sci. **35:** 721-732.

Lennon V.A., Lambert E.H., Whittingham S. and Fairbanks V. (1982) Muscle and Nerve **5:** S21-S25.

Lennon V.A. and Lambert E.H. (1989) Mayo Clin. Proc. **64:** 1498-1504.

Leys K., Lang B., Vincent A. and Newsom-Davis J. Lancet 1989 ii: 1107.

Leys K., Lang B., Johnston I. and Newsom-Davis J. (1991) Ann. Neurol. **29:** 307-314.

Llinas R. and Yarom Y. (1981) J. Physiol. **315:** 569-584.

Lowry O.H., Rosebrough N.J., Farr A.L. and Randall R.J. (1951) J. Biol. Chem. **193:** 265-275.

Marqueze B., Martin-Moutot N., Leveque C. and Couraud F. (1988) Mol. Pharmacol. **34:** 87-90.

McCann F.V., Pettengill O.S., Cole J.J., Russell J.A.G. and Sorenson G.D. (1981) Science **212:** 1155-1157.

McCleskey E.W., Fox A.P., Feldman D.H., Cruz L.J., Olivera B.M., Tsien R.W. and Yoshikami D. (1987) Proc. Natl. Acad. Sci. **84:** 4327-4331.

Mikami A., Imoto K., Tanabe T., Niidome T., Mori Y., Takeshima H.,

Narumiya S. and Numa S. (1989) Nature **340:** 230-233.

Miller R.J. (1987) in: Structure and Physiology of the Slow Inward Calcium Channel (Venter J.C. and Triggle D. eds., Alan R. Liss Inc., New York) pp 161-246.

Miller R.J. and Freedman S.B. (1984) Life Sci. **34:** 1205-1221.

Molenaar P.C., Newsom-Davis J., Polak R.L. and Vincent A. (1982) Neurology **32:** 1061-1065.

Mossman S., Vincent A. and Newsom-Davis J. Lancet 1988 i: 116-119.

Nagel A., Engel A.G., Lang B., Newsom-Davis J. and Fukuoka T. (1988) Ann. Neurol. **24:** 552-558.

Nelson P., Christian C. and Nirenberg M. (1976) Proc. Natl. Acad. Sci. **73:** 123-127.

Newsom-Davis J., Pinching A.J., Vincent A. and Wilson S.G. (1978) Neurology (NY) **28:** 266-272.

Newsom-Davis J. and Murray N.M.F. (1984) Neurology **34:** 480-485.

Newsom-Davis J., Leys K., Vincent A., Ferguson I., Modi G. and Mills K. (1991) J. Neurol. Neurosurg. Psychiatry, in press.

Nowycky M.C., Fox A.P. and Tsien R.W. (1985) Nature **316:** 440-443.

Olivera B.M., McIntosh J.M., Cruz L.J., Luque F.A. and Gray W.R. (1984) Biochemistry **23:** 5090-5095.

Olivera B.M., Gray W.R., Zeikus R., McIntosh J.M., Varga J., Rivier J., de Santos V. and Cruz L.J. (1985) Science **230:** 1338-1343.

Olivera B.M., Cruz L.J., de Santos V., LeCheminant G.W., Griffin D., Zeikus R., McIntosh J.M., Galyean R., Varga J., Gray W.R. and Rivier J. (1987) Biochemistry **26:** 2086-2090.

Olivera B.M., Rivier J., Clark C., Ramilo C.A., Corpuz G.P., Abogadie F.C., Mena E., Woodward S.R., Hillyard D.R. and Cruz L.J.

(1990) Science **249:** 257-263.

O'Neill J.H., Murray N.M.F. and Newsom-Davis J. (1988) Brain **111:** 577-596.

Pearse A.G.E. (1969) J. Histochem. Cytochem. **17:** 303-313.

Peers C., Lang B., Newsom-Davis J. and W.-Wray D. (1990) J. Physiol. **421:** 293-308.

Perez-Reyes E., Kim H.S., Lacerda A.E., Horne W., Wei X., Rampe D., Campbell K.P., Brown A.M. and Birnbaumer L. (1989) Nature **340:** 233-236.

Plummer M.R., Logothetis D.E. and Hess P. (1989) Neuron **2:** 1453-1463.

Prior C., Lang B., Wray D. and Newsom-Davis J. (1985) Ann. Neurol. **17:** 587-592.

Pumplin D.W., Reese T.S. and Llinas R. (1981) Proc. Natl. Acad. Sci. **78:** 7210-7213.

Quarles R.H. (1989) PNEI Perspectives **2:** 109-119.

Reynolds I.J., Snowman A.M. and Snyder S.H. (1986) J. Pharmac. Exp. Ther. **237:** 731-738.

Roberts A., Perera S., Lang B., Vincent A. and Newsom-Davis J. (1985) Nature **317:** 737-739.

Robitaille R., Adler E.M. and Charlton M.P. (1990) Neuron **5:** 773-779.

Rosenberg R.L., Isaacson J.S. and Tsien R.W. (1989) Ann. N.Y. Acad. Sci. **560:** 39-52.

Schwab M., Alitalo K., Klempnauer K.-H., Varmus H.E., Bishop J.M., Gilbert F., Brodeur G., Goldstein M. and Trent J. (1983) Nature **305:** 245-248.

Sher E., Pandiella A. and Clementi F. (1988) FEBS Letters **235:**

178-182.

Sher E., Gotti C., Canal N., Scoppetta C., Piccolo G., Evoli A. and Clementi F. Lancet 1989 ii: 640-643.

Sher E., Denis-Donini S., Zanini A., Bisiani C. and Clementi F. (1989a) J. Cell. Biol. **108:** 2291-2300.

Sher E., Pandiella A. and Clementi F. (1990) Cancer Research **50:** 3892-3896.

Silver R.A., Lamb A.G. and Bolsover S.R. (1990) Nature **343:** 751-754.

Stallcup W.B. (1979) J. Physiol. **286:** 525-540.

Swandulla D., Carbone E. and Lux H.D. (1991) Trends Neurosci. **14:** 46-51.

Takahashi M. and Ogura A. (1983) FEBS Letters **152:** 191-194.

Takahashi M. and Catterall W.A. (1987a) Biochemistry **26:** 5518-5526.

Takahashi M. and Catterall W.A. (1987b) Science **230:** 88-91.

Takahashi M., Seagar M.J., Jones J.F., Reber B.F.X. and Catterall W.A. (1987) Proc. Natl. Acad. Sci. **84:** 5478-5482.

Takahashi M. and Fujimoto Y. (1989) Biochem. Biophys. Res. Commun. **163:** 1182-1188.

Tanabe T., Takeshima H., Mikami A., Flockerzi V., Takahashi H., Kangawa K., Kojima M., Matsuo H., Hirose T. and Numa S. (1987) Nature **328:** 313-318.

Taphoorn M.J.B., Van Duijn H. and Wolters E.C.H. (1988) J. Neurol. Neurosurg. Psychiatry **51:** 880-882.

Tischler A.S., Dichter M.A. and Biales B. (1977) J. Path. **122:** 153-156.

Toll L. (1982) J. Biol. Chem. **257:** 13189-13192.

Triggle D.J. (1987) ISI Atlas of Science: Pharmacology 319-324.

Triggle D.J. and Janis R.A. (1987) in: Structure and Physiology of the Slow Inward Calcium Channel (Venter J.C. and Triggle D. eds., Alan R. Liss Inc., New York) pp 29-50.

Tsien R.W., Lipscombe D., Madison D.V., Bley K.R. and Fox A.P. (1988) Trends Neurosci. **11:** 431-438.

Tumilowicz J.J., Nichols W.W., Cholen J.J. et al (1970) Cancer Research **30:** 2110-2118.

Vaghy P.L., Striessnig J., Miwa K., Knauss H.-G., Itagaki K., McKenna E., Glossman H. and Schwartz A. (1987) J. Biol. Chem. **262:** 14337-14342.

Van Doorn P.A., Brand A. and Vermeulen M. (1987) Neurology **37:** 1798-1802.

Van Doorn P.A., Brand A. and Vermeulen M. (1988) Neurology **38:** 1592-1595.

Vandaele S., Fosset M., Galizzi J.-P. and Lazdunski M. (1987) Biochemistry **26:** 5-9.

Vincent A. and Newsom-Davis J. (1980) J. Neurol. Neurosurg. Psychiatry **43:** 590-600.

Vincent A. and Newsom-Davis J. (1985) J. Neurol. Neurosurg. Psychiatry **48:** 1246-1252.

Vincent A., Lang B. and Newsom-Davis J. (1989) Trends Neurosci. **12:** 496-502.

Vincent A. (1990) in: Neuromuscular transmission: basic and applied aspects (Vincent A. and Wray D. eds., Manchester University Press, Manchester and New York) pp 226-248.

Weiland G.A. and Oswald R.E. (1985) J. Biol. Chem. **260:** 8456-8464.

Willcox N., Demaine A.G., Newsom-Davis J., Welsh K.I., Robb S.A.

and Spiro S.G. (1985) Human Immunol. **14:** 29-36.

Wilson S., Vincent A. and Newsom-Davis J. (1983) J. Neurol. Neurosurg. Psychiatry **46:** 383-387.

Woodward S.R., Cruz L.J., Olivera B.M. and Hillyard D.R. (1990) The EMBO Journal **9:** 1015-1020.

Yamamoto T., Vincent A., Ciulla T., Lang B., Johnston I. and Newsom-Davis J. (1991) Ann. Neurol., in press.

Yoshikami D., Bagabaldo Z. and Olivera B.M. (1989) Ann. N.Y. Acad. Sci. **560:** 230-248.